



This is a repository copy of *Bacterial cellulose : a smart biomaterial with diverse applications*.

White Rose Research Online URL for this paper:
<https://eprints.whiterose.ac.uk/184020/>

Version: Accepted Version

Article:

Gregory, D.A. orcid.org/0000-0003-2489-5462, Tripathi, L., Fricker, A.T.R. et al. (4 more authors) (2021) Bacterial cellulose : a smart biomaterial with diverse applications. *Materials Science and Engineering: R: Reports*, 145. 100623. ISSN 0927-796X

<https://doi.org/10.1016/j.mser.2021.100623>

© 2021 Published by Elsevier B.V. This is an author produced version of a paper subsequently published in *Materials Science and Engineering: R: Reports*. Uploaded in accordance with the publisher's self-archiving policy. Article available under the terms of the CC-BY-NC-ND licence (<https://creativecommons.org/licenses/by-nc-nd/4.0/>).

Reuse

This article is distributed under the terms of the Creative Commons Attribution-NonCommercial-NoDerivs (CC BY-NC-ND) licence. This licence only allows you to download this work and share it with others as long as you credit the authors, but you can't change the article in any way or use it commercially. More information and the full terms of the licence here: <https://creativecommons.org/licenses/>

Takedown

If you consider content in White Rose Research Online to be in breach of UK law, please notify us by emailing eprints@whiterose.ac.uk including the URL of the record and the reason for the withdrawal request.



eprints@whiterose.ac.uk
<https://eprints.whiterose.ac.uk/>

1 **Bacterial cellulose: A smart biomaterial with diverse applications**

2

3 David A. Gregory,^{1*} Lakshmi Tripathi,^{1*} Annabelle T.R. Fricker¹, Emmanuel Asare¹, Isabel

4 Orlando², Vijayendran Raghavendran^{1,3}, Ipsita Roy^{1**}

5

6 ¹Department of Materials Science and Engineering, Faculty of Engineering, University of
7 Sheffield, Sheffield, UK

8 ²Université Clermont Auvergne, CNRS, SIGMA Clermont, ICCF, F-63000 Clermont–Ferrand,
9 France

10 ³Current address: Department of Biology and Biological Engineering, Chalmers University of
11 Technology, Gothenburg, Sweden

12

13 * These authors contributed equally to this work

14 **Corresponding author: I.Roy@sheffield.ac.uk

15

16 **Table of Contents**

17 Abstract

18 Key words

19 1 Introduction

20 2 Production of BC

21 3 Material Properties

22 3.1 Functionalisation of BC

23 4 Applications

24 4.1 Bulk Applications

25 4.1.1 Food

26 4.1.2 Paper

27 4.1.3 Packaging

28 4.1.4 Superabsorbent polymers

29 4.1.5 Textiles

30 4.1.6 Bioconcrete

31 4.2 Bioremediation

32 4.3 Cosmetics

33 4.4 Electronics and Sensors

34 4.5 Biomedical applications

35 4.5.1 Wound healing and antibacterial wound dressings

36 4.5.2 Controlled Drug delivery

37 4.5.3 Tissue engineering

38 4.5.4 Cell culture

39 4.5.5 Artificial blood vessels

40 4.5.6 Additive manufacturing (3D Printing)

41 5 Current commercial status:

42 6 Future Outlook:

43 Abbreviations

44 Funding

45 Declaration of competing interest

46 Biographies

47 References

48

49

50

Tables

51 **Table 1:** Modifications of cellulose nanofibres/BC 14

52 **Table 2:** Summary of selected BC modifications for use as SAPs29

53 **Table 3:** BC modification reported in the recent literature for bioremediation.35

54 **Table 4:** Worldwide bacterial cellulose producing companies. 74

55

56

57

58

59 **Abstract**

60 Natural biomaterials have benefited the human civilisation for millennia. However, in recent
61 years, designing of natural materials for a wide range of applications have become a focus of
62 attention, spearheaded by sustainability. With advances in materials science, new ways of
63 manufacturing, processing, and functionalising biomaterials for structural specificity has
64 become feasible. Our review is focused on bacterial cellulose (BC), an exceptionally versatile
65 natural biomaterial. BC is a unique nanofibrillar biomaterial extruded by microscopic single-
66 cell bacterial factories utilising the chemical energy harvested from renewable substrates. BC
67 is extracellular and is intrinsically pure, unlike other biopolymers that require extraction and
68 purification. BC fibres are 100 times thinner than plant-derived cellulose and exist in a highly
69 porous three-dimensional network that is highly biocompatible. Macro fibres fabricated from
70 BC nanofibrils are stronger and stiffer, have high tensile strength values and can be used as
71 substitutes for fossil fuel-derived synthetic fibres. The increased surface area to volume ratio
72 allows stronger interactions with the components of composites that are derived from BC. The
73 reactive hydroxyl groups on BC allows various chemical modifications for the development of
74 functionalised BC with a plethora of ‘smart’ applications. In this review we consolidate the
75 current knowledge on the production and properties of BC and BC composites, and highlight
76 the very recent advancements in bulk applications, including food, paper, packaging,
77 superabsorbent polymers and the bio-concrete industries. The process simplicity of BC
78 production has the potential for large scale low-cost applications in bioremediation.
79 Furthermore, the emerging high value applications of BC will be in electrochemical energy
80 storage devices as a battery separator, and in transparent display technologies will be explored.
81 Finally, the extensive biomedical applications of BC are discussed including, wound healing,
82 controlled drug delivery, cancer treatment, cell culture and artificial blood vessels. In a further
83 development on this, additive manufacturing considers enhancing the capabilities for

84 manufacturing complex scaffolds for biomedical applications. An outlook on the future
85 directions of BC in these and other innovative areas is presented.

86

87

88 **Key words**

89 Bacterial cellulose, biodegradable, biocompatible, biomaterial, biomedical devices,
90 bioelectronic materials.

91 1 Introduction

92 We live in an age of advanced materials and currently the emphasis is towards green
93 technologies where the circular economy is driving innovation and bringing new paradigms.
94 Of all the natural polymers, cellulose is known to be the most abundant on the planet. With a
95 primary productivity of plant biomass in the range of 100-125 Gt per year, plant-derived
96 cellulose has received enormous attention as a feedstock for the biobased production of fuels,
97 paper, packaging, as well as biomedical applications [1, 2]. Aside from plant-derived cellulose,
98 cellulose can also be produced by a variety of acetic acid producing bacterial strains belonging
99 to the genera *Acetobacter*, *Gluconobacter*, *Gluconacetobacter* and *Komagateibacter*. These
100 bacteria commonly found in fermented foods such as, vinegar, *nata de coco*, kombucha and
101 rotting fruits are capable of oxidising alcohols, aldehydes, sugar, or sugar alcohols in the
102 presence of oxygen to acetic acid. The species of the *Gluconacetobacter* and *Komagateibacter*
103 genera are known to produce a moist extracellular matrix made of crystalline cellulose as a
104 protection against desiccation and UV damage, also referred to as bacterial cellulose (BC) [3].
105 The high-water absorptivity and gaseous permeability of the BC hydrogel allow the exchange
106 of nutrients and materials required for the bacteria's survival. The unique physicochemical
107 properties of bacteria derived cellulose with equivalent characteristics to plant cellulose has
108 been exploited by humankind in numerous applications discussed in this review.
109
110 Compared to plant cellulose BC is 100 times thinner and exists in a three-dimensional network.
111 This results in an increased surface area to volume ratio allowing for stronger interactions with
112 surrounding components and moieties. The BC microfibrils are arranged in a well-defined 3D
113 web-shaped sequence of monomeric units that are linked by regular β -1,4-glycosidic bonds,
114 providing a high mechanical strength, degree of polymerization, and a higher crystallinity
115 index (80-90%), tensile strength and water holding capacity compared to plant cellulose.

116 BC is an exceptionally versatile biomaterial and of commercial interest due to its natural purity,
117 biodegradability, biocompatibility, and non-cytotoxicity. Patent applications filed on BC
118 worldwide reached 7,371 in 2020. The long-term trend shows that patent applications
119 worldwide have grown every year since 1980. BC offers the possibility of custom-designed
120 cellulose matrices from a highly branched, three-dimensional, reticulated structure suitable for
121 production of high-quality paper, and in contrast for the production of a lamellar structure with
122 less significant branching, to be used for medical applications. The numerous hydroxyl
123 functional groups allow it to be functionalised and used in the development of polymer
124 composites [4]. BC can also be blended or chemically grafted with different biopolymers and
125 nanoparticles to acquire new materials with highly desirable properties. In this review paper,
126 we have described the recent advancements reported in the applications of BC including, bulk
127 applications e.g., food, paper, and the packaging and textile industries. BC has also been
128 investigated as a reinforcement material in the construction industries, for bioremediation
129 applications as well as for cosmetic and electronic applications. Furthermore, we describe the
130 use of BC in biomedical applications for wound healing, antibacterial, controlled drug delivery,
131 cancer treatment, tissue engineering, cell culture, and artificial blood vessel applications; and
132 the advances in additive manufacturing focused on biomedical applications. Finally, the current
133 commercial status of BC products is discussed and an outlook on the future directions of the
134 innovative applications of BC is presented.

135

136 **2 Production of BC**

137 Several cellulose-producing bacteria have been reported including the genera, *Acetobacter*,
138 *Gluconobacter*, *Komagataeibacter*, *Rhizobium*, *Agrobacterium* and *Sarcina*. The most
139 commonly known bacterium for BC production is *Komagataeibacter*
140 (formerly *Gluconacetobacter*) *xylinus*, a Gram-negative obligate aerobic bacterium which can

141 efficiently metabolise a wide range of carbon and nitrogen sources to produce BC [5]. The
142 traditional culture medium used for the production of BC is Hestrin and Schramm (HS)
143 medium, containing glucose, peptone and yeast extract as carbon, and nitrogen sources [6].
144 Studies have shown improvements of the BC yield by the addition of methanol to the HS
145 medium [7] and addition of small amounts of endoglucanase to the production culture. As
146 sustainability is highly sought after, the use of agricultural waste and industrial by-products as
147 low-cost medium for BC production has been investigated [8-10]. In a recent study by Skiba
148 *et al.* [11], BC was produced from oat hulls, an agricultural residue, on a pilot-scale, utilising
149 a symbiotic culture of *Medusomyces gisevii*. The authors pre-treated oat hulls with 2–6%
150 HNO₃ solutions which were enzymatically hydrolysed to yield a sugar rich solution which was
151 utilised as a substrate for BC production. The pilot-scale production from oat hulls resulted in
152 a BC yield of 80.5 tons of 98%-wet hydrogel per 100 tons of oat hulls [11]. Other cheap
153 substrates for the production of BC include corn steep liquor (CSL)-fructose medium [12, 13],
154 date syrup and molasses, food-agro residues and petrochemical waste products [14].

155

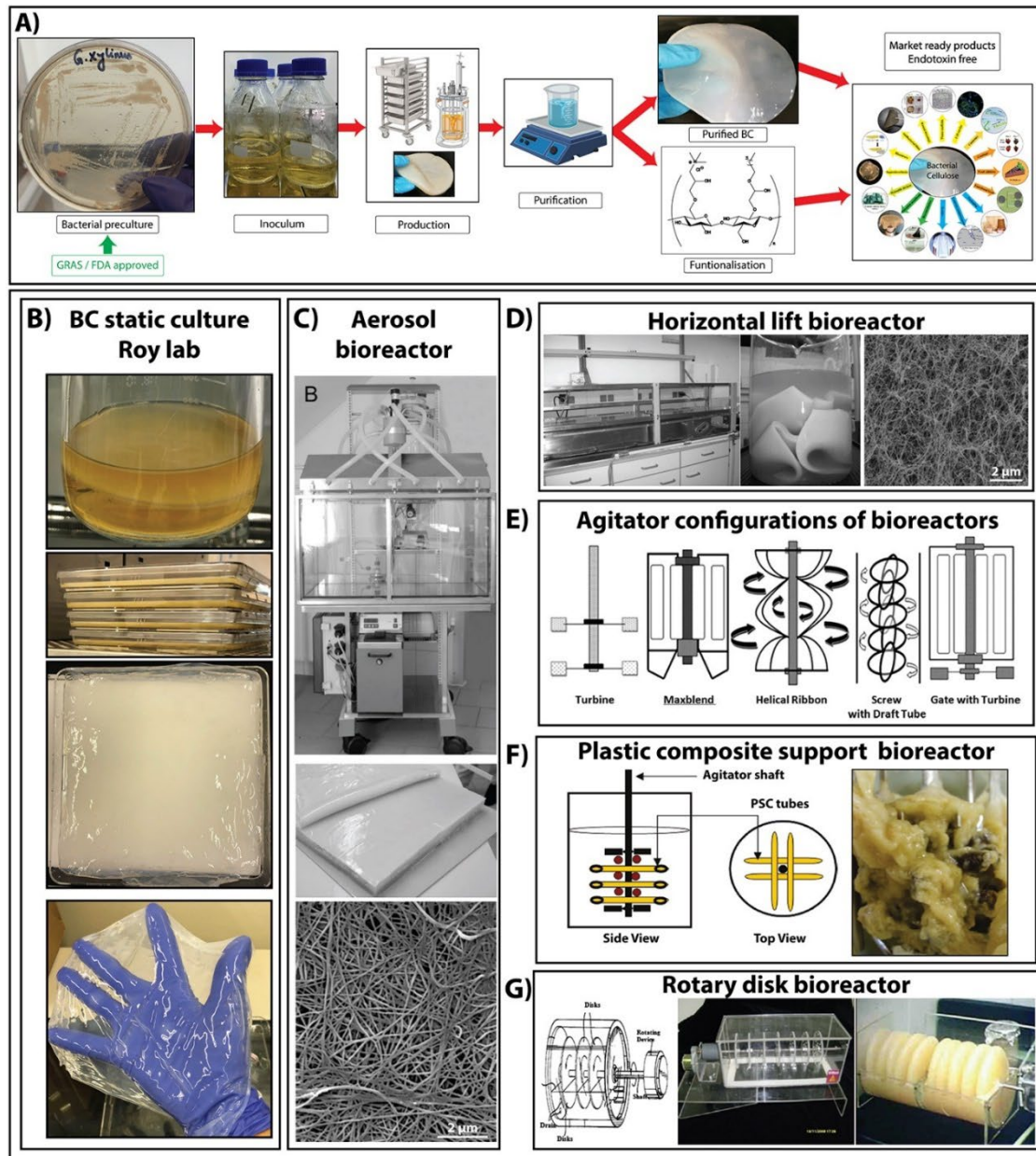
156 The general process required to produce BC from cultivating the organism to the final
157 application product is schematically described in Figure 1 A. BC can be produced under static,
158 agitated or stirred fermentation conditions, resulting in different forms of cellulose. Under
159 static conditions, cellulose microfibrils extruded from the bacteria surface, bundle up to form
160 a pellicle on the air-liquid interface, due to oxygen starvation in the bulk, causing the bacteria
161 to move to the interface, where growth and polymer synthesis occurs [15] (Figure 1 B).
162 However, this static culture method requires large surface areas and long culture periods, which
163 may hinder mass production. Several other bioreactors have been developed that can produce
164 BC pellicles at higher yields under static conditions. These include, aerosol (Figure 1 C) [16]
165 and Horizontal Lift bioreactors (Figure 1 D) [17], and rotary biofilm contactors [18]. In agitated

166 cultivation and stirred fermentation processes three forms of cellulose are produced: fibrous
167 suspensions, spheres and pellets (Figure 1 E-G). It is important to note, compared to the
168 cellulose produced by static culture, BC produced via stirred cultivation methods has been
169 shown to have lower mechanical strengths [19]. Further to this, a lower quantity of BC was
170 reported via the shaking culture method compared to static culture methods, due to the
171 emergence of non-cellulose producing mutants under shaking conditions, thus leading to a
172 decline in the synthesised BC. This phenomenon was observed in *K. xylinus* cells where the
173 uniform aeration of cultures induced cells to grow intensively instead of the polymer synthesis.
174 On the contrary, pellicle formation in stationary cultures limited proper oxygen supply for the
175 cells in the lower parts of the culture. Thus, cellulose producing cells moved towards the
176 oxygen rich medium air-interface which enhanced BC synthesis in static cultures [20].

177

178 This illustrates the importance of considering the target application, to choose the most suitable
179 culture method corresponding to the desirable physical properties of harvested BC. By
180 regulating the cultivation conditions e.g., static or agitated cultivation, the BC microstructure
181 can be custom designed to achieve a distinct fibrillar structure. Agitated cultures result in a
182 highly branched three-dimensional BC pellicle. Static cultures on the other hand result in thick
183 pellicles with less significant branching (Figure 2 F). In this context, if we consider BC-derived
184 from agitated cultures they are useful for applications such as enzyme immobilization [21],
185 adsorption of heavy metal ions, oils and organic solvents [22] due to the high surface area
186 availability for interactions. Furthermore they are applicable as a biocompatible biomaterial for
187 human osteoblast growth [23]. In contrast BC pellicles produced via static cultivations exhibit
188 higher Young's moduli and are widely used for wound dressings [24], membranes and as
189 scaffold material in biomedical applications, discussed further in section (4.5) [25]. The
190 downstream processing involves harvesting of the BC produced from the culture medium and

191 purification of the biopolymer. Harvesting of BC is done manually by simply removing the
 192 pellicle from the surface or by filtering the culture broth containing BC suspensions. By means
 193 of a mild alkali treatment, the cells and other contaminants are removed, and the purified BC
 194 can be used in its native form for numerous applications [26, 27] as described below (Figure 1
 195 A).



197 Figure 1: The production process and various static and agitated bioreactor designs for large-scale BC production.
 198 A) BC producing bacterial cells are propagated aerobically under static conditions. Production can either be done
 199 in stacked trays (produces intact pellicles) or in a bioreactor under agitation (produces spheroids). After 8–10 days
 200 of incubation, BC is harvested, washed with mild and hot alkali. Cell free pristine BC finds applications as a
 201 filtration membrane, as face masks and in making food jellies. BC can also be functionalised with various additives
 202 for diverse applications. (Production and Purification schematic drawings created by Biorender.com) B-G)

203 Production of BC by means of static and agitated fermentation conditions; **B**) BC produced in the Roy Lab under
204 static conditions in tubes, bottles and trays, **C**) BC produced in aerosol bioreactors adapted from [16], **D**) BC
205 produced in horizontal lift bioreactors [28], **E**) BC agitator configurations turbine and maxblend impellers
206 reproduced with permission from [29, 30], **F**) BC produced in a plastic composite support (PCS) bioreactor design
207 adapted with permission from [31], **G**) BC produced in rotary disk bioreactor [29, 32].

208 **3 Material Properties**

209 Cellulose produced by living organisms (native cellulose) can exist in two crystalline forms:
210 *cellulose I* and *cellulose II* (Figure 2A & B) [33]. The majority of native cellulose exists as
211 *cellulose I*, which can be further divided into two different sub-allomorphs I_a and I_b [34, 35]
212 (Figure 2 C & D). Atalla and Vanderhart [34] estimated that the cellulose produced by
213 *Komagataeibacter* contains 60-70 percent of metastable I_a (compared to 30% for plant
214 cellulose), whereas cotton, in contrast, is composed of 60-70 percent I_b .

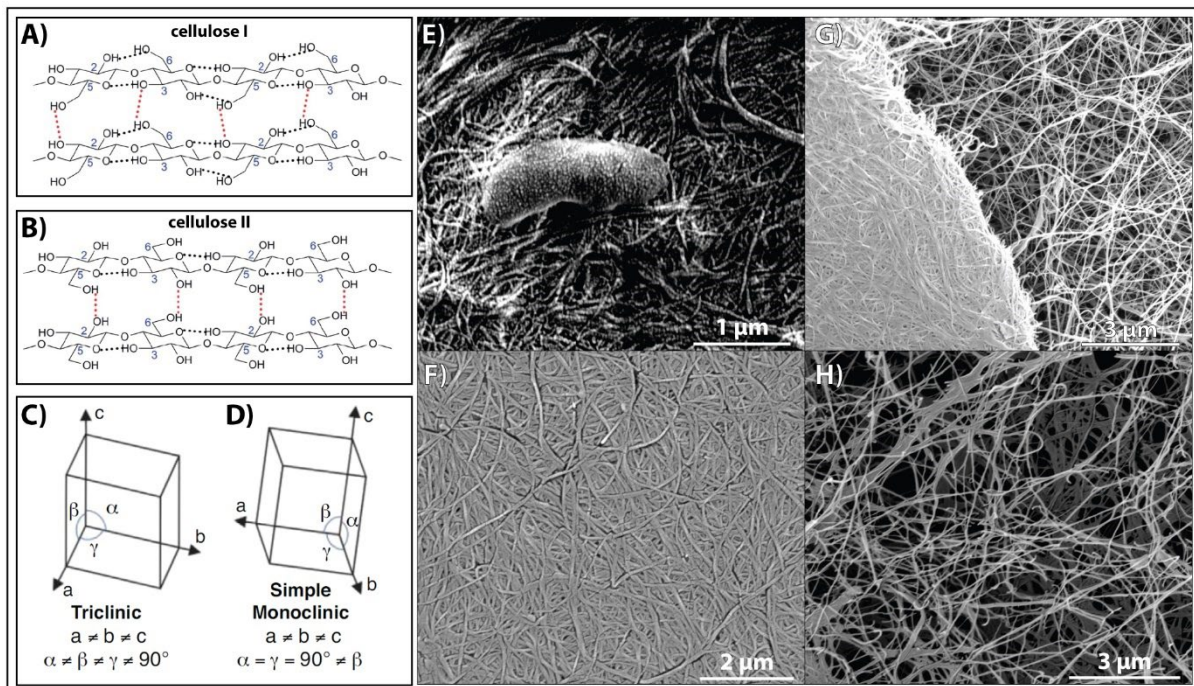
215

216 In static cultures, described above, BC is produced in the form of a mesh of well-defined
217 microfibrils, also referred to as a pellicle [15] (Figure 3E - H). The pellicle consists of a random
218 assembly of microfibrils < 130 nm wide and finer microfibrils, 2 to 4 nm in diameter [36].

219 Although the molecular structure of BC is identical to plant-derived cellulose, the degree of
220 polymerisation (DP) is higher for plant-based cellulose compared to BC, where the DP is
221 13,000 to 14,000 for plant-based cellulose and between 2000 to 6000 for BC [37]. Pure BC is
222 highly crystalline due to the extensive H-bonding and has an open three-dimensional network
223 structure. It is considered a pseudoplastic with fibrils ranging from 25-100 nm in diameter [38].

224 The biosynthesis of BC by *K. xylinus* occurs through the polymerisation of glucose into linear
225 β -(1-4)-glucan chains. The biosynthesis involves four main steps: (i) the phosphorylation of
226 glucose by *glucokinase* (ii) the isomerization of glucose-6-phosphate (Glc-6-P) into glucose-
227 1-phosphate (Glc-1-P) by *phosphoglucomutase* (iii) the synthesis of UDP-glucose by UDPG
228 *phosphorylase* and (iv) and finally the *cellulose synthase* transfers glucosyl residues from
229 UDP-glucose into linear β -(1-4)-glucan chains. [36, 39, 40]. β -(1-4) linked glucan chains are
230 further assembled into an ordered nanostructure called microfibrils of approximately 80 nm

231 [39, 41]. BC has an excellent water holding property and can hold at least 100-fold its own
 232 weight in water. Being polar, it is insoluble in organic solvents. It has high mechanical strength
 233 as evidenced by a high Young's modulus value of up to 30 GPa [42]. The high porosity and
 234 the high surface area make BC highly suitable for impregnation with antimicrobials and other
 235 bio-active compounds, which are discussed in detail in the relevant sections in this review.
 236



238 Figure 2: Chemical structures of cellulose I (A) and II (B) reproduced with permission from [33], C) triclinic crystal
 239 structure of cellulose I α , (D) monoclinic crystal structure of cellulose I β , reproduced with permission from [35],
 240 E-H) Scanning electron microscopy (SEM) micrographs of BC produced under static conditions in H&S media
 241 in the Roy lab; E) *K. xylinus* on the surface of a lab grown pellicle, F) BC fibres as grown in a static culture on
 242 the surface of the pellicle, G) left side showing pellicle surface fibres and right side showing BC fibres below the
 243 surface after being ripped apart H) BC fibres below the pellicle surface.

244

245 3.1 Functionalisation of BC

246 The derivatisation of BC provides the ability to tailor its features and performance, for which
 247 various methods can be adopted to achieve specific functionalities. The modification of BC
 248 can be conducted both *in situ* and *ex situ*, i.e. during the fermentation process or after
 249 biosynthesis.

250 For *in situ* modification, culture conditions are altered through introduction of additives or by
251 changing the carbon source, resulting in the production of functionalised BC or BC-based
252 composites with distinct chemical, physical, mechanical, or morphological features.

253

254 Sun *et al.* demonstrated *in situ* structural modification of BC with the use of sodium fluoride
255 (NaF) to alter the supramolecular arrangement of cellulose fibrils. Increasing concentrations of
256 NaF were added into the culture medium to obtain three different types of membranes labelled
257 as FBC1, FBC2, FBC3 at concentrations of 0.0005%, 0.002, 0.01% (w/v), respectively. At
258 higher NaF concentrations, a lower BC yield was observed with a higher final pH. This is
259 caused by the conversion of glucose into gluconic acid via glucose dehydrogenase enzymes
260 during the fermentation process. This result was ascribed to the formation of hydrofluoric acid
261 (HF), which can easily penetrate through the bacterial membrane and adversely affect their
262 growth. The studies conducted on the hydrogel microstructure by transmission electron
263 microscopy (TEM) showed the formation of smaller and disaggregated microfibrils,
264 proportional to increasing NaF concentration, confirming that HF interferes with the hydrogen
265 bonding network by introducing a competing interaction with the hydroxyl groups of BC. SEM
266 also evidenced lower thicknesses for FBC2 and FBC3, with the pellicles becoming stiffer and
267 denser. In addition to this, a rearrangement of the fibrils occurred upon removal of the fluoride
268 by washing of the membranes, with the fibrils assembling into bulky structures with fibre
269 diameters comparable to those of plant-derived fibrils. This was further corroborated by both
270 a lower degree of crystallinity for NaF-treated BC and a twofold increase in surface area
271 (measured via nitrogen adsorption-desorption) for FBC3 compared to untreated BC. Finally,
272 tensile testing of the materials evidenced increased tensile strengths and Young's moduli as
273 well as a decreased elongation at break (respectively, about four times and six times higher for

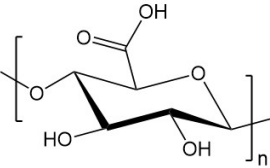
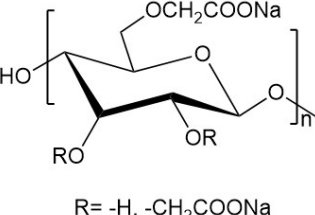
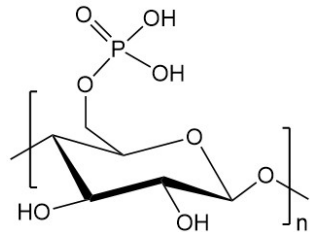
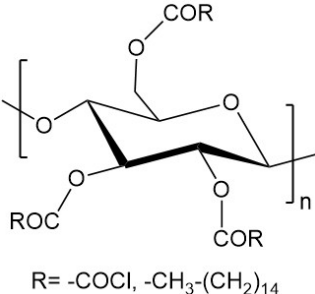
274 FBC3 with respect to untreated BC), ascribed to the rearrangement of the fibrils into bulkier
275 and stiffer ribbons [43].

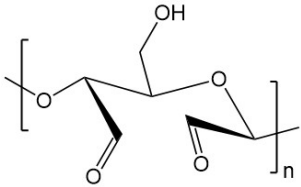
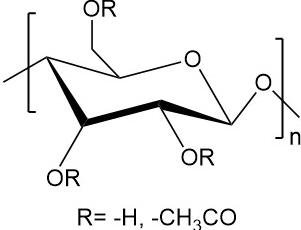
276

277 *Ex situ* modification, on the other hand, is carried out directly on the purified pellicles. The
278 simplest method to achieve this is via physical absorption of active agents. However, without
279 covalent molecular crosslinking, the adsorbed compounds are prone to leaching over time [4].

280 A valid alternative to overcome this problem is the chemical modification of the cellulose
281 structure. Derivatising cellulose interferes with the orderly crystal-forming hydrogen-bonding
282 and promotes the water solubility of even the hydrophobic derivatives. Chemical modifications
283 can be used to introduce charges on the cellulose surface that aids nano-fibrillation. Charged
284 groups generate repulsive forces that weaken the cohesion of H-bonds leading to decreased
285 energy consumption in the polymer processing steps. Specific examples of the BC
286 modifications are listed in Table 1. Chemical modifications of the hydroxyl functional groups
287 include 2,2,6,6-tetramethyl-1-piperidinyloxy (TEMPO) oxidation [44], carboxymethylation
288 [45], phosphorylation, sulfoethylation, acetylation [46-48] and cationisation. In addition,
289 hybridisation with various nanoparticles including, cobalt (Co) [49], copper (Cu) [50], nickel
290 (Ni) [51], gold (Au) [52], silver (Ag) [53], titanium dioxide (TiO₂) [54] and magnetite (Fe₃O₄)
291 [55], surface modifications via adsorption and grafting, and *in situ* shaping during biosynthesis
292 or 3D printing are some of the methods used to functionalise BC [56].

Table 1: Modifications of cellulose nanofibres/BC

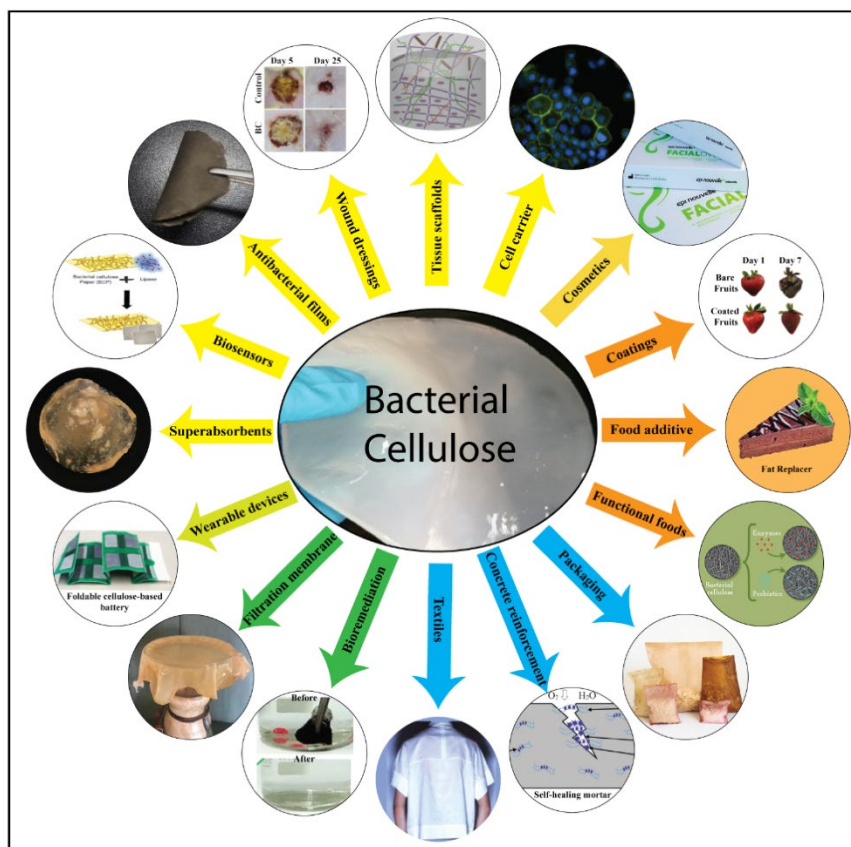
Type of modification	Chemical process	Features	Applications	Chemical Structure	References
Chemical modification of -OH groups	TEMPO oxidation	Introduces charged carboxylic groups at C6 of anhydro- glucose (AGU) units	Bioremediation		[44]
	Carboxymethylation	Monochloroacetic acid reacts with the primary O-6 and secondary O-2 and O-3 hydroxyls groups of the AGU present in BC	Food applications as a thickener, water binder, extrusion aid and film former	 R= -H, -CH ₂ COONa	[45]
	Phosphorylation	Phosphorous linked to two acidic protons is grafted onto the cellulose fibres by impregnating with (NH ₄) ₂ HPO ₄	Orthopaedics, biomedical, textiles or biochemical separation		[57]
	Esterification	Gas-phase esterification of BC with palmitoyl chloride or propionate/acetate using tartaric acid catalyst	Water repellent BC-based materials: cloths, pads, filter paper etc.	 R= -COCl, -CH ₃ -(CH ₂) ₁₄	[47, 48]

Chemical modifications of native BC by ring opening	Periodate oxidation	Introduces aldehyde functions on cellulose chains. Oxidation of OH groups at the C2 and C3 positions results in the formation of aldehyde groups by breaking the C–C bond	Bioabsorbable material for dental medical application	 The diagram shows a repeating unit of a cellulose chain in its cyclic pyranose form. The C2 and C3 positions are oxidized, resulting in aldehyde groups. The C2 carbon is bonded to a hydroxyl group (OH) and an aldehyde group (CHO). The C3 carbon is bonded to an aldehyde group (CHO) and a hydroxyl group (OH). The chain is represented by brackets with a subscript 'n'.	[58]
Surface modification of native BC by adsorption	Adsorption of polyelectrolytes	Regular layers of bacterial nanocellulose (BNC) and polyelectrolyte are formed depending on the polyelectrolyte structure.	Biocompatible drug delivery system	NA	[59]
	Adsorption of hydrophobic polymers	The adsorptions of polystyrene and polytrifluoroethylene from aprotic solvents	Nanopaper for electronics, composites, solvent nanofiltration	NA	[60]
Molecular grafting of BC	Acetylation with toluene and acetic anhydride	Hygroscopicity of BC in composites is reduced, while maintaining their high optical transparency and thermal stability. Acetylation also imparted hydrophobicity	Bionanofibre composite for optoelectronic devices	 The diagram shows a repeating unit of an acetylated cellulose chain. The hydroxyl groups at the C2, C3, and C6 positions are replaced by OR groups. The chain is represented by brackets with a subscript 'n'. Below the structure, it is noted that R = -H, -CH ₃ CO.	[46, 61]
Polymer grafting of BC	Polymerisation	BC is mixed with a monomer and an initiator and then polymerisation is induced at the surface	Antimicrobial BC nanocomposites for wound dressing materials, superabsorbent hydrogels for drug delivery	NA	[62, 63]

295 4 Applications

296 In the following sections, we introduce the vast array of applications for which BC can be
297 extensively utilised (see Figure 3) spanning bulk applications such as food, paper, packaging,
298 textiles and bioconcrete as well as bioremediation, cosmetics, electronics and sensing
299 applications. Biomedical applications are discussed in detail encompassing wound healing and
300 antibacterial wound dressings, controlled drug delivery, cancer treatment, tissue engineering
301 and cell culture, as well as artificial blood vessels. Further, the fabrication of complex structures
302 aided by 3D printing approaches is considered with a focus toward biomedical applications.

303



304

305 Figure 3 The diverse areas of applications of BC. Antibacterial films: BC/graphene oxide-CuO nanocomposite
306 film [64]; Bioremediation: copper coated cellulose aerogels can selectively remove drops of aqueous Sudan III
307 dye in trichloromethane within seven seconds [65]; Cell carrier: dermal fibroblasts and epidermal keratinocytes
308 attached to the BC/Acrylic acid hydrogel [66]; Concrete reinforcement: the high porosity of cellulose fibres helps
309 to absorb water and oxygen and also provides space for the bacteria to grow and heal the crack in concrete [67];
310 Coatings: cellulose nanocrystals reinforced poly-albumen coatings on fruits prolonged the shelf life of
311 strawberries [68]; Cosmetics: pristine BC is used a face mask to support the regeneration of sensitive skin
312 (www.Jenacell.com); Electronics: cellulose-based foldable batteries [69]; Food additives and functional foods: as
313 a US FDA approved dietary fibre BC finds numerous use in the food industry [70]; Filtration membrane: a
314 symbiotic consortium of yeasts and bacteria can act as a living water filtration membrane for gravity filtration
315 [71]; Paper/Biosensors: bioactive paper made with lipase/BC nanocomposite can be used in point-of-use testing
316 devices [72]; Packaging: organic wastes can be converted to BC as an alternative to the single-use plastic

317 packaging (www.julianajschneider.com); Scaffolds: Interpenetrating polymeric hydrogels made with BC
318 exhibited excellent mechanical properties to repair the osteochondral defect [73]; Superabsorbents: BC
319 crosslinked with polyethylene glycol diacrylate and carboxymethyl cellulose [74]; Textiles: BC can be produced
320 in any desirable garment panel shape [75]; Wound dressing: Polydopamine coated BC with *in situ* reduction with
321 silver promotes wound healing [76]. Yellow arrows denote medical applications, cosmetics, and wearable devices;
322 orange arrows denote food and food additives; blue arrows denote industrial applications and green arrows denote
323 bioremediation applications.

324

325 4.1 Bulk Applications

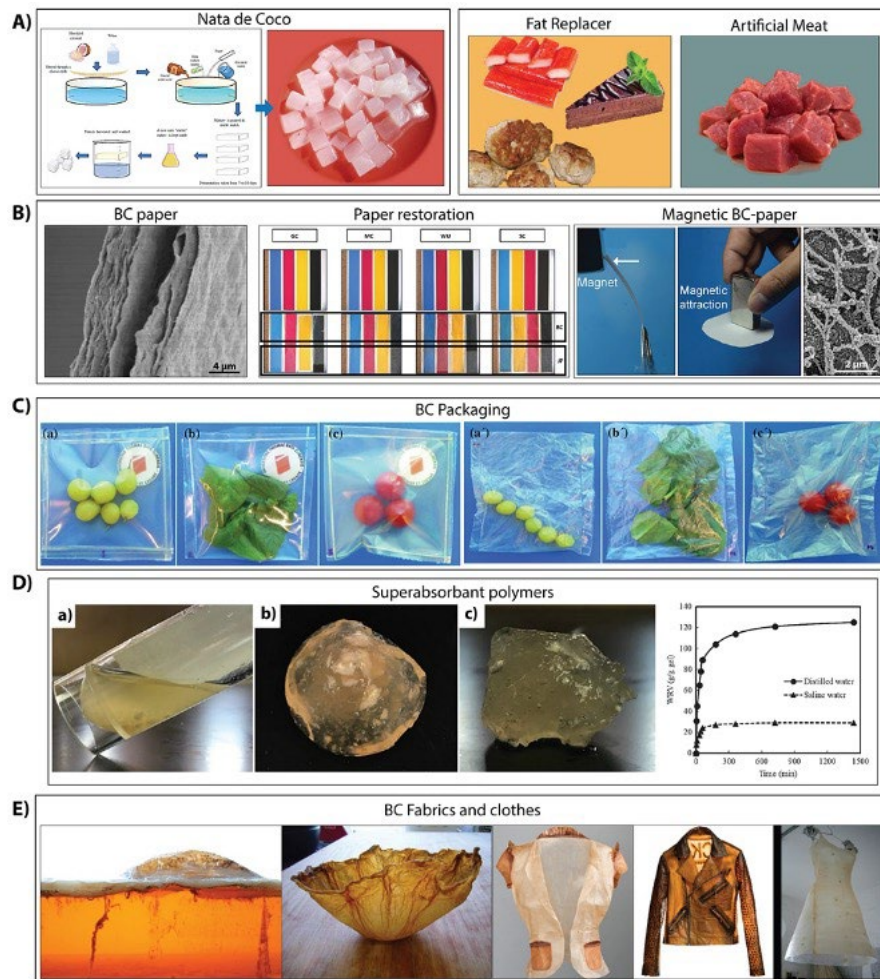
326 4.1.1 Food

327 The superior water-holding capacity, high purity and low-calorie dietary fibres of BC make it
328 an edible biopolymer. Combined with other food ingredients, BC thus has high potential value
329 in the food manufacturing industry [77]. BC is known to be a fibre rich natural food [78] which
330 offers an extensive range of health benefits including a reduction in the risks of chronic diseases
331 such as diabetes, obesity, and cardiovascular ailments, for these reasons, BC was granted
332 ‘generally recognized a safe’ status by the Food and Drug Administration in 1992 [32, 78].

333

334 As previously described the high water-holding properties of BC along with its gelling,
335 thickening and stabilizing properties make it an ideal candidate for food products such as,
336 yoghurt, pastries and salads [78, 79]. The addition of BC to processed foods can preserve their
337 sensorial and original properties for a longer period due to the ability of BC to hold water
338 without distorting the integrity of its shape. Unprocessed BC has a tasteless and hard texture,
339 however when processed with sugar alcohols the texture becomes softer, resembling that of
340 grapes whereas treatment with alginate and calcium chloride modifies its texture to mimic that
341 of squid [79]. Okiyama *et al.* (1993) demonstrated that the addition of BC gel improved the
342 quality of food hydrocolloids, due to its high tensile strength. The authors further demonstrated
343 that BC could be applied as a suspension agent or filler to stabilise foods and improve their
344 integrity, especially to reinforce fragile food hydrogels [80]. In this context, BC-soy protein
345 isolate (SPI) was applied as a stabilising agent to improve the stability and texture profile of

346 ice creams. The effectiveness of the BC/SPI blend could be attributed to the interactions
 347 between the protein molecules and cellulose via hydrogen bonding, Van der Waals forces and
 348 hydrophobic interactions [81]. The low-calories associated with BC offer health benefits when
 349 used to replace the fat components of meats or as a non-caloric bulking agent in jams [80]
 350 (Figure 4A).



351
 352 Figure 4 A) (left) Schematic production of Nata de coco production process reproduced with permission from
 353 [77] (right) fat replacement and artificial meat based on BC reproduced with permission from [70], B) **BC paper**:
 354 reproduced with permission from [82]; **Paper restoration**: reproduced with permission from [83]; **Magnetic BC-**
 355 **paper**: adapted with permission from [84]. C) BC packaging for food, reproduced with permission from [85], D)
 356 Morphology of hydrogels (a, b) crosslinked with PEGDA and (c) without PEGDA at CMBC-g-GMA
 357 concentration of (a) 2 wt% and (b, c) 5 wt%, reproduced with permission from [74] E) BC produced textiles and
 358 fabrics reproduced with permission from BioCouture designed by Suzanne Lee.

359
 360 Another example is the use of BC as the main ingredient for the production of *Nata* (Figure
 361 4A), a sweet native dessert of the Philippines [77]. *Nata de coco*, is a cube shaped delicacy in

362 the *Nata* family that is produced by soaking a specially fermented BC in sugar syrup (Figure
363 4A). The BC used here is obtained via fermentation of *K. xylinus* using different carbohydrate
364 substrates, coconut water and amino acids [32, 70, 77]. *Nata* has a smooth texture feel in the
365 mouth, is simple to manufacture and is considered healthy, this has contributed to its increased
366 popularity around the world [78].

367

368 Probiotics are gaining prominence for their ability to improve digestion by improving the gut
369 microbiota, however, their short shelf-life and instability often limit their application [70, 86].
370 In view of this, researchers have been experimenting the possibility of encapsulating
371 biocompatible and antibacterial materials into probiotics to enhance the latter's long term
372 storage conditions, their resistance to adverse processing conditions, as well as protection from
373 acidic conditions in the gastrointestinal tract (GI). The high crystallinity, biocompatibility, non-
374 toxicity and nanoscale properties make BC a suitable nanomaterial for encapsulation of
375 probiotics. In this context Khorasani and Shojaosadati [87] observed that a composite of pectin
376 and BC preserved *Bacillus coagulans* and extended its shelf life. The authors demonstrated that
377 a 20% and 80% combination of pectin and BC respectively, was an optimal composite that
378 produced the highest survival rate of *B. coagulans* of about 99.43% after microwave drying. In
379 another study BC was used for encapsulating *Lactobacillus acidophilus* 016, enhancing
380 survival rates of the probiotic strain up to 71.1% [88]. Thus, BC can be used as an encapsulating
381 agent to extend the shelf lives of probiotic microorganisms.

382

383 Biopolymers have potential as multifunctional bio-based coatings for active packaging. Bio-
384 polyesters such as poly(3-hydroxybutyrate) (P(3HB)) offer the best opportunities as
385 thermoplastic materials that can be processed by continuous extrusion coating. However, the
386 thermal degradation of P(3HB) at elevated temperatures are assumed to be mainly due to the

387 random polymeric chains of P(3HB), which limit its processing temperature window. The
388 mechanical and thermal instability of P(3HB) can be improved by adding additives or
389 producing blends with other polymer matrices or micro- to nanoscale fillers. When well
390 dispersed in the polymer matrix, fillers can improve the thermal and mechanical properties of
391 P(3HB) due to the improved interactions between filler and polymer matrix. Nanomaterials
392 such as cellulose fibres can be applied in small amounts as fillers to improve the required
393 surface properties. The cellulose fibrils can be isolated from the native cellulose fibres by
394 intensive mechanical treatment grinders and homogenizers or involving high pressure
395 homogenizing systems such as a microfluidizer. Other biopolymers can be applied by
396 dispersion and solvent casting, which may offer the possibility of the application of very thin
397 coating layers with highly specific properties. Chitosan is a linear polysaccharide derived from
398 chitin and can be used as a pre-coating on paper to provide better bonding and a more uniform
399 surface for the application of an additional biopolymer, such as P(3HB) layer, by extrusion
400 coating. Chitosan films reinforced with bacterial cellulose (BC) nanoribbons could improve
401 mechanical and chemical properties of the films, suitable for development of new materials for
402 the food packaging industry [89].

403 404 **4.1.2 Paper**

405 The global impact of the paper industry to deforestation have resulted in the ambition to find
406 alternative ways to produce paper from eco-friendly and sustainable resources. Thus, an
407 emerging trend of recycled papers and non-woody fibres forming constituent raw materials for
408 paper and pulp production is becoming more popular. In 2014 it was reported that 58% of paper
409 produced globally was recycled [90], however the biggest challenge for recycled paper is to
410 maintain original physical and mechanical attributes. The current main non-woody sources for
411 paper are sugarcane bagasse, reeds, bamboo, cereal straw and reeds accounting for only 6.5%
412 of the entire pulp produced annually [90], however, the physical properties of these papers are

413 inferior to traditionally produced paper. As previously discussed BC has the ability to improve
414 mechanical properties of materials it is combined with and is hence a suitable candidate for
415 producing high quality paper or pulp sustainably [91]. In this context Vandamme *et al.*
416 demonstrated BC to be an ultra-strength additive in papermaking due to its fine interwoven
417 smooth fibre network [92]. The unique super-molecular structure of BC due to hydrogen bonds
418 results in a Young's Modulus above 15 GPa, providing these remarkable mechanical
419 properties. BC has been actively used in papermaking since the later part of the 1980s either as
420 a whole or in combination with the traditional and non-traditional sources producing high
421 quality, strong paper [93]. Modified BC has also demonstrated potential in the production of
422 specialized and fire resistant papers [90].

423

424 BC possesses the required characteristics to reinforce degraded papers due to its high
425 crystallinity, high Young's modulus, low internal porosity and long-time stability, thereby
426 making BC an ideal candidate material in papermaking [82].

427

428 A study by Gomez *et al.* [83] assessed BC in the restoration of damaged or degraded paper by
429 observing the variation in visual appearance of printed papers coated with BC and Japanese
430 paper (JP), as shown in Figure 4 B. Very commonly, damaged papers are reinforced by lining
431 with JP. Four different types of commercial papers coated and uncoated including the glossy-
432 finished (GC), the matte-finished (MC), the wood-free uncoated paper (WU) and the super-
433 calendered paper (SC), were printed with cyan, magenta, yellow and black inks. All samples
434 were reinforced with JP and BC sheets. It was expected that the reinforcing material will
435 consolidate the paper properties without changing its visual appearance. JP-lined paper showed
436 a reduction in the print density to >0.5 density points while, the value only slightly decreased
437 to <0.05 for the BC-lined paper. By subjecting the samples to an aging process, BC-lined paper

438 exhibited a significant advantage over JP coated paper, for the restoration of paper, with only
439 slight changes in colour and appearance [83].

440

441 In another study by Jing *et al.*, plant fibres doped with propylene were enhanced by uniformly
442 dispersed fibres of BC to produce tougher paper. A composition containing 3% BC yielded the
443 optimal physical properties for ultra-strong long fibre paper, which showed an increase in
444 tensile index by 12.6%, tear index by 10.1% and bursting index by 7.82% [94].

445

446 Further applications of BC have been used in the development of magnetic papers or magnetic
447 membranes for anti-counterfeiting applications (see Figure 4 B). Sriplai and co-workers
448 fabricated white magnetic paper from a composite sandwich structure that comprised a
449 magnetic BC, which was prepared by incorporating CoFe_2O_4 nanoparticles (NPs) into the
450 structure of BC and a ZnO NPs doped BC via a hot pressing and nanocomposite procedure.
451 The papers exhibited a whiteness of 75–85%, which correlated to a high reflectance in the
452 visible spectral range. Additionally, the white magnetic paper exhibited physical and
453 mechanical features like flexibility, foldability, and rollability similar to the traditional paper
454 [84]. The current drawback, of utilising BC for these applications, however, is the high cost
455 associated with the production of BC and therefore the current research focus is to produce BC
456 more cost effectively. A good starting point for this are the previously mentioned bioreactors
457 as well as the use of waste materials as substrates for the fermentation process.

458

459

460 **4.1.3 Packaging**

461 The global demand for goods and services continue to increase as human activities increase
462 because of rapid population growth. This has caused an explosive growth in the use of plastic
463 packaging. However, the undesirable consequences of petrochemically derived or synthetic

464 plastics have prompted campaigns for reduction and potential elimination in their utility where
465 possible. The impact of non-degradable solid waste in the environment e.g., the oceans and
466 landfill, has prompted a rigorous search for sustainable and eco-friendly solutions in the area
467 of packaging. It has been reported that petroleum based plastics constitute the third largest
468 volume of municipal waste, out of which, only 3% gets recycled [95]. Essentially, the toxic
469 effect of the accumulation or incineration of these wastes and the safety requirements for food
470 materials have shifted attention to biodegradable resources or bioplastics for packaging
471 solutions.

472

473 Cost-effective and green packaging can reduce food waste [96] and decrease carbon emissions
474 [97]. 40–50% of fruits and vegetables are wasted every year and efforts have been made to
475 preserve the freshness of fruits. Bio-based films and coatings are membranes principally
476 consisting of a macromolecule matrix and a plasticizer or other components that are usually
477 applied to reduce the inherent brittleness of some bioplastics and improve their mechanical and
478 barrier properties [98]. It has been reported that pure albumin coatings crack when dried owing
479 to the random organisation of the protein chains. Glycerol has been used as a plasticizer to
480 increase the mobility and flexibility of the albumin protein chains by reducing the
481 intermolecular forces between them. However, glycerol coatings swell in humid environments
482 owing to their hydrophilic nature. Jung *et al.* (2020) prepared an edible and washable
483 micrometre thick coating composed of egg-albumin (54%) and plant derived cellulose
484 nanocrystals that can increase the shelf life of fruits [68]. Coating on papayas, avocados,
485 bananas, and strawberries revealed increased shelf life of fruits while maintaining the flavours
486 of the fruits. The albumen-coating thus served as an oxygen barrier and preserved the freshness
487 of the fruit. To bring mechanical reinforcement, cellulose nanocrystals (CNCs) were
488 incorporated, and this further decreased water and gas permeability of the coating material. The

489 film maintained the flexibility, allowing it to be repeatedly bent and folded without breaking.
490 Addition of a small fraction of egg yolk to the mixture alleviated the susceptibility to moisture.
491 In addition, including curcumin during the coating process imparted antibacterial, antifungal
492 and antibiofilm properties to the coated surface. The CNCs used in the study were derived from
493 plant cellulose material which requires pre-treatment before cellulose can be dislodged from
494 lignin and the hemicellulose network. Here, the plant-based cellulose could easily be replaced
495 with bacteria-derived cellulose, which is naturally 100% pure and does not require any pre-
496 treatment, saving on energy and operation costs.

497

498 Food-packages function as containments to protect food from the risk of contaminating agents
499 such as oxygen, microorganisms, water vapour, and off-flavours and thus extend the shelf life
500 of food. In the last decade, researchers have explored the suitability of BC or BC composites
501 as food-packaging materials with additional benefits such as antimicrobial properties to ward
502 off spoilage microorganisms, similar to the previously mentioned food coatings. Many studies
503 have confirmed that the presence of antimicrobial agents of natural origin in food packaging
504 systems prolong the shelf lives and maintain the quality of food [99]. Stroescu *et al.* (2019)
505 reported that antimicrobial food pads made from superabsorbent materials like bacterial
506 cellulose and its derivatives are able to conserve the sensorial attributes of packaged foods,
507 such as fruits, vegetables and meat products that otherwise, have the tendency of generating
508 exudates while in storage [100]. Being food-grade, BC could also provide edible packaging
509 with unique nutritional and suitable physical and mechanical characteristics [101].
510 Furthermore, BC-based films have been treated with natural flavours such as fruit purees, and
511 used as snacks or wraps for non-traditional sandwiches and sushi [98].

512

513 One major hindrance impeding the commercial implementation of bio-based food packages is
514 that biopolymers fall short of the versatility of synthetic polymers [100]. Thus, current research
515 focuses on addressing this by forming various blends and polymer composites that could
516 imitate the versatility of synthetic plastics depending on the requirements of the application of
517 interest. It is important to note that for hygiene requirements, some edible films and coatings
518 may require complementary outer packaging. Pradrao *et al.* (2016) incorporated bovine
519 lactoferrin (bLF) into bacterial cellulose. Using a highly perishable fresh sausage as a prototype
520 meat product, the modified BC-bLF films were tested for their potential use in antimicrobial
521 edible packaging. The BC-bLF films were characterized in terms of cytotoxicity, water vapour
522 permeability (WVP), mechanical characteristics and antibacterial potency against two food
523 spoilage microorganisms, *Staphylococcus aureus* and *Escherichia coli*. The films were found
524 to be non-toxic on the meat product, exhibited bactericidal properties against the food
525 pathogens and possessed suitable technological attributes for their use as bio-based meat
526 product wrapping [102].

527

528 Thermoplastic corn starch (TPCS), nanobiocomposites comprising of bacterial cellulose nano-
529 whiskers (BCNW) were developed by direct melt mixing and its physical properties like
530 morphology, barrier and tensile strength were subsequently obtained. The morphological
531 studies demonstrated that up to 15 wt% loading of the BCNW dispersed properly into the TPCS
532 matrix led to an improvement in barrier properties. In addition, the incorporation of BCNW led
533 to the stiffening of the nanocomposite resulting in an increase in its elastic modulus. The
534 authors also described the innovative coating of the nanocomposite films with electrospun
535 P(3HB) fibres, forming multi-layered structures that were found to significantly improve
536 barrier properties of the films, making them useful systems in the packaging of foods [103].
537 Salari *et al.* (2018) developed a nanocomposite comprising chitosan, nanocrystals of bacterial

538 cellulose and silver nanoparticles (AgNPs). The BC nanocrystals (BCNC) were obtained using
539 acid hydrolysis. The results showed that the incorporated BCNC and AgNPs significantly
540 influenced the colour and transparency of the chitosan films. Additionally, the mechanical
541 attributes of the nanocomposite improved significantly as well as its water vapour permeability
542 and sensitivity to water. Besides, it was revealed that the nanocomposite film manifested
543 considerable antibacterial activity against food borne pathogens suggesting that BCNC/AgNPs
544 containing nanocomposite films can be applied in active food packaging to increase the shelf
545 life of foods [104].

546
547 Bandyopadhyay *et al.* (2018) determined the physico-chemical, mechanical and bio-adhesive
548 properties of ‘neat BC’ and various combinations of polyvinylpyrrolidone (PVP) and
549 carboxymethyl cellulose (CMC) with bacterial cellulose as the base polymer. They further
550 investigated the potential application of the ‘neat BC’ and composite polymers in food
551 packaging. The mechanical tests revealed that ‘PVP-CMC-BC’ films had the highest tensile
552 strength as well as lowest elastic properties among ‘PVP-BC’ and ‘neat BC’ samples.
553 Additionally, ‘PVP-CMC-BC’ was shown to endure longer stretching and exhibited the fastest
554 deformation rate. Elasticity and deformity are key considerations when selecting materials for
555 food packaging. However, the authors found ‘PVP-CMC-BC’ films an ideal novel, green
556 packaging material due to their superior tensile properties, printability and transparency [105].

557 Zahan and co-workers (2020) incorporated lauric acid (LA) into bacterial cellulose (BC) films
558 and successfully developed biodegradable and antimicrobial (AM) material that has potential
559 applications in the food, medical and pharmaceutical fields. Degradation studies, of samples
560 buried in soil, showed that by the seventh day, *Bacillus sp.* and *Rhizopus sp.* were responsible
561 for the complete degradation of BC. The study revealed that the addition of LA improved the
562 functionality of the BC films by effectively inhibiting the growth of *Bacillus subtilis*. This

563 model BC film proved to be a good candidate to replace synthetic plastics in packaging
564 activities [95].

565

566 In a similar development, Yordshahi *et al.* (2020) designed a BC based antimicrobial packaging
567 using postbiotics of lactic acid bacteria as an active ingredient and demonstrated its potential
568 use as antimicrobial meat wrapping. Films of the BC / postbiotics composite (BC/P) were tested
569 for their antimicrobial activity against *Listeria monocytogenes*. Anti-listeria activity of BC/P
570 films was directly affected by the concentration and impregnation time of the film production.
571 The study also found that following the wrapping of the meat with the films, postbiotics were
572 instantly soluble on the meat surface, coupled with a quick hydration of the BC which resulted
573 in a rapid release of postbiotics into the meat. Such a rapid release of active factors is
574 particularly ideal for foods with finite shelf lives like ground meat as this can effectively control
575 pathogen growth and significantly improve the overall shelf life, while maintaining the sensory
576 attributes of food [106].

577

578 **4.1.4 Superabsorbent polymers**

579

580 The basic human needs for absorbent materials have not changed over the years but how those
581 needs are met have changed considerably. Superabsorbent polymers (SAPs) had a market value
582 of USD 120 billion in 2016 which is expected to grow annually at a rate of 6% to reach about
583 203 billion by 2025 [107]. There is a high demand for diapers, female hygiene products, adult
584 incontinence products, as well as applications in agriculture for controlled release of fertilisers
585 [108] and absorbent systems for wearable artificial kidneys [109].

586

587 The scientific way to describe SAPs are xerogellants: xero meaning a dry material and gellant
588 is the abbreviation for gelling agent. To qualify as a superabsorbent, the dry material must

589 spontaneously imbibe about twenty times its own mass of a liquid. Whilst undergoing this
590 2000% change in volume, the swelling material retains its original identity. The measure of
591 this property is termed as absorbency under load. It describes the amount of physiological
592 saline contained in 1 g of SAP under specified pressure. However, most studies report the
593 swelling in water and not in saline. Currently the most used SAPs are produced from non-
594 renewable and non-biodegradable polymers, therefore increased interest in biodegradable and
595 natural polymers for SAP development is attracting attention [110, 111]. The microbial
596 fermentative production of BC thus makes it an attractive material in the category of SAPs.

597

598 The production of SAPs is a three-step process: **functionalisation** (of the carbohydrate),
599 **crosslinking** and **drying**. Functionalising via etherification or esterification (of hydroxyl
600 groups present in the polysaccharide) allows the formation of water-soluble polysaccharide
601 derivatives. It was determined that solvent evaporation of the hydrogels via freeze-drying
602 produces a microporous structure which however collapses during the formation of the 3D
603 structure. In contrast, drying by means of a supercritical carbon dioxide method maintains the
604 micro and nanostructure effectively. Swelling ratios larger than 500 times the initial mass, in
605 less than an hour, have been achieved through careful choice of crosslinking agents combined
606 with structure retaining, eco-friendly, drying methods [74, 112] (Figure 4 D). A summary of
607 BC modifications employing various crosslinkers and drying agents to produce SAPs is given
608 in Table 2.

609

610 **Table 2:** Summary of selected BC modifications for use as SAPs

Substrate	Crosslinker	Drying agent	Swelling ratio (%)	Maximum absorbency (g/g in distilled water)	Reference
Carboxymethylated and glycidyl methacrylate functionalised BC	Polyethylene glycol diacrylate	Air	12,500*	125	[74]
BC	Citric acid using disodium phosphate and sodium bicarbonate as a catalyst.	Air	3,300	33*	[113]
BC	2-aminoethyl methacrylate, <i>N,N</i> -methylene bis-acrylamide (MBAA)	Air	6,200	62*	[62]
BC	MBAA with potassium persulphate as the initiator	NA	2,500	25*	[63]
BC generated by <i>in situ</i> fermentation on bentonite inorganic gel	<i>N, N'</i> -methylenebis-acrylamide (NMBA)	Oven dried at 80 °C	35,800*	358	[114]
BC grafted acrylic acid copolymer	NMBA	lyophilisation	33,200*	332	[115]

611 * Calculated values

612

613 4.1.5 Textiles

614

615 The most common fibres used in the clothing industry are synthetic and hence not

616 biodegradable. Therefore, it is important to introduce eco-friendly fabrics in the textile

617 industry. Natural and biodegradable BC fibres can be used for textiles given their suitable

618 physicochemical and mechanical properties (Figure 4 E). In this context effort has been put

619 towards the improvement of flexibility of BC, especially after dehydration. Fernandes *et al.* for

620 instance, proposed a method to incorporate two commercial polymers into the structure of BC
621 to achieve this. Here, a softener (S), e.g. polydimethylsiloxane and a hydrophobiser (H),
622 fluorocarbon polymer aqueous nano-emulsion (non-ionic), were absorbed into the matrix by
623 exhaustion, which is a common treatment for textile materials. This process involves placing
624 the fabric in an aqueous solution containing e.g. the dye in a sealed chamber under predefined
625 temperatures and incubation times [116]. Fernandes *et al.* produced various composites, either
626 by exhaustion with S or H at increasing concentrations as well as by exhaustion with S followed
627 by drying and impregnation with H. SEM analysis showed higher mass per unit and surface
628 coverage for the treated samples compared to pure BC, with the softener-modified composites
629 showing the largest change. In addition, mechanical tests evidenced higher elongation at break
630 for higher amounts of additives, assumed to be due to greater mobility of fibrils and weakening
631 of intermolecular bonding of cellulose. Furthermore, higher hydrophobicity was observed, with
632 average water contact angles of about 130° compared to 64° for native BC. Finally, despite the
633 increased thickness of the composites, a porous structure was maintained, as confirmed by the
634 water vapour permeability values, which are in line with footwear materials ($\geq 192 \text{ g}\cdot\text{m}^{-2}$,
635 24 h), and static water absorption results, with <60% absorption for the higher concentrations
636 of both H and S and >100% for the other compositions, making them suitable, respectively, for
637 the development of uppers and linings/insoles [117].

638

639 In another study, Kamiński *et al.* described the use of glycerol to improve the flexibility of BC
640 and stearic acid to protect from moisture. In this case, BC was obtained from the fermentation
641 of a SCOBY (i.e. symbiotic consortium of bacteria and yeast, generally known as kombucha
642 culture), which consists of a combination of various species of yeast and bacteria producing
643 BC under static or dynamic brewing conditions. The composites were prepared by immersion
644 into a glycerol solution and application of stearic acid with a brush, followed by high

645 temperature treatment to achieve a homogenous coating. A significant increase in elongation
646 at break and tensile strengths was demonstrated when comparing treated to untreated samples.
647 The produced composites were then used to produce two proof of concept clothing articles,
648 namely a wristband and a cotton/BC T-shirt. The aim of this study was to produce clothes for
649 astronauts, enabling them to fully recycle their used clothes [118].

650

651 The produced textiles were then subjected to machine sewing, exposure to water and worn by
652 volunteers in space station simulated conditions for two weeks. Data indicated that there was
653 no evidence of microbial colonisation of the fabrics and no adverse skin irritations with the
654 participants. Furthermore, although a loss of flexibility was registered, the treated BC did not
655 show any evidence of tear, unlike untreated BC fabrics. Finally, participants evaluated the
656 textiles based on softness, smell, visual appearance, flexibility and sweat absorption, giving
657 them overall good or neutral responses, indicating that treated BC can be used as a green and
658 waste-free textile [118].

659

660 **4.1.6 Bioconcrete**

661

662 The need for eco-efficient construction materials heralded new frontiers in concrete technology
663 by employing materials with multifunctional properties [119]. Nanoparticles have been
664 extensively used for decades, promoting cement hydration, reinforcement, and densified
665 microstructures, leading to reduced porosity and increased mechanical strength. In this regard,
666 nanocellulose materials are an emerging class of non-toxic and green material with
667 multifunctional properties [120]. The intrinsic hydrophilic and hygroscopic nature of cellulose
668 nano fibres (CNF), together with their tendency to form a percolating network enables them to
669 be used as viscosity modifying agents in self-consolidating concrete [121]. CNFs possess large
670 surface areas and display strong interactions between their surrounding slurry materials [122].

671 However, the production of CNF is an expensive process; this is where the production of BC
672 via simple fermentation can potentially replace CNF.

673

674 Application of bacterial nanocellulose (BNC) coatings on natural fibres has been an effective
675 way to alter fibre-matrix interactions [123, 124]. BNC coated bagasse fibres (0.1 wt%)
676 displayed increased surface energy (owing to its crystalline nature) and increased roughness,
677 properties that are vital for the surface behaviour of nanoparticles. The increased surface –OH
678 groups and increased O/C ratio demonstrated enhanced interfacial adhesion leading to an
679 increased modulus of elasticity compared to natural bagasse (5.2 GPa vs 4.7 GPa) [123]. The
680 close spacing of BNC, their increased presence at crack tips, as well as their high aspect ratio
681 makes them efficient in stabilising and suppressing cracks [125]. BNC cement composites
682 exhibited a higher fracture toughness that enables a cracked concrete material to resist fracture
683 longer. Decreased fibre mineralisation offered by the protective layer of BNC limits the
684 permeation of alkali ions in the cement slurry into the fibre lumens, thus stabilising the cracks
685 [123]. BNC coating accelerated the hydration in the fibre cement interface improving
686 mechanical interlocking of the internal structures. BNC can substitute plant derived cellulose
687 fibres as a bacterial immobilising agent in self-healing concrete. It is therefore of vital
688 importance to improve the upscaling of BNC to enable its use in the concrete industry.

689

690 **4.2 Bioremediation**

691

692 Industrial waste is often released into the environment without any proper treatment.

693 Bioremediation is aimed at offering a permanent solution to these problems transforming
694 pollutants to smaller molecules such as CO₂ and H₂O by utilising microorganisms or by
695 converting them to useful products. Recently, an ultrafiltration membrane was developed using
696 BC prepared by the previously mentioned native kombucha symbiotic culture of bacteria and

697 yeast [126]. BC has been extensively used in bioremediation in a form of functionalized BC
698 used to adsorb specific pollutants [126]. Muhamad *et al.* described an *in situ* method for the
699 fabrication of an adsorbent material to be used for the removal of heavy metals in wastewater.
700 More specifically, pandan extract was added during bacterial fermentation, yielding the
701 production of BC-pandan (BC-P) composites. Pandan is a tropical plant where the leaves are
702 rich in 2-acetyl-1-pyrroline (2AP), a compound largely known in the food industry that has
703 also exhibited the ability to trap heavy metals due to the presence of two functional groups, i.e.
704 cyclic nitrogen and ketone. The removal capacity of the BC-P composites was tested on
705 synthetic wastewater containing chromium (VI). The analysis evidenced a proportional
706 relationship between the removal efficiency and the 2AP content, with a maximum of over
707 80% removal efficiency for the composite biosynthesised in undiluted pandan extract [127].

708

709 Zhuang and Wang adopted an *ex situ* approach and produced nickel hexacyanoferrate BC
710 (BC/NiHCF) in a two-step reaction carried out directly within the BC pellicles. First, Ni^{2+} was
711 loaded by immersion of BC into a solution of nickel chloride. Metal hexacyanoferrates are
712 known for their high selectivity towards caesium allowing the replacement of an alkaline metal
713 located in the centre of their cubic structure with a caesium ion of similar size. Owing to their
714 low cost, such compounds have been widely used, for instance, to treat radioactive wastewater
715 from nuclear power plants. In this case, the removal capacity of the BC/NiHCF composites
716 was tested in a solution containing Cs^+ ions by measuring their residual concentration
717 calorimetrically. The experiment highlighted a fast increase in the removal and adsorption
718 ability in the first 60 minutes, followed by a decrease in the rate of adsorption between 60 and
719 120 minutes. This latter effect was ascribed to the gradual saturation of the surface adsorption
720 sites and the lower concentration gradient of Cs^+ . A third stage was then observed with a near
721 zero diffusion rate constant, and the equilibrium reached after 150 minutes with a final removal

722 ratio of 96%. Increasing the concentration of Cs^+ ions led to an increase in the adsorption
723 capacity, due to a stronger driving force for mass transfer. However, this also led to a decrease
724 in the removal ratio. An adsorbent loading of $100\text{--}300 \text{ mg Cs}^+ \cdot \text{g}_{\text{BC-NiHCF}}^{-1}$ exhibited the highest
725 removal ratio [128].

726

727 Incorporation of carbon nanotubes into BC was investigated by Nie and co-workers to develop
728 oil-absorbent materials for environmental remediation. Two types of nanotubes, namely
729 pristine and carboxylated (CNT and CCNT respectively,) were incorporated at 5 and 10 wt%
730 into BC after ultrasonic treatment followed by freeze-drying. In addition to this, two BC
731 aerogels were prepared, one obtained through freeze-drying and the other one consisting of
732 regenerated BC, i.e. freeze-dried BC previously subjected to homogenisation. All the samples
733 exhibited mesoporous structures with similar pore size; however, the absorption-desorption of
734 nitrogen evidenced that the presence of the carbon nanotubes resulted in an increased surface
735 area. This effect was observed both for CNT and CCNT composites, with about double the
736 surface area in the case of 10 wt% CNT or CCNT content ($\sim 80 \text{ m}^2 \cdot \text{g}^{-1}$ for the two composites
737 vs about $40 \text{ m}^2 \cdot \text{g}^{-1}$ for BC and $44 \text{ m}^2 \cdot \text{g}^{-1}$ for regenerated BC). The absorbing capacity of the
738 materials was then studied using four different oils, namely, paraffin, sunflower seed oil,
739 vacuum oil and propanetriol. Highest absorption was observed for the composites with 10 wt%
740 CNT or CCNT at $120 \text{ g propanetriol oil} \cdot \text{g}_{\text{BC-CNT}}^{-1}$ [129]. Table 3 lists a summary of BC
741 modifications used to capture heavy metals, organic solvents, and synthetic dyes.

742

Table 3: BC modification reported in the recent literature for bioremediation.

Pollutant	BC modification	Results	Reference
Malachite green	Magnetic BCNF /graphene oxide polymer aerogel (MBCNF/GOPA) composed of BC nanofibres (BCNFs), Fe ₃ O ₄ nanoparticles and graphene oxide	A maximum adsorption capacity of 270 mg·g ⁻¹ with a contact time of 35 min for 85% removal; reusable over eight cycles after elution with acetic acid/ethanol.	[130]
Cresol isomers	Molecularly imprinted BC, using polydopamine, TiO ₂ and an imprinting layer	<i>o</i> -cresol (23.7 mg·g ⁻¹), <i>m</i> -cresol (33.9 mg·g ⁻¹), and <i>p</i> -cresol (45.6 mg·g ⁻¹) adsorbed within 20 h; Exhibited excellent regeneration (adsorption/desorption) for up to five cycles	[131]
Tetracycline hydrochloride and 2,4-dichlorophenol	TEMPO-BC is converted to TEMPO-BC Zeolitic imidazolate framework 8 (ZIF). Carbonisation of TEMPO-BC@ZIF-8 yielded a N-carbon@N-ZnO	Particles exhibited a surface area of 1000 m ² ·g ⁻¹ and upon exposure to visible light degraded the pollutants in 100 min. A slight loss (~ 5 %) of reactivity was observed after five consecutive photocatalytic cycles.	[13]
Tellurium (IV) ions	TiO ₂ coated BC	Maximum adsorption capacity of 103.64 mg·g ⁻¹ . Excellent regeneration (adsorption/desorption) with 50% removal efficiency even after the ninth cycle.	[132]
Dimethyl formamide (DMF), cyclohexane	Reduced graphene oxide-BC aerogels	High absorption capacity of up to 147 g DMF and 164 g cyclohexane per g of dry aerogel was observed.	[133]
<i>n</i> -hexane, trichloromethane, pump oil	Copper nanoparticles-coated cellulose aerogel	Maximum absorption capacities achieved were: 70 g·g ⁻¹ for <i>n</i> -hexane, 160 g·g ⁻¹ for trichloromethane and 100 g·g ⁻¹ for pump oil. Absorbency was more stable at higher cellulose content in the aerogels.	[65]
Oil spills	Cellulose-silica composite	High surface area (734 m ² ·g ⁻¹), low thermal conductivity, high oil absorption capability and a high contact angle (145°) after hydrophobic modification making them easily washable and reusable.	[134]

Chromium (VI) ions	BC-Pandan extract	42% higher removal efficiency than the native BC.	[127]
Caesium ions	Nickel hexacyanoferrate BC	An adsorbent loading of 100–300 mg Cs ⁺ ·g _{BC-NiHCF} ⁻¹ exhibited higher removal ratio.	[128]
Paraffin oil, vacuum oil and propanetriol	BC with pristine carbon nanotubes (CNT) and carboxylated CNT	An absorption capacity of 120 g·g _{BC-CNT} ⁻¹ was obtained using propanetriol as a model oil.	[129]
Textile waste effluent	Unmodified BC	Efficient removal of microorganisms/dye after ten filtration cycles for the <i>E. coli</i> suspensions as well as the blue pigmented textile effluent.	[135]

744

745

746 4.3 Cosmetics

747 BC has a huge potential in the field of cosmetics and skincare due to its excellent material

748 properties such as, biocompatibility, capacity to hold water, ability to take up and release

749 substances, as well as excellent skin adhesion properties, whilst providing a sustainable option

750 which could replace many non-biodegradable cosmetic components [136]. In a study by

751 Pacheco *et al.* [137], researchers developed skin masks by incorporating cosmetic actives (e.g.

752 skin moisturisers and astringents) into BC nanofibre membranes. The masks were tested by

753 volunteers who assessed their skin moisture after mask use, which concluded a good skin

754 adhesion and improvement in the skin moisture level. Hyaluronic acid (HAc) is another natural

755 polymer that has been shown to be a good ingredient in cosmetic moisturisers. HAc is a key

756 molecule for retaining moisture in the skin, and a loss of this is something that contributes to

757 the aging of the skin. It also plays a role in tissue healing as it enhances the immune response

758 by activating inflammatory cells, in addition to curating the response of fibroblasts and

759 epithelial cells to the injury [138]. In a study by Wang *et al.* [139], researchers functionalised

760 BC membranes with integrated silk sericin (SS) and HAc and found that these membranes had

761 improved cell viability when compared to membranes of pure BC. This study introduces a
762 novel BC composite which has potential in applications in both cosmetics and wound
763 dressings, the latter application is discussed in more detail in the Biomedical application section
764 of this paper.

765

766 A thorough study into the *in vivo* effectiveness of BC based face masks was carried out by
767 Perugini *et al.* [140]. Here the researchers looked at factors such as skin moisturisation,
768 elasticity, smoothness, reduction of wrinkles, homogeneity of the dermal layer, and renewal of
769 the outermost layer of cells (stratum corneum) in a variety of BC masks containing different
770 compounds. Masks aimed at anti-aging were shown to significantly decrease the breadth of
771 wrinkles and skin surface roughness, masks with an aim of ‘lifting’ improved the skins
772 elasticity and firmness, and cell renewal masks had an exfoliating effect which was shown to
773 encourage new skin cell production over the course of one month when using a mask three-
774 times each week. The study showed that BC is a well-tolerated material for cosmetic use, and
775 a suitable delivery system for the release of active compounds into the skin.

776

777 As was previously discussed in the section on food (Section 4.1.1), BC can be used as a
778 stabilising or thickening agent, which is also applicable to cosmetic products. In this context it
779 has been assessed for its ability to stabilise oil and water emulsions, and for texture
780 improvement of cosmetic products [141]. The media in which BC is cultivated can also
781 influence the cosmetic benefits it can provide. For example, a study by Amorim *et al.*[142]
782 grew *Komagataeibacter hansenii* (formerly *Glucanacetobacter hansenii*) in a tropical fruit
783 residue media to produce BC, as the fruit media has multiple characteristics which aid in the
784 prevention of free radical damage to the skin: these include its good vitamin and mineral
785 content, for example antioxidants such as ascorbic acid (vitamin C). Therefore, the cosmetic

786 BC face mask not only hydrates and moisturises but can also be used as a carrier of active
787 ingredients from the fruit.

788

789 A more extreme cosmetic application of BC, which links cosmetics directly to biomedical
790 wound healing applications, is for the treatment of burn wounds. Khalid *et al.*, [143] decided
791 to create a wound dressing from BC due to its ideal mechanical properties, incorporating zinc
792 oxide nanoparticles to give the dressings an antimicrobial function. Initial studies to assess the
793 dressing's antimicrobial properties were carried out on four common pathogens associated with
794 burns, with between 87.4% and 94.3% activity against them. This research was taken to the *in*
795 *vivo* level where burn model mice treated with BC-ZnO nanocomposites showed 66% wound
796 healing, which was significant, and histological analysis confirmed that there was regeneration
797 of tissue.

798

799 Overall, the positive effects that BC can have on cosmetic products provides the potential that
800 it could replace many other commonly used synthetic polymers in cosmetics, reducing the
801 negative environmental effects of the cosmetics industry.

802

803 **4.4 Electronics and Sensors**

804 Another key application area of BC is its use in electrical applications, which inadvertently
805 means that components become more sustainable and recyclable. For example, Dhar *et al.* used
806 reduced graphene oxide (RGO) to improve the electrical conductivity of BC as well as its
807 mechanical performance. RGO sheets were found to be homogeneously incorporated in the BC
808 network thanks also to the reducing capacity of the hydroxyl groups on its surface, thus
809 improving their dispersion as well as the interconnection between the two systems. The
810 nanocomposites showed significant increase in the ultimate tensile strength (UTS), Young's

811 moduli and toughness values compared to pristine BC for all RGO concentrations. In addition
812 to this, electrical conductivity of about $140\text{-}150\text{ S}\cdot\text{cm}^{-1}$ was obtained for a film containing
813 3 wt% RGO, confirming that the material presented suitable characteristics for the development
814 of flexible electronic devices, including free-standing films and paper-based electronics [144].
815 Current marketing strategies are aimed at developing devices that are sustainable as well as
816 being flexible for the use in human-machine interface units, medical monitoring systems and
817 other wearable devices. These include electronic paper, flexible organic light emitting diode
818 displays [145] as well as countless other electronic components (e.g. transistors) as well as
819 flexible energy storage devices [69, 146]. A key material for the fabrication of these devices is
820 cellulose which is considered to be an excellent natural biopolymer with good biodegradability,
821 mechanical performance, piezoelectricity and dielectricity [69]. As previously mentioned,
822 compared to plant-based cellulose, BC has distinct advantages of which a key advantage for
823 electronic applications is having a greater resistance to insulating/ionic liquids (ILs) [147, 148].
824 One important processing technique of using BC for electronic applications is the carbonisation
825 of BC, here the entire BC structure is converted into a highly conductive carbon network
826 according to the 3D nanofibrous BC network structure of the sample [149-151]. This is often
827 referred to as carbonised bacterial cellulose (CBC). The resulting structures have been shown
828 to be excellent electrode material for flexible storage devices such as capacitors with ample
829 space for electrolytes and have been reported to have excellent mechanical stability under
830 bending and stretching strains [152]. Wang *et al.* [153] also described the fabrication of a high-
831 performance yarn supercapacitor based on a twisted CNT / BC membrane with
832 electrochemically deposited polypyrrole (PPy) (Figure 5A). They reported an excellent areal
833 capacitance of $458\text{ mF}\cdot\text{cm}^{-2}$ at $0.8\text{ mA}\cdot\text{cm}^{-2}$, furthermore it withstood a high cycling stability
834 with no notable degradation after 2000 cycles. In contrast to this another common application
835 of BC is the use as a dielectric in form of electrical insulating paper (Figure 5B), here BC has

836 been reported to have a greater breakdown voltage compared to standard plant-based paper as
837 well as better mechanical properties and a better resistance to the denaturing effects of
838 insulating liquids [147]. Another slightly different approach reported by Zhou *et al.* [154] was
839 the use of BC in the fabrication of a Layer-by-Layer (LBL) silicon-based sandwich nanomat
840 for use as a flexible anode for lithium-ion batteries (Figure 5C). Here in brief, BNC was
841 functionalised with 2,2,6,6-tetramethylpiperidine-1-oxyl (TOBC) and then reinforced with
842 silica nanoparticles and sandwiched LBL with graphite microsheets.

843

844 Di Pasquale *et al.* [155] describe the production and characterisation of a biodegradable
845 deformation sensor based on BC. Deformation sensors are of particular interest for applications
846 such as assisted rehabilitation as well as for being key sensing devices in the recreational
847 market for virtual reality, augmented reality as well as gaming applications. Here they utilise
848 the piezo-ionic properties of BC to produce a workable paper-based sensor. Furthermore, the
849 produced BC sensor is compared to sensors with respect to environmental impact and
850 considered the most environmentally friendly.

851

852 The sensor was made by impregnating BC with ILs, i.e. 1-Ethyl-3-Methylimidazolium
853 tetrafluoroborate (EMIMBF₄) and then covering the structure with conductive polymers (e.g.
854 Poly-(3,4-ethylenedioxythiophene)-polystyrene-sulfonic acid (PEDOT)), where they report a
855 sensitivity of $4.3 \times 10^5 \text{ V}\cdot\text{mm}^{-1}$ at 21 Hz, estimated at a resolution of 0.04 mm (Figure 5D)
856 [155]. Similarly, another BC-IL-based sensor is described by Trigona *et al.* [156] explaining
857 how this can potentially also be used to harvest electronic energy via mechanical vibration. It
858 is important to note that this sensor is fundamentally the same except that the energy gained
859 via the piezo effect is exploited. In conclusion, it appears that BC has many physical advantages
860 for use in the fabrication of electronic devices as compared to plant-based cellulose and

861 therefore holds much promise for future applications in this area which needs expanding.
862 Furthermore, most if not all plant based cellulose applications should be transferrable to BC
863 cellulose and due to the enhanced features BC has over plant cellulose, there is a strong
864 potential of better-quality devices being produced.

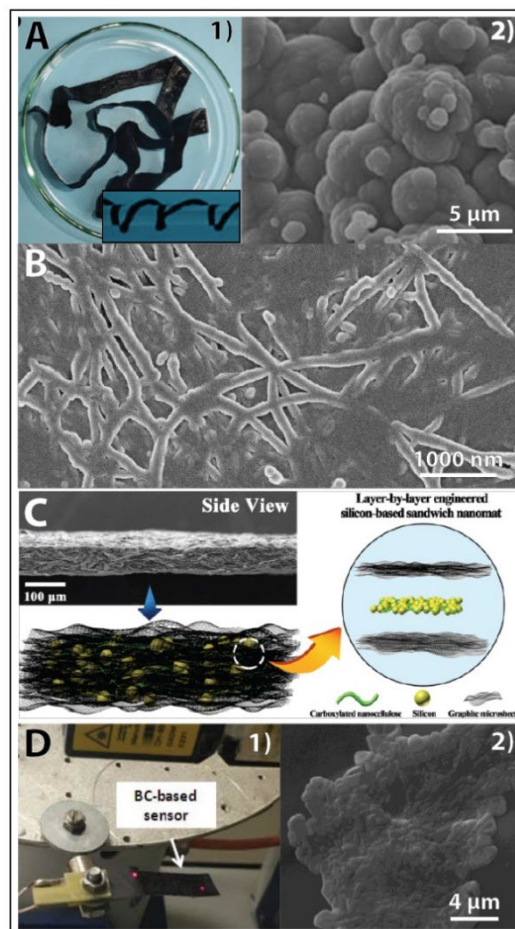
865

866 In the context of chemical modifications carried out to confer antibacterial properties to BC, a
867 different approach was undertaken by Farooq *et al.* for the development of a phage-based
868 biosensor able to detect live *S. aureus* cells. First, carboxylated multiwall carbon nanotubes
869 (c-MWCNTs) were produced through acid treatment and incorporated into the cellulose matrix
870 at increasing concentration through sonication. This was a necessary step to impart electrical
871 conductivity to the hydrogel and obtain an electrochemical biosensor capable of detecting any
872 change in the conductivity of the medium or interface with the material. To improve the
873 efficiency of the phage immobilisation, the polymer surface was then coupled with
874 polyethylene imine (PEI), through interaction between the carboxyl groups of c-MWCNTs and
875 the hydroxyl groups of cellulose with the positively charged amino groups on PEI. The
876 presence of a positive charge on the surface of the nanocomposite allowed in fact the
877 stabilisation of the phage through electrostatic conjugation with its negative capsid, leaving the
878 positive tails exposed for bacterial capture. The antibacterial assays carried out clearly
879 evidenced that the BC/cMWCNTs-PEI structure presented high inhibition zone even after
880 sonication for 15 minutes, whereas, in the absence of PEI, the treatment resulted in the complete
881 detachment of the phage.

882

883 The electrochemical characterisation of the c-MWCNTs composites as working electrodes was
884 conducted through differential pulse voltammetry (DPV). First, DPV was conducted in PBS in
885 the presence of *S. aureus* only. After 10 minutes, a decrease in the current response was

886 observed, followed by an increase after 25 minutes, probably indicating, respectively,
 887 deposition of the cells onto the electrode upon phage capturing (thus blocking the electron
 888 transfer) and consequent cell lysis with release of intracellular components and higher medium
 889 conductivity. The specificity of the sensor was then assessed, and significant current variation
 890 response was registered only in the case of pure *S. aureus* and mixed culture containing *S.*
 891 *aureus*, whereas the test on non-specific bacteria, including *E. coli* and *Pseudomonas*
 892 *aeruginosa*, caused negligible response. Finally, the activity was tested in milk: linear
 893 correlation between the signal and CFU concentration was observed, with a maximum
 894 detection concentration up to 5×10^6 CFU·mL⁻¹ and high level of accuracy, as confirmed by
 895 comparison with the values obtained by quantification of the cells recovered from milk samples
 896 through the plate count method [157].



897

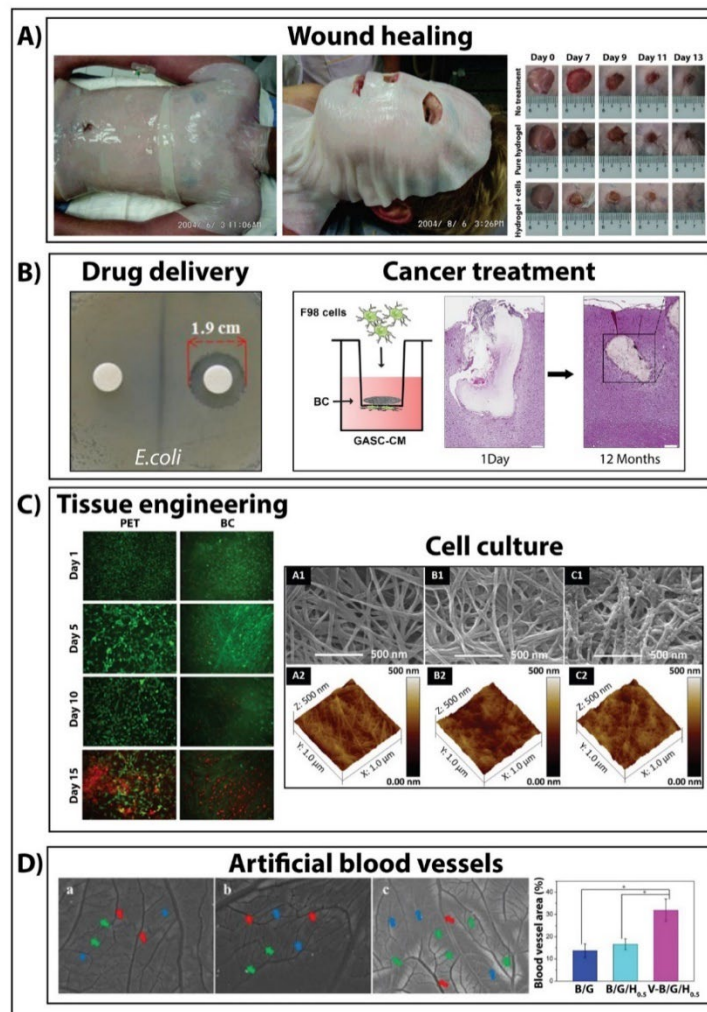
898 Figure 5: A 1) CNT/BC membrane, inset) twisted CNT/BC yarn, 2) PPy/CNT/BC yarn after polymerization at
 899 2 V for 40 min and 5 V for 60 min, adapted from Wang *et al.* [153]; B The structure of the BC paper, adapted

900 from Zhuravleva *et al.* [147]; C Layer-by-layer engineered silicon-based BC sandwich nanomat, adapted from
901 Zhou *et al.* [154]; D 1) BC-based deformation sensor setup showing the two lasers used to measure the
902 deformation (anchor and tip displacement, respectively), 2) BC/EMIMBF₄/PEDOT sensor, adapted from Di
903 Pasquale *et al.* [155].

904

905 **4.5 Biomedical applications**

906 In the biomedical area, extensive research has been devoted to the modification of BC to target
907 specific applications, while at the same time taking advantage of its great intrinsic
908 biocompatibility as well as previously discussed attributes such as its structural variability,
909 robust mechanical strength, 3D fibrous structure, porosity, water retention capacity and
910 transparency, among others. This places BC as a prominent biomaterial of interest in many
911 biomedical applications [158-160], in particular in the fields of wound healing, drug delivery,
912 tissue engineering, and artificial blood vessels.[161, 162]



913

914 Figure 6 A), Wound healing for large-scale burns (left and middle), reproduced with permission from [163], (right)
 915 Healing process of wound excised (15 mm diameter) on a rat, reproduced with permission from [27], B), **Drug**
 916 **Delivery:** Disk diffusion of Ciprofloxacin (CIP) from β -cyclodextrin-grafted bacterial cellulose nanowhiskers
 917 (BCNC-g- β CD) to prevent bacterial colonization. Left disk: unmodified BCNC; and right disk: BCNC-g- β CD-
 918 CIP, reproduced with permission from [164], **Cancer Treatment:** Histological section of rat brain one day and
 919 twelve months after BC membrane implementation. Scale bar 200 μ m, reproduced with permission from [165]
 920 C), **Tissue Engineering:** Live-dead staining results of the triple culture of brain microvascular endothelial cells
 921 (BMECs), astrocytes, and pericytes on PET and BC membranes on 1st, 5th, 10th and 15th days. Live cells are green
 922 (Calcein AM) and dead cells are red (Ethidium Homodimer-1). Some dead cells are observed on the 10th day; and
 923 the number of dead cells increases on the 15th day, Scale bars 100 μ m, reproduced with permission from [166],
 924 **Cell culture:** Surface morphology of the (A1, A2) unmodified BCM, (B1, B2) poly(acrylic acid)-BCM (PAA-
 925 BCM) and (C1, C2) plant-derived recombinant human osteopontin-BCM (p-rhOPN-BCM), as evaluated by (A1,
 926 B1, C1) FE-SEM and (A2, B2, C2) AFM analyses, respectively. Images shown are representative of those seen
 927 from at least 3 such fields of view per sample and 3 independent samples, reproduced with permission from [167],
 928 D), Effects of vascular endothelial growth factor (VEGF) provision by the VEGF-loaded BC/gelatin heparin
 929 modified (V-B/G/H_{0.5}) scaffolds on vascularization using a chick chorioallantoic membrane (CAM) assay.
 930 Representative images of the CAM vascularization in response to B/G scaffold (a), B/G/H_{0.5} scaffold (b), and
 931 V-B/G/H_{0.5} scaffold (c). (B) Quantification of the blood vessels, reproduced with permission from [168].

932

933 4.5.1 Wound healing and antibacterial wound dressings

934 Wound healing is a key application area where the natural properties of BC can be exploited.
935 Due to the unique physicochemical attributes of BC it has great potential in wound and burn
936 recovery (Figure 6A), where there is a growing demand for non-invasive and innovative
937 approaches that can trigger rapid and full recovery of critical wounds and burns [27]. In
938 addition to biocompatibility and non-toxicity, candidate materials for wound healing must
939 satisfy certain key requirements including the ability to maintain a moist environment around
940 the wound site, ability to absorb wound exudate and enhance re-epithelisation, high porosity
941 and permissiveness to gaseous exchange, as well as being accommodative to antimicrobial and
942 drug delivery properties [27]. Furthermore, wound healing involves a complex interaction
943 between different cells, soluble compounds, and components of the extracellular matrix
944 (ECM), therefore, the material must serve as a suitable interphase to facilitate this. The
945 aforementioned properties of BC are highly suited for this purpose and, in particular, its water-
946 holding ability allows it to maintain a moist environment around the wound site [169].

947

948 In a study conducted by Beekmann *et al.* [170], the addition of water-soluble polyethylene
949 glycol (PEG) in the BC structure was proposed to achieve the production of a highly transparent
950 substrate to be utilised as a drug-delivery platform. PEG₄₀₀ and PEG₄₀₀₀ were added with
951 increasing concentrations to the BC production medium in an attempt to improve drug loading
952 uptake. As predicted, PEG-modified BC demonstrated larger pore sizes and increased water
953 uptake capacity, resulting in improved drug loading and release capacity, which was more
954 pronounced for PEG₄₀₀ doped BC. An anti-inflammatory drug model was incorporated, namely
955 the sodium salt of diclofenac. Diclofenac is a non-steroidal drug that presents several side
956 effects when administered orally, therefore the development of topical gels would offer a
957 promising alternative to minimise these side effects. The best results were reported for a

958 composite containing 8% PEG₄₀₀, with an increase in loading from 1.06 mg diclofenac·g_{BC}⁻¹
959 for pristine BC to 1.49 mg diclofenac·g_{BC}⁻¹, making it a suitable candidate for the development
960 of both transdermal patches and active wound dressings [170].

961

962 By using a solution impregnation method, Lamboni *et al.* (2016) [171] integrated silk sericin
963 (SS) into the BC network, sufficiently coating the BC fibres and effectively encapsulating the
964 fibres. The study aimed to improve the cytoprotective and mitogenic effects of the composite
965 while maintaining the original mechanical and thermal attributes of BC. The morphological
966 analysis of the BC/SS composite showed many interconnected pores that improved oxygen
967 permeation and adsorption of wound exudate. Biocompatibility tests with fibroblasts showed
968 high cell proliferation and viability.

969

970 In another study Chang and Chen [172] blended alginate and chitosan with oxidised BC, from
971 which they formulated a dry-fabricated biofilm (DFBF) and assessed its wound dressing
972 potential. The study demonstrated that the DFBF, based on hydrogen peroxide oxidised BC,
973 exhibited suitable mechanical properties, hydrophobicity, biocompatibility, and excellent cell
974 proliferation of Detroit 551 cells (derived from a skin biopsy of a normal Caucasian female
975 embryo) for wound dressing applications. Moreover, the modified DFBF successfully adsorbed
976 wound exudate and released anti-inflammatory substances in a controlled manner.

977

978 In order to combat the intrinsic lack of antibacterial functionalities in BC, due to its chemical
979 structure, some of the most common class of active agents loaded into BC consist of therapeutic
980 metals such as silver, zinc, and copper. A recent study conducted by Phutanon *et al.* [173] for
981 example, relied on the use of copper to confer antibacterial features to the BC substrate. In this
982 case, CuO was produced directly onto the membranes through a forced hydrolysis technique.

983 This method enables the uniform distribution of precipitated metal oxides by controlling pH
984 and temperature of the hydrolysis [126]. The CuO nanoparticles were directly formed onto the
985 fibrillar network of BC in an evenly dispersed pattern, probably due the involvement of the
986 hydroxyl groups of the polymer in the CuO synthesis. Once again, the agar diffusion test on
987 BC-based composites showed promising results against both *E. coli* and *S. aureus*; in
988 particular, inhibition zone values comparable with the positive control (namely, tetracycline)
989 were registered in the case of *S. aureus* [173].

990

991 Besides metals, a wide range of antibacterial agents have been incorporated within BC,
992 including various antibiotics. Silver sulfadiazine (SSD) is known for its antibacterial effect and
993 has been largely utilised for topical treatments on wounds. BC sheets containing SSD at
994 different concentrations (0.2%, 0.4%, 0.8%, 1.0% v/w) were prepared by immersion processing
995 for 24h. The activity of the modified pellicles was evaluated by disc diffusion assay against the
996 most common bacterial strains found in diabetic foot ulcer, i.e. *E. coli*, *P. aeruginosa* and
997 *S. aureus*, demonstrating good inhibition in all cases. In addition, the incorporation of SSD
998 resulted in a significant increase in the tensile strength in a concentration dependent manner
999 (~0.03 kPa at 0% SSD to ~0.14 kPa at 1% SSD), owing to the reduced degree of porosity of
1000 the material and interactions between the matrix and the nanoparticles [174].

1001

1002 Along with physical absorption into the hydrogel, BC modification processes to develop
1003 antibacterial materials can also involve the chemical functionalisation of the polymer
1004 backbone. Inoue *et al.* [58] presented an optimised method to obtain 2,3-dialdehyde BC
1005 (DABC) through oxidation with metaperiodate. Periodate is capable of selectively oxidising
1006 the polymer at positions C2 and C3, yielding a bioabsorbable (pristine BC is non-degradable)
1007 and biocompatible material. The oxidation method was improved by increasing the periodate

1008 concentration to achieve the highest number of aldehydic groups. Since the substrate was
1009 intended to be utilised as a bioabsorbable membrane for the treatment of periodontal diseases,
1010 an antibiotic was then loaded into the structure to ensure protection against bacterial
1011 contamination. More specifically, the authors incorporated chlorhexidine both on its own and
1012 upon formation of an inclusion complex with β -cyclodextrin, with the aim to control the
1013 absorption into BC and DABC as well as its release. It was observed that oxidised BC loaded
1014 with the inclusion complex released the highest amount of drugs: this was explained both by
1015 the presence of β -cyclodextrin, which shielded the antibiotic from interacting with the hydroxyl
1016 groups of BC, as well as by the degradation of DABC, which contributed to the higher release
1017 rate [58].

1018

1019 Cacicedo *et al.* [175] incorporated ciprofloxacin into BC to develop an antibacterial film for
1020 application as a wound dressing material. BC was chemically modified to improve the
1021 absorption ability and the controlled release process by cross-linking with chitosan, using
1022 tripolyphosphate, with a final chitosan concentration of ~ 37 wt% with respect to BC. At the
1023 morphological level, scanning electron microscopy (SEM) showed that the presence of
1024 chitosan induced a smoothing of the surface and filling of the interfibrillar space, suggesting
1025 the formation of an intertwined network between the two polysaccharides. Thermogravimetric
1026 analysis (TGA) evidenced nearly twice the water content after freeze-drying for the BC-
1027 chitosan films as compared to BC and chitosan, suggesting a much tighter network that allowed
1028 water molecules to remain trapped between the chains. A tighter network possibly contributed
1029 to the hyperbolic drug release profile with a 30% decrease in ciprofloxacin release compared
1030 to pristine BC where 90% of the total payload was released after the first hour. The composites
1031 presented a water vapour transmission rate of about four times the value obtained for unloaded

1032 BC, making the composite an optimal wound dressing, able to balance the humidity of the
1033 wound and maintain an appropriate level of hydration [175].

1034

1035 Orlando *et al.* used a green-chemistry approach to react BC with two active agents, namely
1036 glycidyl trimethylammonium chloride and glycidyl hexadecyl ether, via a heterogenous
1037 reaction under basic aqueous conditions.[176] The resulting functionalised BC patches
1038 exhibited a reduction in bacterial cells of 43% and 54%, against *E. coli* ATCC 8739TM and *S.*
1039 *aureus* subsp. *Aureus* Rosenbach 6538PTM , respectively. Furthermore, the treated and
1040 untreated samples exhibited excellent cell viabilities of 90-100% for keratinocytes (HaCaT cell
1041 line) and scratch assays revealed good wound closure rates of complete coverage after 5 days.

1042

1043 In the pursuit of producing commercially viable wound healing patches, bandages, and
1044 dressings, the processing and upscaling is of critical importance. For this novel emerging
1045 methodologies need to be considered such as the production of fibrous materials via gyration,
1046 including both pressured gyration [177-180] as well as centrifugal gyration [181] and
1047 Electrohydrodynamic (EHD) processes.

1048 EHD processes such as electrospinning and electrospraying have been predominantly used for
1049 cellulose derivatives due to their solubility in organic solvents. EHD processes utilize an
1050 electrically charged jet of polymer solution to produce fibres or particles at the micron,
1051 submicron and nanoscale with several structural and functional advantages. For example,
1052 Crabb-Mann *et al.* [182] electrospun three cellulose derivatives; ethyl cellulose (EC), cellulose
1053 acetate (CA) and carboxymethyl cellulose (CMC) to produce a wide range of microstructures
1054 with the one step EHD process, using the green solvents ethanol, acetone and water. During
1055 the electrospinning of EC using 17 to 25 wt% solutions, morphological changes from particles
1056 to thick fibres were observed. While when CA was electrospun with acetone using 10 wt%

1057 samples, fibres with heavy beading were produced. The beading was successfully reduced by
1058 adjusting the solvent ratio to 80:20 acetone/water which resulted in the production of smooth
1059 fibres. Further, the fibre diameter or the morphology could be adjusted by varying the
1060 CMC/PEO blend concentration. A change in the molecular weight of CMC from M_w 250,000
1061 to M_w 700, 000 increased the entanglements between polymer chains, leading to an increase in
1062 fibre diameter which consequently reduced the polymeric jet instabilities, leading to smoother
1063 fibre deposition. The authors thus optimised the processing conditions of cellulose derivatives
1064 suitable for development of non-woven fibrous wound healing patches. A similar EHD
1065 processing method was utilised for BC to produce biocompatible ultrafine nanoscale fibres
1066 suitable for biomedical and tissue engineering applications. BC was functionalized with
1067 sulphate groups through acetosulphation, enhancing its solubility in aqueous media. Bacterial
1068 cellulose sulphate/polyvinyl alcohol (BCS/PVA) were then blended in 1:9 (10 mg), 2:8 (20
1069 mg), and 3:7 (30 mg) w/w ratio, respectively, in deionized water. BCS/PVA nanofibers were
1070 thus fabricated via electrospinning. The BCS/PVA nanofibres were reported to be highly
1071 biocompatible with a cell viability >90%, as confirmed by cytotoxicity and cell adhesion
1072 results. BCS nanoscale fibres have therefore, great potential in several biomedical applications
1073 including wound healing, tissue engineering, and regenerative medicine [183]. Another study
1074 showed that electrospinning BC after a chemical treatment with N, N-dimethylacetamide and
1075 lithium chloride (DMA/LiCl) solvent system was much more reproducible. The modified BC
1076 was easily electrospun in chloroform or acetone compared to unmodified BC [184]. Recently,
1077 in the context of electrospinning, a novel directed deposition method was developed by Cam
1078 *et al.* [185], where the material is directly deposited on the wound. The authors described the
1079 use of a portable electrohydrodynamic gun to fabricate wound healing patches directly on skin,
1080 in a point of need application. Here, the authors applied a composite material containing BC
1081 and gelatine (GEL) as well as metformin (Met) or glybenclamide (Gbc) active factors for

1082 treating wounds on diabetic subjects. They found that the simple application of the BC/GEL
1083 patches drastically improved the recovery, however the addition of Gbc and Met further
1084 improved this, where the BC/GEL/Gbc doped patched resulted in the best recovery of the
1085 wound. The results demonstrated that the directly administered patches were able to protect
1086 and promote regeneration, giving a long and sustained release of doped drugs, resulting in
1087 specific wound healing patches with great potential for clinical use. Furthermore, this technique
1088 enables the perfect coverage of wounds as the patch is produced *in situ*, avoiding any issues
1089 with patch dimensions and adhesion.

1090

1091 Pressurised gyration has also been gaining increased attention in the context of upscaling the
1092 production of wound healing bandages. The material produced via this technology has been
1093 shown to produce well-defined fibres of 60-1000 nm in diameter, dependant on the polymer
1094 concentration, at production rates of up to 6 kg per hour [177]. Furthermore, this process can
1095 also be used to produce well-defined core-sheath bicomponent polymer nanofibres on a large
1096 scale [178], which is of particular interest for wound healing patches and regenerative medicine
1097 applications. In this context Aydogdu *et al.* [186] investigated a variety of different PLA, PCL
1098 and BC combinations to produce well-defined fibres via centrifugal gyration. With orifice
1099 diameters of 0.5 mm, the authors found that above 10 wt% BC, the fibre yields started to
1100 reduce. However, using the blends it was possible to produce fibres with > 30 wt % of BC,
1101 giving the fibres enhanced mechanical properties, but at reduced yield. The produced band-like
1102 mats have high potential for mass production of wound healing patches. In another study by
1103 Altun *et al.* [187] BC / PMMA composite fibres were produced via pressurised gyrospinning
1104 incorporating Cu-Ag-Zn/CuO and Cu-Ag-WC (tungsten carbide) nanoparticles which were
1105 shown to result in higher ultimate tensile strengths and Young's moduli, as well as adding
1106 antibacterial function to the produced wound dressing materials.

1107 4.5.2 Controlled Drug delivery

1108 BC is often combined with other materials for the purpose of controlled drug release. For
1109 example, graphene-based nanoparticles have been widely researched for drug carrying and are
1110 able to prevent premature drug release, however, when placed in an aqueous solution they tend
1111 to clump together, and therefore BC has been researched as an embedding material. Luo *et al.*
1112 [188] embedded graphene oxide in a porous BC 3D network and tested it as a carrier of
1113 ibuprofen. It was shown to release the ibuprofen by non-Fickian diffusion *in vitro*, and
1114 researchers also showed that the incorporation of graphene oxide increased cell viability in
1115 comparison to BC alone. A different approach of drug carrying was researched by Ullah *et al.*
1116 [189], who investigated the use of drug-loaded BC microparticles. These microparticles
1117 exhibited immediate drug release in addition to antibacterial activity. The drug adsorption and
1118 release rates of porous BC microparticles have also been researched and it was shown that these
1119 properties can be controlled [190], giving these microparticles the ability to be tuned for use in
1120 many different biomedical applications which require different drug release rates.

1121

1122 BC as a drug carrier material also has much potential in the field of dentistry, specifically for
1123 wound healing and drug delivery applications, for example after the removal of a tooth. In
1124 addition to the drug carrying properties of BC, it is possible to tune its degradability via
1125 periodate-oxidation which is useful in these types of applications. Weyell *et al.* [191] created
1126 a wound covering using BC loaded with doxycycline as a defence against infection, and found
1127 that it had a biphasic release of the drug and the antibiotic was effective against pathogenic
1128 bacteria found in the mouth. Furthermore, BC also has potential for use as bioabsorbable barrier
1129 membranes for the treatment of bacterial infection related periodontal diseases. The degree to
1130 which the BC is oxidised can regulate the rate of bio-absorption and the bactericidal effect of
1131 drugs/antibiotics that it has been loaded with. In a study by Inoue *et al.* [58], BC was selectively

1132 oxidised using sodium periodate and loaded with inclusion complexes of the drug
1133 chlorhexidine with β -cyclodextrin. This combination of oxidation and β -cyclodextrin loading
1134 led to a ten-fold increase in the rate of chlorhexidine, and this drug release was shown to inhibit
1135 the growth of *E. coli*, *S. aureus*, and *C. albicans*.
1136

1137 **4.5.2.1 Controlled drug delivery for cancer treatment**

1138
1139 BC has been shown to be a suitable material for prolonged drug release, making it ideal as a
1140 drug carrier for cancer treatment. A significant advantage of using a drug carrier such as BC is
1141 that it enables controlled and localised chemotherapy which therefore can increase the
1142 concentration of the drug at the tumour site. It also reduced the overall drug exposure in the
1143 body and mitigated many side effects linked with the current standard chemotherapy treatment
1144 [192].

1145
1146 In a study by Cacicedo *et al.* (2016) [193], researchers improved the loading capacity of the
1147 chemotherapy drug doxorubicin (Dox) onto BC through *in situ* incorporation of sodium
1148 alginate during the fermentation of *K. hansenii*. After purification of the membranes, the drug
1149 was introduced by the absorption method through immersion into a Dox-containing solution.
1150 A thermogravimetric analysis performed on both unmodified BC and BC/alginate composites
1151 evidenced increased water content in the presence of alginate, probably because of its high
1152 hydrophilicity, which could enhance the loading capacity of water-soluble molecules such as
1153 Dox. In addition to this, the nitrogen adsorption/desorption assay showed 84% higher surface
1154 area and 200% higher pore size in the case of the composites compared to pure BC. This result
1155 was ascribed to the formation of a cooperative network between the two polymers, as
1156 confirmed by the shifts in the peaks of the FTIR spectra of the materials. Drug encapsulation
1157 studies further corroborated such findings, with a three times higher loading value for the
1158 BC/alginate system, probably due to the strong interactions between the two polymers, which
1159 created a dense interpenetrated network. The negative charges of the carboxylate groups of
1160 alginate enables electrostatic interaction with the positively charged Dox. Cytotoxicity studies
1161 carried out on HT-29 human colorectal adenocarcinoma cells highlighted that, when the drug
1162 was loaded onto BC/alginate, lower viability values were observed both after 24 and 48 hours,

1163 whereas in the case of free Dox, a reduction in the viability was noted only after 48 hours. In
1164 addition to this, optical images evidenced that free Dox was more prone to form crystallites
1165 and precipitate, thus resulting in lower availability of the drug to the cells [193].

1166

1167 A further study by Cacicedo *et al.* (2018) [192] loaded BC hydrogels with lipid nanoparticles
1168 loaded with Dox. They found that using neutral Dox showed over double the encapsulation
1169 efficiency of cationic Dox (97% vs. 48%), and the neutral Dox enabled sustained drug release
1170 compared to fast release in the cationic form. By using a combination of the two to achieve
1171 optimal drug release, an *in vivo* study revealed a significant reduction in the growth of tumours
1172 and metastatic events.

1173

1174 In a study by Khattab and Dahman (2019) [164], the researchers created BC nanowhiskers with
1175 β -cyclodextrin as an excipient to improve drug stability and solubility. The aim of their study
1176 was to obtain functionalised BC nanowhisiker-grafted- β -cyclodextrin as a drug carrier with a
1177 high grafting ratio, which would then have increased drug loading capabilities and controlled,
1178 prolonged drug release. The nanowhiskers were then loaded with the anticancer drugs
1179 doxorubicin and paclitaxel, as well as the antibiotic ciprofloxacin, and they found that these
1180 functionalised constructs had increased drug loading, as well as a more controlled and sustained
1181 drug release (Figure 6B). In another study [194] researchers oxidised BC with nitrogen dioxide
1182 in chloroform/cyclohexane to produce carboxylated BC as a scaffold for the sustained release
1183 of drugs. They then immobilised the antitumour drug cisplatin on the oxidised BC and studied
1184 its release *in vitro*, finding that its release was sustained and did have the desired cytotoxic
1185 effect on HeLa cells. These studies show the extensive research focusing on the controlled and
1186 sustained release of drugs using BC, for applications such as cancer therapy.

1187 In a study by Chaabane *et al.* [195], magnetite nanoparticles ($\text{Fe}_3\text{O}_4\text{NPs}$) were used to produce
1188 a chemotherapeutic system based on BC. To achieve this, the polymer was first oxidised using
1189 sodium periodate to yield 2,3-dialdehyde BC (DABC) followed by the grafting of
1190 ethylenediamine (EDA). Two different compounds, namely (DABC-EDA-Bzl) and
1191 $[\text{Fe}(\text{DABC-EDA-Bzl})\text{Cl}_2]$, were then formed through addition of either benzyl (Bzl) or benzyl
1192 and iron (II) chloride, respectively. Finally, the magnetite nanoparticles-containing the
1193 complex $[\text{Fe}_3\text{O}_4\text{NP-INS-(DABC-EDA-Bzl)}]$ was obtained by *in situ* co-precipitation of
1194 $[\text{Fe}(\text{DABC-EDA-Bzl})\text{Cl}_2]$ with iron(III) chloride and ammonium hydroxide within the cavity
1195 of the tetra-aza macrocyclic Schiff base ligands. The materials developed were tested both *in*
1196 *vitro* and *in vivo* with respect to their cytotoxic and anticancer behaviour. The *in vitro*
1197 evaluation carried out with CT26 colon cancer cells evidenced that the magnetic complex
1198 presented a lower IC_{50} value as compared to $[\text{Fe}(\text{DABC-EDA-Bzl})\text{Cl}_2]$ ($6 \mu\text{g}\cdot\text{mL}^{-1}$ for
1199 $[\text{Fe}_3\text{O}_4\text{NP-INS-(DABC-EDA-Bzl)}]$ vs $62 \mu\text{g}\cdot\text{mL}^{-1}$ for $[\text{Fe}(\text{DABC-EDA-Bzl})\text{Cl}_2]$), owing to the
1200 oxidative stress induced by reactive oxygen species (ROS) generated through the Fenton
1201 reaction of Fe^{3+} with endogenous hydrogen peroxide. In addition to this, the selectivity of the
1202 materials towards cancer cells was investigated through cytotoxicity assays using peripheral
1203 blood mononucleocyte cells as blood cells are the first type of cells exposed to their action.
1204 After 48 hours of contact with the magnetic complex, no significant reduction in the cell
1205 viability was observed, whereas $[\text{Fe}(\text{DABC-EDA-Bzl})\text{Cl}_2]$ caused a 65% decrease in the cell
1206 viability, probably due to the coordination of Fe(II) with the normal cell membrane. An *in vivo*
1207 study was then performed on CT-26 cells subcutaneously implanted in female BALB/c mice.
1208 Tumour images at day 0 and day 10 clearly evidenced a significant reduction in the volume for
1209 the group treated with $[\text{Fe}_3\text{O}_4\text{NP-INS-(DABC-EDA-Bzl)}]$ as compared to the control (i.e.
1210 saline solution). The $[\text{Fe}(\text{DABC-EDA-Bzl})\text{Cl}_2]$ group, on the other hand, did not show the

1211 same trend, suggesting that the presence of Fe₃O₄NPs is required to ensure high
1212 chemotherapeutic efficiency [195].

1213

1214 **4.5.2.2 Cancer cell entrapment via BC**

1215

1216 Modified BC has also been used to trap cancer cells [165]. Glioblastoma (GB) is an aggressive

1217 form of tumour formed in the brain or spinal cord; it is a highly recurring type of tumour due

1218 to its infiltrative nature which causes residual cells to remain in the area after surgery. A way

1219 in which to remove these residual cells without causing damage to fragile brain tissue is

1220 required, with BC showing promise for this purpose due to its biocompatibility and suitable

1221 structure for cell entrapment. This was proposed by Autier *et al.* [165] in a study in which BC

1222 membranes were implanted into the surgical cavity after tumour removal to act as cancer cell

1223 traps. Loading the scaffold with chemo-attractants helped to concentrate the cancer cells, thus

1224 facilitating targeted therapies such as stereotactic radiosurgery. The migration of F98 rat glioma

1225 cells was assessed in response to the secretion of chemo-attractants by GB-associated stromal

1226 cells (GASCs). Such cells, generally found in the peritumoral brain area, can produce

1227 cytokines, chemokines, and extracellular matrix proteins, that promote the migration of

1228 residual GB cells towards the margins of the resection or in the normal brain parenchyma. The

1229 chemo-attractive potential of BC loaded with normal medium and with GASCs conditioned

1230 medium (GASC-CM) was assessed by the Transwell migration assay, and higher cell migration

1231 rates through the Transwell were noted towards GASC-CM loaded BC compared to BC loaded

1232 with normal medium. SEM analysis clearly highlighted good cell adhesion, with no further

1233 migration for up to 72 hours of contact. It was also demonstrated that BC is visible through

1234 MRI and diffusion images owing to the presence of many water molecules trapped in the

1235 polymer network. This feature was found to be particularly important when the membranes

1236 were implanted in the brain parenchyma of female syngeneic Fisher rats and their behaviour

1237 was monitored over time. The imaging showed no signs of degradation for up to one year after
1238 implantation, making it possible for targeted therapies to clearly isolate the area of interest.
1239 Histological studies showed that only a mild inflammation reaction (which decreased over
1240 time) with formation of a thin fibrous capsule around the membrane occurred upon BC
1241 implantation. Nevertheless, no major adverse effects were observed in the time frame
1242 considered, with deposition of brain cells on the surface of the scaffold after 12 months,
1243 highlighting the biocompatibility of the material (Figure 6 B) [165].

1244

1245 **4.5.3 Tissue engineering**

1246 Material scientists have been exploiting the water responsive and mechanically adaptive
1247 properties of BC to develop smart materials [110, 196] for use in cornea replacements [197],
1248 and in biology-device interfaces [198].

1249

1250 An interesting study by Niamsap *et al.* [199] presented a method to develop a BC-based
1251 composite for bone tissue engineering through *in situ* addition of plant-derived cellulose
1252 nanocrystals (CNC) and hydroxyapatite (HA). CNCs were obtained through extraction from
1253 sugarcane bagasse by steam-explosion, bleaching with sodium chlorite, followed by hydrolysis
1254 with sulphuric acid; calcium hydroxide and phosphoric acid were then mixed with the CNCs
1255 to yield the formation of CNC/HA nanocrystals (HC). The scaffolds were then produced by
1256 the introduction of both HC and HA at different concentrations (namely, 0.25 and 0.5%) into
1257 the culture medium of BC to obtain, respectively, BC/HA/CNC (BHC) and BC/HA (BHA).
1258 The elemental dispersion spectroscopy analysis highlighted that the amount of HA
1259 nanoparticles was higher in the BHC system, with Ca and P concentrations twice as high as
1260 compared to BHA for both loadings. The result was ascribed by the authors to the stabilisation
1261 effect of the CNC, which prevented the aggregation of the HA nanoparticles through hydrogen

1262 bonding and/or interaction between the negative hydroxyl groups of cellulose and the cationic
1263 charges of HA. In addition to this, an increasingly higher degradation temperature was
1264 registered for the BHC composites in a proportional manner to the HC content as compared to
1265 pristine BC, probably due to the close interconnection between the mineral phase and the
1266 nanofibrillar network of BC achieved through the *in situ* modification approach. The
1267 cytotoxicity of the extracts of the material with 0.5% HC concentration was also evaluated
1268 towards a mouse fibroblast cell line, and higher cell viability was observed with respect to the
1269 positive control, i.e. polyurethane film with 0.1% zinc diethyldithiocarbamate, proving the
1270 applicability of the composites as potential scaffolds in the field of bone tissue engineering
1271 [199].

1272

1273 Zhang *et al.* [200] proposed an interesting method to develop 3D BC/collagen porous
1274 microspheres for applications in bone tissue engineering through oxidation of cellulose
1275 followed by chemical cross-linking with collagen. More specifically, 2,3-dialdehyde BC
1276 (DABC) was obtained through the Malaprade reaction using sodium periodate. Afterwards, a
1277 Schiff-base formation reaction was carried out between the aldehydic groups of DABC and the
1278 free amino groups of type I collagen to yield collagen-DBAC (CDABC). The microspheres
1279 were then produced by the template method combined with the solvent releasing method by
1280 the means of an ionic liquid (IL) [201]. The procedure consisted of the dispersion of CDABC
1281 into the IL phase, followed by the addition of hexadecane to form an emulsion. This was then
1282 poured into n-butyl alcohol to generate the microspheres through precipitation. Bone
1283 morphogenetic protein 2 (BMP-2) was also loaded by physical absorption to induce bone
1284 regeneration. A nitrogen adsorption/desorption assay was conducted to quantify the specific
1285 surface area and pore diameter distribution of the microspheres, which showed a mesoporous
1286 behaviour, with the adsorption isotherm non-coincident with the desorption isotherm. The cell

1287 biocompatibility of the scaffolds was then evaluated towards mice pre-osteoblasts MC3T3-E1
1288 cells, and their osteogenic performance was observed over 14 days by alkaline phosphatase
1289 (ALP) and alizarin red staining. Cell viability in the range of 105-130%, as compared to the
1290 positive control, Tissue Culture Plastic (TCP), was observed in the case of BC, collagen, and
1291 BC/collagen microspheres up to 96 hours after contact, showing that the protein treatment
1292 successfully promoted the proliferation. In addition, stronger osteoblast differentiation ability
1293 was shown by the BC/collagen scaffold even without BMP-2, as compared to pristine BC and
1294 collagen, probably because of the larger specific surface area [200].

1295

1296 A different approach was undertaken by Klinthoophamrong *et al.* [167] who worked on the
1297 incorporation of osteopontin into BC through surface chemical functionalisation (Figure 6C).
1298 Osteopontin (OPN) is a phosphoprotein present in the bone and at the interface with the tissue
1299 promoting bone formation and cell adhesion. OPN can be extracted from the leaves of the
1300 tobacco plant (*Nicotiana benthamiana*), to yield a plant-derived recombinant OPN (p-rhOPN)
1301 with the same structure as the one obtained from mammalian cells. In this study, the protein
1302 was incorporated into BC through conjugation with poly(acrylic acid) (PAA). To achieve this,
1303 PAA was first grafted onto the surface of BC by reversible addition fragmentation chain-
1304 transfer (RAFT) polymerisation using 4,4'-Azobis(4-cyanovaleric acid) as the initiator. First,
1305 the mechanical characterisation of the modified material in wet conditions was carried out, and
1306 no significant difference was observed as compared to pristine BC, proving that the
1307 incorporation of PAA did not influence the performance of the hydrogel. After this, the
1308 carboxyl groups of PAA were reacted with the amino-groups of p-rhOPN via an amide bond
1309 formation to covalently immobilise the protein on the surface of the membrane. An ELISA
1310 assay was then conducted to quantify the unbound protein as compared to the initial loading,
1311 and an immobilisation efficiency of 97% was registered. The biocompatibility studies towards

1312 human periodontal ligament stem cells (hPDLSCs) evidenced significantly higher cell viability
1313 with respect to BC (both with and without PAA), with better cell adhesion and no adverse
1314 effect on the cell morphology as compared to the positive control (i.e. commercial rh-OPN). In
1315 addition to this, ALP and Alizarin Red S staining showed improved osteogenic differentiation
1316 ability and higher calcium deposition levels with respect to unmodified BC, suggesting the
1317 capacity of the p-rhOPN containing composite to support bone regeneration [167].

1318

1319 In the context of soft tissue engineering, the development of BC sheets for the regeneration of
1320 gut muscle has been recently proposed by Lamboni *et al.* [171]. The gastrointestinal tract can
1321 be subjected to surgical resection of impaired segments that cannot guarantee the peristalsis,
1322 i.e. physiological motility. This approach, however, can result in short bowel syndrome, which
1323 can in turn alter the absorption of nutrients and cause malnutrition in the long term. To
1324 overcome this issue, tissue engineering strategies have been investigated involving the
1325 replacement of the damaged tissue. In this context, it is fundamental to ensure good cell
1326 alignment of smooth muscle cells (SMCs) to ensure the contraction of SM layers for the
1327 transport of nutrients and waste. In the work presented, BC was modified with silk sericin (SS)
1328 to produce a matrix that can support the growth and orientation of SMCs while interacting with
1329 the enteric nervous system (ENS) cells. SS demonstrated good cell adhesion and proliferation
1330 towards neuronal cells as well as angiogenic properties, whereas the nanofibrillar network of
1331 BC naturally resembles that of ECM. To achieve this, microstructured BC (mBC) was
1332 produced by *in situ* moulding with a poly(dimethylsiloxane) (PDMS) template to obtain a
1333 microgroove pattern, which was confirmed by SEM analysis. Microgrooves of 10 μm width
1334 were formed, as it has been observed that widths in the range between 5 and 20 μm can support
1335 cell alignment. After this, SS was incorporated through immersion of the pellicles into different
1336 solutions at increasing SS concentrations (i.e. 1 and 2 wt%) to obtain two composites

1337 (respectively, BC-SS1 and BC-SS2). Mechanical testing of the composites evidenced a
1338 decrease in the stiffness, with lower elongation at break and higher Young's modulus probably
1339 due to the brittle nature of SS; nevertheless, the values were found to be in the optimal range
1340 for applications in gut tissue repair. The biological performance of the materials was then
1341 evaluated and compared to random BC (rBC), i.e. BC not treated with the PDMS template.
1342 SMCs were seeded directly onto the samples, and improved alignment, but lower cell number
1343 was observed in the case of mBC as compared to rBC. mBC-SS, on the other hand, presented
1344 higher cell viability, with highest values for mBC-SS1, without the disruption of cell alignment.
1345 In addition to this, the effect of the sericin composites towards the differentiation of neural
1346 stem cells was assessed. Enhanced neurite outgrowth and cell patterning was shown in the
1347 presence of sericin, highlighting the ability of the system to successfully induce cell growth
1348 and differentiation [202].

1349

1350 **4.5.4 Cell culture**

1351 Over the last few decades scientists have been constantly improving the *in vitro* culture of cells
1352 to obtain best results. Zhou *et al.* [203] worked on the improvement of cell adhesion and
1353 viability onto BC to further optimise its biomedical performance. The chemical structure of BC
1354 was modified by incorporation of a carboxymethyl group through addition of lyophilised
1355 carboxymethyl cellulose into the fermentation medium. The resulting membrane was analysed
1356 by scanning electron microscopy (SEM), which evidenced a much denser network with a
1357 decrease in the average pore size from 0.32–1.18 μm for pristine BC to 0.07–0.72 μm for
1358 carboxymethyl BC (CMBC). In addition to this, the BC titre increased by $\sim 28\%$, probably due
1359 to the higher viscosity of the culture broth, thereby promoting the production of BC on the
1360 surface. The biological analyses carried out on BC and CMBC also outlined a different
1361 behaviour for the two hydrogels. First, human corneal endothelial cells were seeded on their

1362 surface: much higher cell adhesion was observed for CMBC upon cell membrane staining,
1363 especially at the early stage, while BC had uneven distribution after seven days and 12% lower
1364 cell viability. An *in vivo* experiment was conducted by implanting the two materials into the
1365 back muscles of rabbits. The test confirmed the previous results, with lower inflammatory
1366 response in the case of CMBC and improved attachment of the tissue to the membrane. This
1367 was explained by the increased protein affinity and altered contact angles and zeta potentials
1368 of CMBC, which could facilitate the interaction with cell membrane proteins [203].

1369

1370 He *et al.* [204] developed a multi-layered tubular cellulose hydrogel and demonstrated that
1371 L929 cells could adhere and proliferate on the surface of the layers and in the interior space,
1372 showing great potential for use as a scaffolding material in tissue engineering, and as a cell
1373 culture carrier. Injectable hydrogels reinforced with CNCs [205] retained their original shape
1374 in water or in a buffer even after 60 days. Moreover, no significant cytotoxicity was observed
1375 using 3T3 fibroblasts using a biochemical assay.

1376

1377 3D models for cell culture, considered current state of the art, have also been developed to
1378 improve the *in vitro* investigation of cellular responses in various conditions. The use of BC to
1379 study glioblastoma (GB) was investigated by Unal *et al.* [206]. They focused on the
1380 development of a 3D model to mimic the chemical composition and topography of the GB
1381 extracellular matrix (ECM). To achieve this, they used BC as a reinforcing phase to be
1382 incorporated into a polycaprolactone/gelatin (PCL/Gel) composite. First, BC nanocrystals were
1383 prepared through dehydration of the pellicles followed by acid hydrolysis using sulphuric acid.
1384 The 3D scaffold was then obtained via electrospinning of a 1:1 acetic acid/formic acid
1385 suspension containing 1:1 w/w PCL:gelatin (in the form of pellets) with increasing BC content,
1386 namely, 0.5% and 1 wt%, to yield, respectively, PCL/Gel/BCNC0.5 and PCL/Gel/BCNC1.0.

1387 The random nano-fibres were collected and tested with respect to their structural and biological
1388 properties. The SEM analysis revealed lower homogeneity for higher BC concentration,
1389 probably due to the increased repulsive force caused by its interaction with gelatin, which
1390 resulted in higher charge density on the jet coming out of the needle during electrospinning.
1391 The cytotoxicity of the composites towards GB cells was also evaluated, and improved cell
1392 viability was registered in the presence of cellulose as compared to the PCL/Gel scaffold. In
1393 addition to this, SEM imaging clearly showed the adhesion and spreading of the cells over the
1394 surface of the samples, with infiltration at a depth of 45 μm into the PCL/Gel/BCNC0.5
1395 scaffold after seven days of incubation and enhanced axonal growth and elongation. The result
1396 was ascribed to the suitable pore size between the nanofibres, which allowed the penetration
1397 of cells and nutrients, making the system a suitable environment for the proliferation of tumour
1398 cells [206]. A similar approach was proposed by Luo *et al.* [207] who developed an *in vitro*
1399 tumour model based on BC and cellulose acetate (CA). First, sub microfibrils of CA were
1400 produced via electrospinning of 15 wt% CA solution in 1:1 acetic acid/acetone. *In situ*
1401 incorporation was then achieved during BC production by *K. xylinus* X-2. A BC/CA scaffold
1402 was in fact produced by the growth of BC into the CA scaffold through deposition of the culture
1403 medium directly onto the fibres. Morphological characterisation of the hydrogel showed an
1404 interconnected network of nanofibrillar BC and sub-micro-fibrous CA, with homogeneous
1405 distribution of each component both on the surface and in the cross-sectional region. The
1406 porosity of the materials was also estimated through the liquid displacement method using
1407 ethanol, and over 90% of porosity was registered for BC/CA, which could facilitate cellular
1408 ingrowth into the scaffold. Significantly higher proliferation of MCF-7 breast cancer cells was
1409 observed for BC/CA as compared to pristine BC and CA, and larger cell clusters were formed,
1410 as evidenced by rhodamine phalloidin and DAPI staining. The infiltration of cells into the
1411 scaffolds was also investigated, and enhanced penetration was noted for CA and, especially,

1412 BC/CA, probably because of the small pore size of pristine BC. In addition to this, higher
1413 resistance was demonstrated by cells seeded onto BC/CA as compared to those seeded on CA
1414 and BC respectively, towards doxorubicin (an anticancer drug), highlighting the similarity of
1415 the system with *in vivo* conditions, where cell-to-cell and cell-to-matrix interactions can
1416 promote 3D proliferation and contribute to increased drug tolerance [207].

1417

1418 Bayir *et al.* [208] reported the use of BC as a basement membrane (BM) to develop an *in vitro*
1419 static model of a blood-brain barrier (BBB). The BBB deals with maintaining the homeostasis
1420 of the central nervous system (CNS) by regulating the permeability of various substances from
1421 the blood vessels to the brain. However, the BBB can also prevent drugs from reaching the
1422 CNS, for instance in the treatment of neurodegenerative diseases and brain tumours. To test
1423 the permeability of drugs, several studies focused on the design of *in vitro* BBB models. In this
1424 work, a static model was produced, i.e., a model not involving blood flow, as opposed to
1425 dynamic models that simulate the effect of the shear stress of the blood flow. BC and
1426 polyethylene terphthalate (PET) were then used as the BM. The BM is a specific type of
1427 extracellular matrix (ECM) that coordinates with the BBB in modulating the intercellular
1428 signalling, supporting its structure and mediating cell attachment and migration [208]. Through
1429 the use of Transwell inserts, three different culturing methods were applied, namely
1430 monoculture, co-culture and triple culture; more specifically, the upper and the lower sides of
1431 the Transwell were used to mimic, respectively, the luminal and the abluminal part of the blood
1432 vessel (i.e. BC or PET, attached to the inserts). In all cultures, brain microvascular endothelial
1433 cells were seeded on the luminal side; in the contact co-culture (where the second cell type is
1434 seeded on the abluminal side) astrocytes or pericytes were used, whereas in the triple culture
1435 both pericytes and astrocytes were seeded on the abluminal side (Figure 6C). Transendothelial
1436 electrical resistance (TEER) was then measured to evaluate the barrier properties of the two

1437 BMs. This value, which indicates the integrity of the barrier, is generally higher in dynamic
1438 models, probably because of more realistic conditions. In the study performed, statistically
1439 significant, higher TEER was observed in the case of BC compared to PET, especially in the
1440 co-culture models. In particular, TEER values closer to $150 \Omega \cdot \text{cm}^2$ were obtained vs $100 \Omega \cdot \text{cm}^2$
1441 for the PET models; this is considered the minimum value that is suitable for pharmaceutical
1442 studies, therefore making BC a better alternative for the development of BBB *in vitro* models
1443 [166].

1444

1445 **4.5.5 Artificial blood vessels**

1446

1447 BC has been researched for some years as a material for the production of artificial blood
1448 vessels due to the suitability of many of its properties, including its biocompatibility, fine
1449 fibrous network architecture, and good tensile strength.

1450

1451 As previously mentioned, BC is a biomaterial that can be used effectively as a drug carrier.
1452 This was utilised in research by Li *et al.* [209] in which they included chitosan into small
1453 vascular grafts made of bacterial nanocellulose (BNC), created using double silicone tube
1454 bioreactors; the addition of chitosan increased the grafting ability of the artificial blood vessel
1455 constructs. Heparin, an anticoagulant drug, was grafted into the construct and bonded to both
1456 the BC hydroxyl groups as well as the additional amino groups of the chitosan. These tubes of
1457 BC plus chitosan and heparin had an increased level of cell biocompatibility compared to
1458 constructs with BC alone, and the authors suggest that this may be due to the heparin
1459 encouraging water retention in the BC which then aids in nutrient transport to the cells. It was
1460 also hypothesised that due to chitosan's degradability *in vivo*, there is potential that this could
1461 aid in the controlled slow release of drugs such as heparin once the construct is implanted, and
1462 this is suggested as a topic of further study.

1463 A key issue that can arise with creating tubular tissue engineered constructs is trying to seed
1464 the construct with cells in its tubular state, whereas cells will much more easily adhere onto a
1465 flat scaffold in culture. For example, a study by Li *et al.* [210] created small-diameter blood
1466 vessels using shape-memory BC. This was achieved by rolling BC into a tubular structure and
1467 subsequently lyophilising it, creating creases and an arrangement of fibres which produced an
1468 inner stress on the inside layers of BC, thus causing the self-rolling shape-memory nature of
1469 the BC. The researchers found that this enabled them to flatten out the BC membrane in order
1470 to seed it with cells using microfluidics-based patterning, whilst being able to reroll it into its
1471 previous tubular structure. The use of microfluidics-based patterning allows different cell
1472 types, here endothelial cells, fibroblasts, and smooth muscle cells, to be seeded in a controlled
1473 design. This study went as far as animal studies in a rabbit model, and the main result shown
1474 was that there was no thrombus formation over three weeks post-implantation. An advantage
1475 for the use of BC in this application and technique is that it provides a quicker way to create
1476 cell populated vascular replacements [210].

1477

1478 Whilst BC can be used for the creation of artificial blood vessels, it can also be used to
1479 encourage the growth of new native blood vessels by promoting neovascularisation. In a study
1480 by Wang *et al.* (2018) [168] BC and gelatin 3D porous scaffolds were made, modified with
1481 heparin and subsequently loaded with vascular endothelial growth factor (VEGF). Heparin is
1482 able to bind growth factors such as VEGF through electrostatic interactions, and it also protects
1483 VEGF from proteolytic degradation, thus retaining its bioactivity. Previous studies had
1484 heparinised materials including ePTFE, PEG, and collagen, however PTFE and PEG lack a
1485 nanofibrous structure which promotes cell adhesion, and collagen has drawbacks in terms of
1486 immunogenicity. The use of BC, however, enabled the researchers to achieve a controlled
1487 release of VEGF over time through heparinisation, whilst exhibiting a lack of immunogenicity

1488 as well as a nanofibrous structure. In this study BC was combined with gelatin with eliminated
1489 antigenicity as it has a similar chemical composition to that of collagen without the
1490 immunogenicity issues. Through *in vitro* studies, the VEGF-loaded scaffolds exhibited
1491 increased cell migration and proliferation as compared to scaffolds without VEGF (Figure 6D).
1492 As seen with the other studies using BC, this scaffold had good biocompatibility *in vivo* and
1493 results showed that this scaffold increased the amount of angiogenesis that occurred *in vivo*.

1494

1495 **4.5.6 Additive manufacturing (3D Printing)**

1496 The advancement of biomedicine has also resulted in the requirement of more complex
1497 biomedical devices and scaffold materials. In the pursuit of better ways to repair tissue damage,
1498 materials are needed with tuneable properties as well as the ability to produce complex
1499 structures. As discussed above, production of blends or composite materials result in tuneable
1500 properties. These materials by themselves often do not have the necessary structural designs
1501 for them to be applied to specific biomedical applications. It is here where 3D printing is
1502 proving to be an excellent tool to enable the production of complex structures in three
1503 dimensions. 3D printing, also known as additive manufacturing, can be used to produce 3D
1504 structures via a layer by layer (LBL) process. In additive manufacturing the material deposition
1505 is controlled by means of computer aided design (CAD) technology allowing for simple
1506 bottom-up production of complex designs. Very few examples currently exist where BC is
1507 explicitly used in the fabrication of 3D scaffolds.

1508

1509 Recently, a tuneable scaffold material based on TEMPO-oxidised (2,2,6,6-
1510 tetramethylpiperidiny1-1-oxyl) BC, Alginate (Al) and laponite nanoclay (XI) was described
1511 by Wei *et al.* They produced 3D printed scaffolds via gel extrusion and were able to tune the
1512 scaffold degradability as well as the release of bovine serum albumin (BSA), as a model

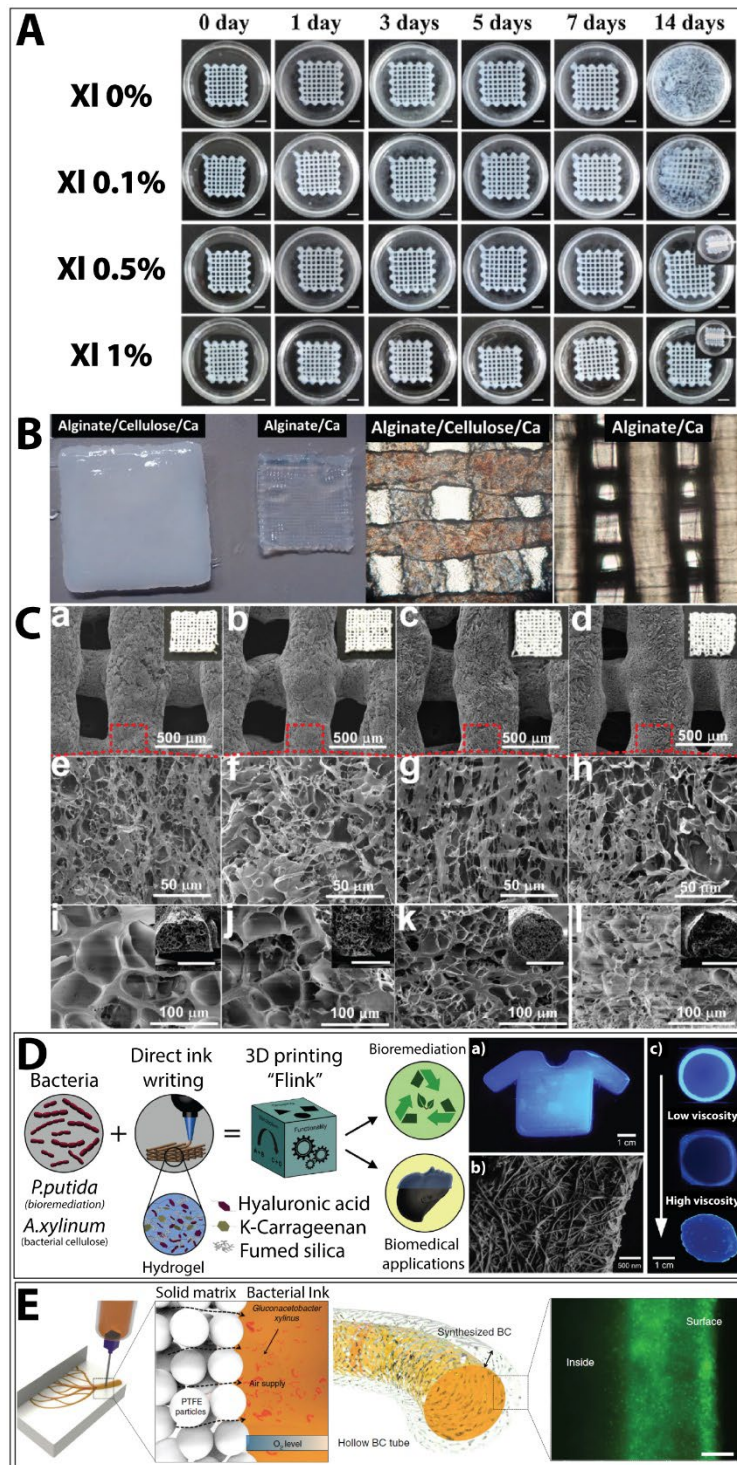
1513 compound, *in vitro*. With increasing the amount of XI, the *in vitro* scaffold degradation time
1514 (in PBS at 37 °C) increased, also decreasing the rate of BSA release (Figure 7A). However,
1515 cell studies with fibroblasts showed that increasing the content of XI above a threshold of
1516 0.5 % slowed the release of BSA so significantly that this was detrimental for cell proliferation
1517 [211]. Another example of a BC/Alginate hydrogel matrix was described by Gutierrez *et al.*
1518 [212] where they incorporated copper nanostructures into the matrix to produce a printable and
1519 antimicrobial 3D printed structures. The authors discussed how the addition of BC into the
1520 alginate hydrogel helps to enhance the mechanical properties of the hydrogel and additionally
1521 enhances the printability of complex structures. They found that an alginate concentration of
1522 4 wt % gave good printability and the addition of BC at a ratio of 70/30 wt % enhanced the
1523 structural integrity of the hydrogel significantly (Figure 7B). The copper doped scaffolds hold
1524 antimicrobial functions against *E. coli* and *S. aureus*. Another example of enhanced mechanical
1525 properties of 3D printed hydrogel structures by the addition of BC was described by Huang *et*
1526 *al.* [213]. Here the authors 3D printed a BC/silk fibroin/gelatin/glycerol composite hydrogel
1527 ink and cross linked this by rinsing with ethanol or freeze drying the printed scaffolds. The
1528 hydrogels were printed at 25–30 °C to decrease the viscosity (arising from gelatin) and at print
1529 speeds of 3–5 mm·s⁻¹. With increasing BC ink content, the resulting mechanical properties of
1530 the 3D printed scaffolds increased drastically from tensile strengths of 100 kPa to 800 kPa
1531 (from 0 wt % to 0.7 wt% of BC). The scaffolds demonstrated a good self-recovery and
1532 compressive stress of 65 kPa at 30% strain, 2 times that of scaffolds without the addition of
1533 BC which the authors claim match natural tissue mechanical properties for human meniscus
1534 tissue applications. Further to this the resulting 3D scaffolds demonstrated an excellent
1535 hierarchical porous structure ideal for soft tissue repair applications (Figure 7C).
1536

1537 Another interesting concept of implementing BC into 3D printed scaffolds is the actual 3D
1538 printing of live bacteria and *in situ* formation/production of BC within the scaffold, enabling
1539 accurate directed growth of the fibres. In a study reported by Schaffner *et al.* [214] the authors
1540 printed a hydrogel consisting of hyaluronic acid (HAc), k-carrageenan, and fumed silica also
1541 called functional living ink (Flink) including the bacteria (*Acetobacter xylinum* for BC) The
1542 authors explained how the areas of the scaffold with higher oxygen content produced denser
1543 BC networks (Figure 7D). The resulting construct could be used both in bioremediation as well
1544 as for biomedical applications. In a similar approach, Shin *et al.* [215] 3D printed live
1545 *A. xylinum* bacteria in a growth medium containing mannitol into a solid matrix-assisted
1546 scaffold containing polytetrafluoroethylene (PTFE) microparticles and cellulose nanofibers
1547 (CNFs) (Figure 7E). Areas with high oxygen content led to increased production of BC. The
1548 authors used this to their advantage to produce hollow BC tubes postulated for use as potential
1549 vascular systems. After a 7-day incubation the CNF/BC tubes were washed, and collagen was
1550 crosslinked onto the surface. After this the bacteria were removed from the scaffolds and these
1551 sterilised prior to *in vitro* cell culture studies. The cytotoxicity on fibroblast cells was then
1552 investigated and the scaffold deemed viable.

1553

1554 In contrast to the previous mentioned studies Sämfors *et al.* [216], employed a sacrificial 3D
1555 Printing technique, where CT scan data of the outer edge of a kidney was used to produce a
1556 hollow kidney template made from clay to be used as a mould, in addition to this, a tree-like
1557 vasculature structure was printed separately with PLA. These two structures were then placed
1558 together and a homogenised, degassed blend of alginate and BC (10/90% w/w) was cast into
1559 the mould. This when then placed in a -80°C freezer for 24 hours and then gently heated to
1560 remove the outer mould and cooled down to -80°C for an additional 2 hours after which the
1561 structure was freeze-dried. Finally, the dried structure was crosslinked by submersion in

1562 100 mM CaCl₂ solution. The authors did not perform any further cell culture studies of the
1563 produced scaffolds, however this method may have merits in producing highly permeable
1564 complex 3D scaffolds with vasculature for future organ applications [216]. Despite there not
1565 being many current works on the 3D-printing of BC, research relating to 3D printing of
1566 cellulose containing inks are most likely to be extendable to BC containing inks. Currently 3D-
1567 printing of structures containing cellulose is mostly performed using commercial inks
1568 containing plant-based cellulose. However, there is no doubt that similar methodologies could
1569 be used for 3D-printing of BC-derived inks, which would result in a more eco-friendly and
1570 sustainable future for these inks.



1571

1572 Figure 7 **A)** Optical images of 3D-printed BC/Al/XI scaffolds in PBS solution showing the scaffolds degradation
 1573 over 14 days (Scale bar: 5 mm), adapted from Wei *et al.* [211]; **B)** Comparative photographic and optical
 1574 microscopy images of 3D-printed hydrogel scaffolds produced using pure alginate inks at 4 wt % (right-side) and
 1575 the hydrogel scaffolds using BC/alginate inks having a solid content composition of 70/30 wt % (left-side), after
 1576 24 h immersion in a CaCl₂ solution, adapted from Gutierrez *et al.* [212]. **C)** SEM images of (a, e, i) BCNFs-0
 1577 wt%, (b, f, j) BCNFs-0.35 wt%, (c, g, k) BCNFs-0.70 wt%, (d, h, l) BCNFs-1.40 wt% scaffolds. (a–h) Surface
 1578 microstructure of printed scaffolds. (i–l) Cross section of printed filaments (Inserted scale bars: 500 μm), adapted
 1579 from Huang *et al.* [213]. **D)** Schematics of the 3D bacteria-printing platform for the creation of functional living
 1580 materials. Multifunctional bacteria are embedded in a bioink consisting of biocompatible HAC, k-carrageenan,
 1581 and Fumed silica (FS) in bacterial medium. **a)** *In situ* formation of bacterial cellulose by *A. xylinum* was used to
 1582 generate a 3D-printed scaffold with a 4.5 wt% Flink in the shape of a T-shirt. Bacterial cellulose is visualized with

1583 a specific fluorescent dye at 365 nm. **b)** Bacterial cellulose nanofibril network under SEM printed with a 3wt %
1584 Flink. **c)** Growth of bacterial cellulose dependent on oxygen availability and the viscosity of the Flink. Images
1585 shown, from top to bottom, circular prints using 3, 6, and 9 wt% Flinks, adapted from Schaffner *et al.* [214]. **E)**
1586 (left) Solid matrix-assisted 3D printing of bacteria containing ink: Bacteria containing ink were printed inside of
1587 solid matrix. Oxygen was supplied through the solid particles to the surface of the CNF ink containing *G. xylinus*,
1588 allowing the bacteria to metabolize. (right) Schematic illustration of a hollow CNF/BC tube. Utilizing the region-
1589 specific biosynthesis of BC at the surface of the printed CNF hydrogel. Movement of bacteria to the surface of
1590 the printed CNF/BC hydrogel structure after incubation for 7 days, adapted from Shin *et al.* [215].

1591

1592

1593 **5 Current commercial status:**

1594 The wide-range applications of BC across various sectors have led to an exponential growth in
1595 the commercialisation of BC. The global BC market was approximately USD 299 million in
1596 2019, which is expected to reach around 777 million by 2027 [217]. Edible BC is produced at
1597 a commercial scale in several Asian countries including Philippines, Thailand, Vietnam and
1598 Malaysia, sold under the trade name *nata de coco*.

1599

1600 Recently, biomedical applications of BC have gained considerable significance. In the
1601 biomedical sector; ‘Cellulose solutions LLC’ have developed, a non-toxic biocompatible
1602 wound dressing sold under the name Dermafill™. Another silver-based antimicrobial wound
1603 dressing, Nanoderm™, has been created by the Axcelon Biopolymers corporation.
1604 Furthermore, several other commercialised BC-based wound dressings are sold under the trade
1605 names Biofill®, Cellulon® and Gengiflex®. For another key application area BC Cosmetic
1606 face masks were developed by *Forschungszentrum für Medizintechnik und Biotechnologie*
1607 (*fzmb*), GmbH, Germany. Further to this JeNacell have extensively developed innovative BC-
1608 based materials for wound dressings, tissue engineering, cosmetics and filtration membranes.

1609

1610 The mechanical properties of BC make it an ideal candidate for another lucrative market in the
1611 manufacturing of diaphragms for electroacoustic transducers. Several manufacturers including,
1612 Acer. Audioquest, Creative, Klipsch, and Panasonic have developed headphones that are

1613 equipped with BC diaphragms. In other applications Puraffinity have developed ultrafiltration
 1614 membranes from bacterial-derived cellulose to target micro pollutants in wastewater.
 1615 Furthermore, CP Kelco have developed a BC-derived activated structurant sold under the brand
 1616 name ‘CELLULON™ Cellulose Liquid’ for laundry detergents and surfactant-based
 1617 formulations. In the textile industry, Biofabricate founded by a British fashion designer
 1618 Suzanne Lee have created fabrics using BC named *Biocouture* with leather like qualities
 1619 (Figure 4 E). Undoubtedly, due to its unique features BC can be utilized to produce value-
 1620 added products for many industrial applications and bio-medical sectors as shown in **Table 4**.

1621

1622 **Table 4:** Worldwide bacterial cellulose producing companies.

#	Name	Type of BC	Applications	Company
1	<i>Nata-de-coco</i>	Pristine	Candied food in Asian countries	Profood International Corp, Borman’s, Buenas, Filtaste, Tita Ely, Mega Prime
2	Cellulon™	Pristine	Food hydrocolloids	CP Kelco
3	Nanoderm™ Ag	Pristine	Wound dressing	Axcelon Biopolymers Corp
4	Dermafill	Pristine	Wound dressing	Cellulose solutions Ltd
5	Gengiflex®	Pristine	Wound dressing	BioFill--Productos Biotecnologicos
6	Biofill®	Pristine	Wound dressing	Robin goad
7	Epicite, Epinouvelle, Biocellic	Functionalised BC	Cosmetics	JeNaCell GmbH
8	Nanomasque	Pristine	Cosmetics, veterinary, medical	fzmb GmbH
9	Biocellulose	Pristine	Diaphragms for headphones	Acer, Audioquest, Creative, Klipsch, Panasonic
10	Coated bacterial cellulose	Pristine	Rheology modifier in detergents	The Procter & Gamble Company
11	Biofabricate	Pristine/Dyed	Textiles – fashion	BioCouture
12	Adsorbent beads	Functionalised BC	Filtration	Puraffinity

1623

1624 **6 Future Outlook:**

1625 In the pursuit of sustainable green materials BC offers an excellent opportunity to meet the
1626 recent trends. It is suitable for a large variety of applications in industrial and biomedical
1627 sectors, however, current high production costs and low-yields has limited the large-scale
1628 production of BC and its commercial applications. In order to address this the development of
1629 novel bioreactor designs has greatly helped improve the yields obtained and thus these new
1630 systems will need to be applied at industrial scale, resulting in vastly lowered production costs.
1631 Another possibility of reducing production costs, especially useful when integrating BC for
1632 large-scale bioconcrete applications, is a portable onsite production of BC, which would
1633 eliminate transportation costs of the cellulose suspensions.

1634

1635 In its natural form, cellulose is insoluble in water but its derivatised forms, such as ethyl
1636 cellulose (EC), cellulose acetate (CA) and carboxymethyl cellulose (CMC), sodium
1637 carboxymethyl cellulose (NaCMC), methyl cellulose (MC), hydroxypropyl cellulose (HPC)
1638 and hydroxypropylmethyl cellulose (HPMC), are more soluble and good film formers. This
1639 enables them to be highly suitable for wound healing, tissue engineering, food packaging
1640 industry and used as edible films in coating applications e.g. for fruits.

1641

1642 Another key advantage of BC is its low endotoxin content, high-water holding capacity, as well
1643 as natural purity, giving it great potential for a vast array of biomedical applications including
1644 the development of wound dressings, 3D scaffolds for tissue engineering, as well as for drug-
1645 delivery applications. *In situ* and *ex situ* modifications of BC can be utilised to achieve
1646 application oriented custom designed materials. This can include the functionalisation of BC
1647 to introduce antibacterial functional groups to develop antibacterial and biocompatible wound
1648 dressings. Furthermore, novel techniques such as pressurised gyration as well as the novel

1649 portable electrohydrodynamic gun mentioned previously will help in the upscaling and
1650 administering of novel customisable wound healing patches. Similarly, highly biocompatible
1651 ultrafine cellulosic nanofibers can be prepared using BC via the electrospinning technique in
1652 order to produce highly directional scaffolds, ideal for tissue engineering applications, where
1653 directed cell alignment is essential, such as for neural applications. To further develop the
1654 production of highly complex structures aimed at mimicking natural tissues and organs, the use
1655 of 3D printing (additive manufacturing) with BC represents an ideal technology. Here in
1656 particular, the high tensile strengths and excellent permeability of BC are of high value to
1657 produce highly suitable composites via 3D Printing. Bioelectronics and sensors based on BC
1658 are eco-friendly options with longevity due to their excellent mechanical properties. For the
1659 treatment of industrial wastewater and elimination of pollutants, metallic catalytic
1660 nanoparticles can be stabilised with BC. Furthermore, superabsorbent BC composites for
1661 bioremediation applications also give rise to the potential for multiple regeneration cycles, thus
1662 lowering the overall costs when applying these composites in these applications. In the paper
1663 industry BC is the ideal candidate for coating paper as it gives excellent properties of gloss,
1664 smoothness, ink receptivity and holdout, and surface strength, therefore, suitable for printing
1665 materials as well as in paper restoration applications.

1666
1667 Many applications currently based on plant-cellulose could easily be replaced with bacteria-
1668 derived cellulose, which is naturally 100% pure and does not require any pre-treatment, saving
1669 on energy and operation costs. In conclusion, BC, is a highly versatile green material that has
1670 a huge potential for the development of novel smart materials of varied usage in numerous
1671 technologies, including bulk, biomedical and electronic applications, creating incredible eco-
1672 friendly opportunities for future industrial applications.

1673

1674 **Abbreviations**

- 1675 2AP: 2-acetyl-1-pyrroline
1676 AgNPs: Silver nanoparticles
1677 AGU: Anhydro Glucose Units
1678 Al: Alginate
1679 ALP: Alkaline Phosphatase
1680 AM: antimicrobial
1681 AP: Acetyl-1-Pyrroline
1682 BBB: Blood Brain Barrier
1683 BC: Bacterial Cellulose
1684 BCNC: Bacterial Cellulose Nanocrystal
1685 BCNW: Bacterial Cellulose Nano-Whiskers
1686 BCP: bacterial cellulose postbiotic composite
1687 BC-P: Bacterial Cellulose-Pandan
1688 BCS/PVA: Bacterial cellulose sulphate/polyvinyl alcohol
1689 BHA: Bacterial Cellulose - Hydroxyapatite
1690 BHC: Bacterial Cellulose - Hydroxyapatite - Cellulose nanocrystal
1691 BLF: Bovine Lactoferrin
1692 bLF: bovine lactoferrin
1693 BM: Basement membrane
1694 BMP: Bone Morphogenetic Protein
1695 BNC: Bacterial Nano Cellulose
1696 BSA: Bovine Serum Albumin
1697 Bzl: Benzyl
1698 CA: Cellulose Acetate
1699 CAD: Computer Aided Design
1700 CBC: Carbonised Bacterial Cellulose
1701 CCNT: Carboxylated Carbon Nano Tubes
1702 CDABC: Collagen Dialdehyde Bacterial Cellulose
1703 CFU : Colony Forming Unit
1704 CIP: Ciprofloxacin
1705 CM: Conditioned Medium
1706 CMBC: Carboxymethyl Bacterial Cellulose
1707 CMC: Carboxymethyl Cellulose
1708 c-MWCNTs: Carboxylated Multiwall Carbon Nanotubes
1709 CNC: Cellulose Nanocrystals
1710 CNF: Cellulose Nano Fibres
1711 CNS: Central Nervous System
1712 CNT: Carbon Nano Tubes
1713 CO₂: Carbon Dioxide
1714 CT: Computed Tomography
1715 Cu-Ag-WC: Copper, Silver and Tungsten (Wolfram) carbide nanoparticles
1716 Cu-Ag-Zn/CuO: Copper, Silver, Zinc and Copper oxide nanoparticles
1717 DABC: 2,3-Dialdehyde Bacterial Cellulose
1718 DAPI : 4',6-Diamidino-2-Pheny Lindole
1719 DFBBF - dry-fabricated biofilm
1720 DMA/LiCl: N, N-dimethylacetamide and lithium chloride
1721 DMF: Dimethyl Formamide
1722 Dox - Doxorubicin

1723 DP: Degree of Polymerisation
1724 DPV: Differential Pulse Voltammetry
1725 DVS: Divinyl Sulphone
1726 EC: Ethyl Cellulose
1727 ECM: Extracellular Matrix
1728 EDA: Ethylenediamine
1729 EMIMBF4: 1-Ethyl-3-Methyl Imidazolium Tetra FluoroBorate
1730 EMIMBF4: 1-Ethyl-3-Methylimidazolium tetrafluoroborate
1731 ENS: Enteric Nervous System
1732 FBC: Fluoride Bacterial Cellulose
1733 Flink: Functional Living Ink
1734 FTIR: Fourier Transform Infra-Red
1735 GASC: Glioblastoma Associated Stromal cells
1736 GB: Glioblastoma
1737 Gbc: Glybenclamide
1738 GC: glossy-finished coating
1739 GEL: gelatine
1740 GI: gastrointestinal tract
1741 Glc-1-P: Glucose-1-phosphate
1742 Glc-6-P: Glucose-6-phosphate
1743 GOPA: Graphene Oxide Polymer Aerogel
1744 GPa: GigaPascals
1745 Gt: Gigatons
1746 HA: Hydroxy Apatite
1747 HAc: Hyaluronic Acid
1748 HCF: Hexa Cyano Ferrate
1749 HEC: Hydroxy Ethyl Cellulose
1750 HF: Hydro Fluoric
1751 HNO₃: Nitric acid
1752 HPC: Hydroxypropyl Cellulose
1753 hPDLSC - human periodontal ligament stem cells
1754 HPMC: Hydroxypropyl Methylcellulose
1755 IC50: Half maximum Inhibitory concentration
1756 IL: Ionic Liquid
1757 JP: Japanese paper
1758 LA: lauric acid
1759 LBL: Layer By Layer
1760 LCA: Life Cycle Assessment
1761 mBC: Microstructured Bacterial Cellulose
1762 MC: matte-finished coating
1763 MC: Methylcellulose
1764 Met: Metformin
1765 MRI: Magnetic Resonance Imaging
1766 NaCMC: Sodium Carboxyl Methyl Cellulose
1767 NaF: Sodium Fluoride
1768 NCM: Nano Cellulose Material
1769 NiHCF: Nickel Hexacyanoferrate
1770 NMBA: N,N-Methylene Bis-Acrylamide
1771 NP: nanoparticles
1772 OPN: Osteopontin

1773 PAA: Poly Acrylic Acid
1774 PBS: Phosphate Buffered Saline
1775 PCL: Poly Capro Lactone
1776 PCS: Plastic Composite Support
1777 PDMS: Poly Di Methyl Siloxane
1778 PEDOT: Poly-(3,4-Ethylene Dioxy Thiophene
1779 PEG: Polyethylene Glycol
1780 PEI: Polyethylene Imine
1781 PEO: Poly(ethylene oxide)
1782 PET: Polyethylene terephthalate
1783 PLA: Polylactic acid
1784 PPy: Polypyrrole
1785 p-rhOPN - plant-derived recombinant OPN
1786 PTFE: Poly Tetra Fluoro Ethylene
1787 PVP: polyvinyl pyrrolidone
1788 RAFT: Reversible Addition Fragmentation Chain-Transfer
1789 rBC: Random Bacterial cellulose
1790 RGO: Reduced Graphene Oxide
1791 ROS - reactive oxygen species
1792 SAP: Super Absorbent Polymers
1793 SC: super-calendered paper
1794 SCOPY: Symbiotic Culture of Bacteria and Yeast.
1795 SEM: Scanning Electron Microscopy
1796 SMC: Smooth Muscle Cells
1797 SPI: Soy protein isolate
1798 SS: Silk Sericin
1799 SSD: Silver Sulfadiazine
1800 TCP - tissue culture plastic
1801 TEER: Trans Endothelial Electrical Resistance
1802 TEM: transmission electron microscopy
1803 TEMPO: 2,2,6,6-Tetramethyl-1-piperidinyloxy
1804 TGA: Thermogravimetric Analysis
1805 TiO₂: Titanium Dioxide
1806 TO: 2,2,6,6-Tetramethylpiperidine-1-Oxyl
1807 TOBC: 2,2,6,6-tetramethylpiperidine-1-oxyl functionalised BC
1808 TPCs: thermoplastic corn starch
1809 TPCS: Thermoplastic Corn Startch
1810 UTS: Ultimate Tensile Strength
1811 UV: Ultra Violet
1812 VEGF: Vascular Endothelial Growth Factor
1813 WU: Wood-free uncoated
1814 WVP: Water Vapour Permeability
1815 XI: lamponite Nanoclay
1816 ZIF: Zeolitic Imidazolate Framework

1817
1818 **Funding**

1819 IR, DAG and VR were supported by the BBI/JU H2020 projects PolyBioSkin (Grant
1820 Agreement No. 745839) and ECOFUNCO (Grant Agreement No. 837863). LT and EA were
1821 supported by the BBI/JU H2020 project, ECOFUNCO (Grant Agreement No. 837863). AF

1822 was supported by a scholarship from the Department of Materials Science and Engineering,
1823 Faculty of Engineering, University of Sheffield. IO was supported by the European Union's
1824 Horizon 2020 research and innovation programme under the Marie Skłodowska-Curie grant
1825 agreement No 643050.

1826

1827 **Declaration of competing interest**

1828 The authors declare that they do not have any conflict of interests.

1829

1830 **Biographies**

Dr. David A. Gregory is a Post-Doctoral Research Associate in the Department of Materials Science and Engineering at the University of Sheffield. He received his PhD in 2015 on “Catalytic Micromotors” fully funded by an EPSRC scholarship and is an expert in on active colloids and additive manufacturing comprising Reactive Inkjet printing, Fused deposition modelling as well as gel extrusion printing technologies. David has a multidisciplinary background including production of bacterial derived polymers, material science, cell culture, physics, biochemistry, mathematics, programming and prototype development. Prior to his PhD he completed a MSc run jointly between Leeds and Sheffield Universities in Bionanotechnology, for which received a Sheffield University scholarship to cover course fees. He also undertook a BSc at the University of Lancaster in Physics and Astrophysics with Cosmology as well as a dual Honours BSc at Keele University in Biochemistry and Music. He has presented at several international conferences as an invited speaker, won best poster prizes and has published in several high impact peer reviewed journals as well as written three book chapters.



Dr. Lakshmi Tripathi is a Post-Doctoral Research Associate in Biochemical Engineering at the University of Sheffield. She received her PhD in Microbiology from the Tsinghua University, Beijing, China. She was a recipient of the prestigious Doctoral Scholarship awarded by the China Scholarship Council (CSC), the Government of China. She has worked with cross-functional teams for the discovery of new products from the discovery stage, through the development pipeline to proof-of-concept and commercialisation. Her areas of interest include Microbiology, Molecular Biology and Biochemical Engineering with expertise in upstream and downstream process development, bio-based polymers and microbial strain development for value-added compound production including Polyhydroxyalkanoates (PHAs), Bacterial Cellulose, Biosurfactants and Bio-emulsifiers. She has published in several SCI-indexed peer-reviewed journals.



Annabelle Fricker is a PhD student working in the tissue engineering group at The University of Sheffield. She received a BSc in Biology from The University of Bath and an MSc in Stem Cells and Regeneration from The University of Bristol. She was awarded a scholarship from the University of Sheffield to carry out her PhD research, which focuses on bioengineering heart tissue for the treatment of heart failure, and she has experience in the production of bacterial derived polymers, material processing techniques including 3D printing, and cell culture including that of induced pluripotent stem cells. She has published in peer-reviewed journals and contributed to a handbook of PHAs.



Emmanuel Asare is a University of Sheffield funded PhD student, undertaking a research project in the development of a PHA-based functional nerve guide conduit aimed at supporting the optimal regeneration and recovery of injured peripheral nerves. He has a BSc in Biological Sciences from the Kwame Nkrumah University of Science and Technology in Ghana, and an MSc in Applied Biotechnology at the University of Westminster in London. Also, he is currently involved in a European Union project BBI/JU H2020 – ECOFUNCO where he produces PHAs and bacterial cellulose for consortium partners for further use in various applications. He has gained hands-on experience in fermentation techniques, cell culture techniques and the use of various analytical and polymer processing techniques including 3D printing and CAD designing of tissue engineering scaffolds. He has published 2 peer reviewed papers and was awarded a prestigious travel grant, University of Westminster Fund125 for outstanding student initiative.



Dr Isabel Orlando obtained her BSc and MSc in Industrial Chemistry from the University of Bologna (Italy). In 2016 she joined an industrial doctoral programme named HyMedPoly, which she carried out between the University of Westminster in London and Vornia Biomaterials, a company producing medical grade polymers in Dublin. Her main research interest is the chemical modification of natural polymers and low molecular weight compounds to develop active materials for biomedical applications. More recently, she focused on the regulatory compliance of a range of polymers for food packaging in the context of EVASUMOD, a collaborative project between the Industrial technical centre for plastics and composites (IPC) and SIGMA graduate school of engineering in Clermont-Ferrand (France).



Dr. Vijayendran Raghavendran received his PhD in microbial biotechnology from Technical University of Denmark in 2005. He has had postdoctoral research experience at University of Pennsylvania (USA), University of Campinas (Brazil), Chalmers Institute of Technology (Sweden), University of Sheffield (UK) in addition to teaching chemistry at a secondary school (UK). He has expertise in bioethanol and biopolymers production and is a Fellow of the Higher Education Academy in the UK.



Professor Ipsita Roy has internationally recognized research expertise in sustainable natural biomaterials and their use in the manufacturing of biomedical scaffolds for hard and soft tissue engineering. She is currently a Professor at the Department of Materials Science and Engineering, Faculty of Engineering, University of Sheffield. Professor Roy completed her doctorate at the University of Cambridge and won many awards for her work including the Cambridge University Philosophical Society Fellowship Award. Her postdoctoral work was at the University of Minnesota, USA. She has published over 100 papers in biomaterials journals (H index of 39) and has delivered plenary and invited talks at numerous international conferences. Her group is currently focused on the production of a range of biobased polymers including Polyhydroxyalkanoates (PHAs), Bacterial Cellulose, γ -Polyglutamic acid, Alginate, and their use in biomedical and green bulk applications. She has pioneered the production of non-immunogenic PHAs from Gram-positive bacteria. Her total grant profile is currently worth 10 million.



1831
1832

1833 **References**

- 1834
1835 [1] S.Y. Lee, H.U. Kim, T.U. Chae, J.S. Cho, J.W. Kim, J.H. Shin, D.I. Kim, Y.-S. Ko, W.D.
1836 Jang, Y.-S. Jang, *Nature Catalysis* 2 (2019) 18-33.
1837 [2] A.K. H.P.S, A. Adnan, E. Yahya, N. Olaiya, S. Safrida, M. Hossain, V. Balakrishnan, D.
1838 Gopakumar, C. Abdullah, A.A. Oyekanmi, D. Pasquini, *Polymers* 12 (2020) 1759.
1839 [3] W.S. Williams, R.E. Cannon, *Appl Environ Microbiol* 55 (1989) 2448-2452.
1840 [4] F. Rol, M.N. Belgacem, A. Gandini, J. Bras, *Progress in Polymer Science* 88 (2019) 241-
1841 264.
1842 [5] P. Ross, R. Mayer, M. Benziman, *Microbiological reviews* 55 (1991) 35-58.
1843 [6] M. Schramm, S. Hestrin, *Microbiology* 11 (1954) 123-129.
1844 [7] Z. Lu, Y. Zhang, Y. Chi, N. Xu, W. Yao, B. Sun, *World Journal of Microbiology and*
1845 *Biotechnology* 27 (2011) 2281-2285.
1846 [8] M.U. Rani, N.K. Rastogi, K.A. Appaiah, *J Microbiol Biotechnol* 21 (2011) 739-745.
1847 [9] A. Vazquez, M.L. Foresti, P. Cerrutti, M. Galvagno, *Journal of Polymers and the*
1848 *Environment* 21 (2013) 545-554.
1849 [10] P. Carreira, J.A. Mendes, E. Trovatti, L.S. Serafim, C.S. Freire, A.J. Silvestre, C.P. Neto,
1850 *Bioresour Technol* 102 (2011) 7354-7360.
1851 [11] E.A. Skiba, V.V. Budaeva, E.V. Ovchinnikova, E.K. Gladysheva, E.I. Kashcheyeva, I.N.
1852 Pavlov, G.V. Sakovich, *Chemical Engineering Journal* 383 (2020) 123128.
1853 [12] H. Toyosaki, T. Naritomi, A. Seto, M. Matsuoka, T. Tsuchida, F. Yoshinaga,
1854 *Bioscience, Biotechnology, and Biochemistry* 59 (1995) 1498-1502.
1855 [13] Z. Cheng, R. Yang, X. Liu, X. Liu, H. Chen, *Bioresour Technol* 234 (2017) 8-14.
1856 [14] S. Kongruang, *Applied Biochemistry and Biotechnology* 148 (2008) 245.
1857 [15] S. Hestrin, M. Aschner, J. Mager, *Nature* 159 (1947) 64-65.
1858 [16] M. Hornung, M. Ludwig, H.P. Schmauder, *Engineering in Life Sciences* 7 (2007) 35-41.
1859 [17] D. Kralisch, N. Hessler, D. Klemm, R. Erdmann, W. Schmidt, *Biotechnology and*
1860 *Bioengineering* 105 (2010) 740-747.
1861 [18] Y.-J. Kim, J.-N. Kim, Y.-J. Wee, D.-H. Park, H.-W. Ryu, *Applied Biochemistry and*
1862 *Biotechnology* 137 (2007) 529.
1863 [19] K. Watanabe, M. Tabuchi, Y. Morinaga, F. Yoshinaga, *Cellulose* 5 (1998) 187-200.
1864 [20] A. Krystynowicz, W. Czaja, A. Wiktorowska-Jeziarska, M. Gonçaves-Miśkiewicz, M.
1865 Turkiewicz, S. Bielecki, *Journal of Industrial Microbiology and Biotechnology* 29 (2002)
1866 189-195.
1867 [21] Q. Cai, C. Hu, N. Yang, Q. Wang, J. Wang, H. Pan, Y. Hu, C. Ruan, *International*
1868 *Journal of Biological Macromolecules* 109 (2018) 1174-1181.
1869 [22] H. Zhu, S. Jia, H. Yang, Y. Jia, L. Yan, J. Li, *Biotechnology & Biotechnological*
1870 *Equipment* 25 (2011) 2233-2236.
1871 [23] Y. Hu, J.M. Catchmark, E.A. Vogler, *Biomacromolecules* 14 (2013) 3444-3452.
1872 [24] J. Kim, Z. Cai, H.S. Lee, G.S. Choi, D.H. Lee, C. Jo, *Journal of Polymer Research* 18
1873 (2011) 739-744.
1874 [25] V.I. Legeza, V.P. Galenko-Yaroshevskii, E.V. Zinov'ev, B.A. Paramonov, G.S.
1875 Kreichman, I.I. Turkovskii, E.S. Gumenyuk, A.G. Karnovich, A.K. Khripunov, *Bulletin of*
1876 *Experimental Biology and Medicine* 138 (2004) 311-315.
1877 [26] F.G. Blanco Parte, S.P. Santoso, C.-C. Chou, V. Verma, H.-T. Wang, S. Ismadji, K.-C.
1878 Cheng, *Critical Reviews in Biotechnology* 40 (2020) 397-414.
1879 [27] R. Portela, C.R. Leal, P.L. Almeida, R.G. Sobral, *Microbial Biotechnology* 12 (2019)
1880 586-610.

1881 [28] D. Kralisch, N. Hessler, D. Klemm, R. Erdmann, W. Schmidt, *Biotechnology and*
1882 *Bioengineering* (2009).

1883 [29] A. Sani, Y. Dahman, *Journal of Chemical Technology & Biotechnology* 85 (2010) 151-
1884 164.

1885 [30] T. Kouda, H. Yano, F. Yoshinaga, *Journal of Fermentation and Bioengineering* 83
1886 (1997) 371-376.

1887 [31] K.-C. Cheng, J.M. Catchmark, A. Demirci, *Biomacromolecules* 12 (2011) 730-736.

1888 [32] Z. Shi, Y. Zhang, G.O. Phillips, G. Yang, *Food Hydrocolloids* 35 (2014) 539-545.

1889 [33] J. Credou, T. Berthelot, *J. Mater. Chem. B* 2 (2014) 4767-4788.

1890 [34] R.H. Atalla, D.L. Vanderhart, *Science* 223 (1984) 283.

1891 [35] E.M. Van Zyl, J.M. Coburn, *Current Opinion in Chemical Engineering* 24 (2019) 122-
1892 130.

1893 [36] R.M. Brown, Jr., J.H. Willison, C.L. Richardson, *Proc Natl Acad Sci U S A* 73 (1976)
1894 4565-4569.

1895 [37] R. Jonas, L.F. Farah, *Polymer Degradation and Stability* 59 (1998) 101-106.

1896 [38] K.-Y. Lee, G. Buldum, A. Mantalaris, A. Bismarck, *Macromolecular Bioscience* 14
1897 (2014) 10-32.

1898 [39] I.M. Saxena, K. Kudlicka, K. Okuda, R.M. Brown, Jr., *J Bacteriol* 176 (1994) 5735-
1899 5752.

1900 [40] K. Zaar, *J Cell Biol* 80 (1979) 773-777.

1901 [41] R.M. Brown Jr., *Journal of Polymer Science Part A: Polymer Chemistry* 42 (2004) 487-
1902 495.

1903 [42] Y. Nishi, M. Uryu, S. Yamanaka, K. Watanabe, N. Kitamura, M. Iguchi, S. Mitsuhashi,
1904 *Journal of Materials Science* 25 (1990) 2997-3001.

1905 [43] B. Sun, L. Zhang, F. Wei, A. Al-Ammari, X. Xu, W. Li, C. Chen, J. Lin, H. Zhang, D.
1906 Sun, *Carbohydrate Polymers* 231 (2020) 115765.

1907 [44] X. Chen, X. Xu, J. Cui, C. Chen, X. Zhu, D. Sun, J. Qian, *Journal of Hazardous*
1908 *Materials* 392 (2020) 122331.

1909 [45] K. Schlufter, T. Heinze, *Macromolecular Symposia* 294 (2010) 117-124.

1910 [46] M. Nogi, K. Abe, K. Handa, F. Nakatsubo, S. Ifuku, H. Yano, *Applied Physics Letters*
1911 89 (2006) 233123.

1912 [47] S. Berlioz, S. Molina-Boisseau, Y. Nishiyama, L. Heux, *Biomacromolecules* 10 (2009)
1913 2144-2151.

1914 [48] J.A. Ávila Ramírez, C.J. Suriano, P. Cerrutti, M.L. Foresti, *Carbohydrate Polymers* 114
1915 (2014) 416-423.

1916 [49] T. Kamal, I. Ahmad, S.B. Khan, A.M. Asiri, *International Journal of Biological*
1917 *Macromolecules* 135 (2019) 1162-1170.

1918 [50] T. Kamal, I. Ahmad, S.B. Khan, M. Ul-Islam, A.M. Asiri, *Journal of Polymers and the*
1919 *Environment* 27 (2019) 2867-2877.

1920 [51] T. Kamal, I. Ahmad, S.B. Khan, A.M. Asiri, *Reactive and Functional Polymers* 145
1921 (2019) 104395.

1922 [52] Y. Chen, S. Chen, B. Wang, J. Yao, H. Wang, *Carbohydrate Polymers* 160 (2017) 34-42.

1923 [53] S. Pal, R. Nisi, M. Stoppa, A. Licciulli, *ACS Omega* 2 (2017) 3632-3639.

1924 [54] J. Hu, D. Wu, Q. Feng, A. Wei, B. Song, *Fibers and Polymers* 21 (2020) 1760-1766.

1925 [55] E. Akaraonye, J. Filip, M. Safarikova, V. Salih, T. Keshavarz, J.C. Knowles, I. Roy,
1926 *Journal of Nanomaterials* 2016 (2016) 1-14.

1927 [56] T.R. Stumpf, X. Yang, J. Zhang, X. Cao, *Materials Science and Engineering: C* 82
1928 (2018) 372-383.

1929 [57] F. Rol, C. Sillard, M. Bardet, J.R. Yarava, L. Emsley, C. Gablin, D. Léonard, N.
1930 Belgacem, J. Bras, *Carbohydrate Polymers* 229 (2020) 115294.

- 1931 [58] B.S. Inoue, S. Streit, A.L. dos Santos Schneider, M.M. Meier, *International Journal of*
1932 *Biological Macromolecules* 148 (2020) 1098-1108.
- 1933 [59] Y. Pöttinger, M. Rabel, H. Ahrem, J. Thamm, D. Klemm, D. Fischer, *Cellulose* 25
1934 (2018) 1-22.
- 1935 [60] K.S. Kontturi, K. Biegaj, A. Mautner, R.T. Woodward, B.P. Wilson, L.-S. Johansson,
1936 K.-Y. Lee, J.Y.Y. Heng, A. Bismarck, E. Kontturi, *Langmuir* 33 (2017) 5707-5712.
- 1937 [61] J.A. Ávila Ramírez, C. Gómez Hoyos, S. Arroyo, P. Cerrutti, M.L. Foresti,
1938 *Carbohydrate Polymers* 153 (2016) 686-695.
- 1939 [62] A.R.P. Figueiredo, A.G.P.R. Figueiredo, N.H.C.S. Silva, A. Barros-Timmons, A.
1940 Almeida, A.J.D. Silvestre, C.S.R. Freire, *Carbohydrate Polymers* 123 (2015) 443-453.
- 1941 [63] M. Pandey, M.C.I. Mohd Amin, N. Ahmad, M.M. Abeer, *International Journal of*
1942 *Polymer Science* 2013 (2013) 905471.
- 1943 [64] Y.-Y. Xie, X.-H. Hu, Y.-W. Zhang, F. Wahid, L.-Q. Chu, S.-R. Jia, C. Zhong,
1944 *Carbohydrate Polymers* 229 (2020) 115456.
- 1945 [65] Z. Li, L. Zhong, T. Zhang, F. Qiu, X. Yue, D. Yang, *ACS Sustainable Chemistry &*
1946 *Engineering* 7 (2019) 9984-9994.
- 1947 [66] E.Y.X. Loh, N. Mohamad, M.B. Fauzi, M.H. Ng, S.F. Ng, M.C.I. Mohd Amin,
1948 *Scientific Reports* 8 (2018) 2875.
- 1949 [67] H. Singh, R. Gupta, *Journal of building engineering* 28 (2020) 101090.
- 1950 [68] S. Jung, Y. Cui, M. Barnes, C. Satam, S. Zhang, R.A. Chowdhury, A. Adumbukulath,
1951 O. Sahin, C. Miller, S.M. Sajadi, L.M. Sassi, Y. Ji, M.R. Bennett, M. Yu, J. Friguglietti, F.A.
1952 Merchant, R. Verduzco, S. Roy, R. Vajtai, J.C. Meredith, J.P. Youngblood, N. Koratkar,
1953 M.M. Rahman, P.M. Ajayan, *Advanced Materials* 32 (2020) 1908291.
- 1954 [69] D. Zhao, Y. Zhu, W. Cheng, W. Chen, Y. Wu, H. Yu, *Adv Mater* (2020) e2000619.
- 1955 [70] H.M.C. Azeredo, H. Barud, C.S. Farinas, V.M. Vasconcellos, A.M. Claro, *Frontiers in*
1956 *Sustainable Food Systems* 3 (2019).
- 1957 [71] C.G. Eggensperger, M. Giagnorio, M.C. Holland, K.M. Dobosz, J.D. Schiffman, A.
1958 Tiraferri, K.R. Zodrow, *Environmental Science & Technology Letters* 7 (2020) 213-218.
- 1959 [72] C. Buruaga-Ramiro, S.V. Valenzuela, C. Valls, M.B. Roncero, F.I.J. Pastor, P. Díaz, J.
1960 Martínez, *Cellulose* 27 (2020) 3413-3426.
- 1961 [73] X. Zhu, T. Chen, B. Feng, J. Weng, K. Duan, J. Wang, X. Lu, *ACS Biomaterials Science*
1962 *& Engineering* 4 (2018) 3534-3544.
- 1963 [74] A. Chaiyasat, S. Jearanai, L.P. Christopher, M.N. Alam, *Polymer International* 68 (2019)
1964 102-109.
- 1965 [75] C.K. Chan, J. Shin, S.X.K. Jiang, *Clothing and Textiles Research Journal* 36 (2018) 33 -
1966 44.
- 1967 [76] S. Jiji, S. Udhayakumar, K. Maharajan, C. Rose, C. Muralidharan, K. Kadirvelu,
1968 *Carbohydr Polym* 245 (2020) 116573.
- 1969 [77] A. Arévalo Gallegos, S. Carrera, R. Parra, T. Keshavarz, H. Iqbal, *BioResources* 11
1970 (2016) 5641-5655.
- 1971 [78] E. Sukara, R. Meliawati, 2016 4 (2016).
- 1972 [79] A. Okiyama, M. Motoki, S. Yamanaka, *Food Hydrocolloids* 6 (1992) 479-487.
- 1973 [80] A. Okiyama, M. Motoki, S. Yamanaka, *Food Hydrocolloids* 6 (1993) 503-511.
- 1974 [81] Y. Guo, X. Zhang, W. Hao, Y. Xie, L. Chen, Z. Li, B. Zhu, X. Feng, *Carbohydrate*
1975 *Polymers* 198 (2018) 620-630.
- 1976 [82] S.M. Santos, J.M. Carbajo, E. Quintana, D. Ibarra, N. Gomez, M. Ladero, M.E. Eugenio,
1977 J.C. Villar, *Carbohydrate Polymers* 116 (2015) 173-181.
- 1978 [83] N. Gómez, S.M. Santos, J.M. Carbajo, J.C. Villar, 2017 12 (2017) 13.
- 1979 [84] N. Sriplai, P. Sirima, D. Palaporn, W. Mongkolthanaruk, S.J. Eichhorn, S. Pinitsoontorn,
1980 *Journal of Materials Chemistry C* 6 (2018) 11427-11435.

- 1981 [85] N. Saha, O. Zaandra, S. Bandyopadhyay, P. Saha, Bacterial Cellulose Based Hydrogel
 1982 Film for Sustainable Food Packaging, in: V. Katiyar, R. Gupta, T. Ghosh (Eds.), Advances in
 1983 Sustainable Polymers: Processing and Applications, Springer Singapore, Singapore, 2019, pp.
 1984 237-245.
- 1985 [86] G.K. Gbassi, T. Vandamme, *Pharmaceutics* 4 (2012) 149-163.
- 1986 [87] A.C. Khorasani, S.A. Shojaosadati, *International Journal of Biological Macromolecules*
 1987 83 (2016) 9-18.
- 1988 [88] T. Jayani, B. Sanjeev, S. Marimuthu, S. Uthandi, *Carbohydrate Polymers* 250 (2020)
 1989 116965.
- 1990 [89] J. Velásquez-Cock, E. Ramírez, S. Betancourt, J.L. Putaux, M. Osorio, C. Castro, P.
 1991 Gañán, R. Zuluaga, *International Journal of Biological Macromolecules* 69 (2014) 208-213.
- 1992 [90] M. Skočaj, *Cellulose* 26 (2019) 6477-6488.
- 1993 [91] G. Lavrič, D. Medvešček, M. Skočaj, Papermaking properties of bacterial nanocellulose
 1994 produced from mother of vinegar, a waste product after classical vinegar production, 2020.
- 1995 [92] E.J. Vandamme, S. De Baets, A. Vanbaelen, K. Joris, P. De Wulf, *Polymer Degradation*
 1996 *and Stability* 59 (1998) 93-99.
- 1997 [93] S. Yamanaka, K. Watanabe, N. Kitamura, M. Iguchi, S. Mitsunashi, Y. Nishi, M. Uryu,
 1998 *Journal of Materials Science* 24 (1989) 3141-3145.
- 1999 [94] Y. Jing, Z. Chuanshan, J. Yifei, H. Wenjia, The research of adding bacterial cellulose to
 2000 improve the strength of long-fiber paper, 2016 4th International Conference on Machinery,
 2001 Materials and Computing Technology, Atlantis Press, 2016, pp. 390-393.
- 2002 [95] K.A. Zahan, N.M. Azizul, M. Mustapha, W.Y. Tong, M.S.A. Rahman, I.S. Sahuri,
 2003 *Materials Today: Proceedings* (2020).
- 2004 [96] G. Schmidt-Traub, M. Obersteiner, A. Mosnier, *Nature* 569 (2019) 181-183.
- 2005 [97] J. Zheng, S. Suh, *Nature Climate Change* 9 (2019) 374-378.
- 2006 [98] C.G. Otoni, R.J. Avena-Bustillos, H.M.C. Azeredo, M.V. Lorevice, M.R. Moura, L.H.C.
 2007 Mattoso, T.H. McHugh, *Comprehensive Reviews in Food Science and Food Safety* 16 (2017)
 2008 1151-1169.
- 2009 [99] K.N. Turhan, *Journal of Hygienic Engineering and Design* 5 (2013) 13-17.
- 2010 [100] M. Stroescu, G. Isopencu, C. Busuioc, A. Stoica-Guzun, Antimicrobial Food Pads
 2011 Containing Bacterial Cellulose and Polysaccharides, *Cellulose-Based Superabsorbent*
 2012 *Hydrogels*, 2019, pp. 1303-1338.
- 2013 [101] K.A. Zahan, N.M. Azizul, M. Mustapha, W.Y. Tong, M.S. Abdul Rahman, I.S. Sahuri,
 2014 *Materials Today: Proceedings* 31 (2020) 83-88.
- 2015 [102] J. Padrão, S. Gonçalves, J.P. Silva, V. Sencadas, S. Lanceros-Méndez, A.C. Pinheiro,
 2016 A.A. Vicente, L.R. Rodrigues, F. Dourado, *Food Hydrocolloids* 58 (2016) 126-140.
- 2017 [103] M.J. Fabra, A. López-Rubio, J. Ambrosio-Martín, J.M. Lagaron, *Food Hydrocolloids*
 2018 61 (2016) 261-268.
- 2019 [104] M. Salari, M. Sowti Khiabani, R. Rezaei Mokarram, B. Ghanbarzadeh, H. Samadi
 2020 Kafil, *Food Hydrocolloids* 84 (2018) 414-423.
- 2021 [105] S. Bandyopadhyay, N. Saha, U.V. Brodnjak, P. Saha, *Materials Research Express* 5
 2022 (2018) 115405.
- 2023 [106] A. Shafipour Yordshahi, M. Moradi, H. Tajik, R. Molaei, *International Journal of Food*
 2024 *Microbiology* 321 (2020) 108561.
- 2025 [107] G. Research, Biodegradable superabsorbent materials market size, share & trends
 2026 analysis report by product, Grandview Research, 2016. [Online]. Available:
 2027 [https://www.grandviewresearch.com/industry-analysis/biodegradable-superabsorbent-](https://www.grandviewresearch.com/industry-analysis/biodegradable-superabsorbent-materials-market)
 2028 [materials-market](https://www.grandviewresearch.com/industry-analysis/biodegradable-superabsorbent-materials-market) (2016).
- 2029 [108] R.A. Ramli, *Polymer Chemistry* 10 (2019) 6073-6090.

2030 [109] E. Doelker, Swelling Behavior of Water-Soluble Cellulose Derivatives, in: L. Brannon-
2031 Peppas, R.S. Harland (Eds.), Studies in Polymer Science, vol 8, Elsevier, 1990, pp. 125-145.
2032 [110] M. Jorfi, E.J. Foster, Journal of Applied Polymer Science 132 (2015).
2033 [111] J. Ma, X. Li, Y. Bao, RSC Advances 5 (2015) 59745-59757.
2034 [112] L. Baldino, S. Zuppolini, S. Cardea, L. Diodato, A. Borriello, E. Reverchon, L.
2035 Nicolais, The Journal of Supercritical Fluids 156 (2020) 104681.
2036 [113] D. Ciecholewska-Juško, A. Żywicka, A. Junka, R. Drozd, P. Sobolewski, P. Migdał, U.
2037 Kowalska, M. Toporkiewicz, K. Fijałkowski, bioRxiv (2020) 2020.2003.2004.975003.
2038 [114] M.-T. Luo, C. Huang, H.-L. Li, H.-J. Guo, X.-F. Chen, L. Xiong, X.-D. Chen,
2039 Carbohydrate Polymers 208 (2019) 421-430.
2040 [115] M.-T. Luo, H.-L. Li, C. Huang, H.-R. Zhang, L. Xiong, X.-F. Chen, X.-D. Chen,
2041 Polymers 10 (2018) 702.
2042 [116] A. Cay, I. Tarakçioğlu, A. Hepbasli, Applied Thermal Engineering 29 (2009) 2554-
2043 2561.
2044 [117] M. Fernandes, M. Gama, F. Dourado, A.P. Souto, Microbial Biotechnology 12 (2019)
2045 650-661.
2046 [118] K. Kamiński, M. Jarosz, J. Grudzień, J. Pawlik, F. Zastawnik, P. Pandyr, A.M.
2047 Kołodziejczyk, Cellulose 27 (2020) 5353-5365.
2048 [119] F. Sanchez, K. Sobolev, Construction and Building Materials 24 (2010) 2060-2071.
2049 [120] A. Balea Martin, E. Fuente, A. Blanco, C. Negro, Polymers 11 (2019) 518.
2050 [121] O.A. Hisseine, N. Basic, A.F. Omran, A. Tagnit-Hamou, Cement and Concrete
2051 Composites 94 (2018) 327-340.
2052 [122] D. Trache, M.H. Hussin, M.K.M. Haafiz, V.K. Thakur, Nanoscale 9 (2017) 1763-1786.
2053 [123] F. Mohammadkazemi, K. Doosthoseini, E. Ganjian, M. Azin, Construction and
2054 Building Materials 101 (2015) 958-964.
2055 [124] K.-Y. Lee, K.K.C. Ho, K. Schlufter, A. Bismarck, Composites Science and Technology
2056 72 (2012) 1479-1486.
2057 [125] S.J. Peters, T.S. Rushing, E.N. Landis, T.K. Cummins, Transportation Research Record
2058 2142 (2010) 25-28.
2059 [126] Forced Hydrolysis and Chemical Co-Precipitation, in: Z.L. Wang, Y. Liu, Z. Zhang
2060 (Eds.), Handbook of Nanophase and Nanostructured Materials, Springer US, Boston, MA,
2061 2002, pp. 55-71.
2062 [127] I.I. Muhamad, S.N.H. Muhamad, M.H. Salehudin, K.A. Zahan, W.Y. Tong, N. Pa'e,
2063 Materials Today: Proceedings 31 (2020) 89-95.
2064 [128] S. Zhuang, J. Wang, Journal of Molecular Liquids 294 (2019) 111682.
2065 [129] X. Nie, P. Lv, S.L. Stanley, D. Wang, S. Wu, Q. Wei, Journal of Applied Polymer
2066 Science 136 (2019) 48000.
2067 [130] P. Arabkhani, A. Asfaram, Journal of Hazardous Materials 384 (2020) 121394.
2068 [131] X. Xu, X. Chen, L. Yang, Y. Zhao, X. Zhang, R. Shen, D. Sun, J. Qian, Chemical
2069 Engineering Journal 382 (2020) 123007.
2070 [132] Z. Qiu, M. Wang, T. Zhang, D. Yang, F. Qiu, Cellulose 27 (2020) 4591-4608.
2071 [133] Y. Wang, S. Yadav, T. Heinlein, V. Konjik, H. Breitzke, G. Buntkowsky, J.J.
2072 Schneider, K. Zhang, RSC Advances 4 (2014) 21553-21558.
2073 [134] H. Sai, L. Xing, J. Xiang, L. Cui, J. Jiao, C. Zhao, Z. Li, F. Li, T. Zhang, RSC
2074 Advances 4 (2014) 30453-30461.
2075 [135] A.A. Alves, W.E. Silva, M.F. Belian, L.S.G. Lins, A. Galembeck, International Journal
2076 of Environmental Science and Technology 17 (2020) 3997-4008.
2077 [136] R.T. Bianchet, A.L. Vieira Cubas, M.M. Machado, E.H. Siegel Moecke, Biotechnol
2078 Rep (Amst) 27 (2020) e00502.

2079 [137] G. Pacheco, C.V. de Mello, B.G. Chiari-Andréo, V.L.B. Isaac, S.J.L. Ribeiro, É.
2080 Pecoraro, E. Trovatti, *J Cosmet Dermatol* 17 (2018) 840-847.

2081 [138] E. Papakonstantinou, M. Roth, G. Karakiulakis, *Dermatoendocrinol* 4 (2012) 253-258.

2082 [139] X. Wang, J. Tang, J. Huang, M. Hui, *Colloids and Surfaces B: Biointerfaces* 195
2083 (2020) 111273.

2084 [140] P. Perugini, M. Bleve, R. Redondi, F. Cortinovis, A. Colpani, *J Cosmet Dermatol* 19
2085 (2020) 725-735.

2086 [141] R.T. Bianchet, A.L. Vieira Cubas, M.M. Machado, E.H. Siegel Moecke, *Biotechnology*
2087 *Reports* 27 (2020) e00502.

2088 [142] J. Amorim, A. Costa, C. Galdino, G. Vinhas, E. Santos, L. Sarubbo, *Chemical*
2089 *Engineering Transactions* 74 (2019) 1165-1170.

2090 [143] A. Khalid, R. Khan, M. Ul-Islam, T. Khan, F. Wahid, *Carbohydrate Polymers* 164
2091 (2017) 214-221.

2092 [144] P. Dhar, B. Pratto, A.J. Gonçalves Cruz, S. Bankar, *Journal of Cleaner Production* 238
2093 (2019) 117859.

2094 [145] Y. Yang, W. Liu, Q. Huang, X. Li, H. Ling, J. Ren, R. Sun, J. Zou, X. Wang, *ACS*
2095 *Sustainable Chemistry & Engineering* 8 (2020) 3392-3400.

2096 [146] W. Lei, D. Jin, H. Liu, Z. Tong, H. Zhang, *ChemSusChem* 13 (2020) 3731-3753.

2097 [147] N. Zhuravleva, A. Reznik, D. Kiesewetter, A. Stolpner, A. Khripunov, *Journal of*
2098 *Physics: Conference Series* 1124 (2018) 031008.

2099 [148] J.D.P. de Amorim, K.C. de Souza, C.R. Duarte, I. da Silva Duarte, F. de Assis Sales
2100 Ribeiro, G.S. Silva, P.M.A. de Farias, A. Stingl, A.F.S. Costa, G.M. Vinhas, L.A. Sarubbo,
2101 *Environmental Chemistry Letters* 18 (2020) 851-869.

2102 [149] K. Yoshino, R. Matsuoka, K. Nogami, S. Yamanaka, K. Watanabe, M. Takahashi, M.
2103 Honma, *Journal of Applied Physics* 68 (1990) 1720-1725.

2104 [150] Z.-Y. Wu, C. Li, H.-W. Liang, J.-F. Chen, S.-H. Yu, *Angewandte Chemie International*
2105 *Edition* 52 (2013) 2925-2929.

2106 [151] N. Islam, S. Li, G. Ren, Y. Zuo, J. Warzywoda, S. Wang, F. Zhaoyang, *Nano Energy*
2107 40 (2017).

2108 [152] H.-W. Liang, Q.-F. Guan, Z. Zhu, L.-T. Song, H.-B. Yao, X. Lei, S.-H. Yu, *NPG Asia*
2109 *Materials* 4 (2012) e19-e19.

2110 [153] W. Wang, Y. Yang, Z. Chen, Z. Deng, L. Fan, W. Guo, J. Xu, Z. Meng, *Cellulose* 27
2111 (2020) 7649-7661.

2112 [154] X. Zhou, Y. Liu, C. Du, Y. Ren, R. Xiao, P. Zuo, G. Yin, Y. Ma, X. Cheng, Y. Gao,
2113 *ACS Applied Materials & Interfaces* 11 (2019) 39970-39978.

2114 [155] G.D. Pasquale, S. Graziani, A. Pollicino, C. Trigona, *IEEE Transactions on*
2115 *Instrumentation and Measurement* 69 (2020) 2561-2569.

2116 [156] C. Trigona, S. Graziani, G. Pasquale, A. Pollicino, R. Nisi, A. Licciulli, *Sensors* 20
2117 (2020) 136.

2118 [157] U. Farooq, M.W. Ullah, Q. Yang, A. Aziz, J. Xu, L. Zhou, S. Wang, *Biosensors and*
2119 *Bioelectronics* 157 (2020) 112163.

2120 [158] N. Eslahi, A. Mahmoodi, N. Mahmoudi, N. Zandi, A. Simchi, *Polymer Reviews* 60
2121 (2020) 144-170.

2122 [159] M. Ul-Islam, T. Khan, W.A. Khattak, J.K. Park, *Cellulose* 20 (2013) 589-596.

2123 [160] Y. Huang, C. Zhu, J. Yang, Y. Nie, C. Chen, D. Sun, *Cellulose* 21 (2014) 1-30.

2124 [161] M. Moniri, A. Boroumand Moghaddam, S. Azizi, R. Abdul Rahim, A. Bin Ariff, W.
2125 Zuhainis Saad, M. Navaderi, R. Mohamad, *Nanomaterials* 7 (2017) 257.

2126 [162] C. Zhong, *Frontiers in Bioengineering and Biotechnology* 8 (2020).

2127 [163] W.K. Czaja, D.J. Young, M. Kawecki, R.M. Brown, *Biomacromolecules* 8 (2007) 1-
2128 12.

2129 [164] M.M. Khattab, Y. Dahman, *The Canadian Journal of Chemical Engineering* 97 (2019)
2130 2594-2607.

2131 [165] L. Autier, A. Clavreul, M.L. Cacicedo, F. Franconi, L. Sindji, A. Rousseau, R. Perrot,
2132 C.N. Montero-Menei, G.R. Castro, P. Menei, *Acta Biomaterialia* 84 (2019) 268-279.

2133 [166] E. Bayir, M.M. Celtikoglu, A. Sendemir, *Int J Biol Macromol* 126 (2019) 1002-1013.

2134 [167] N. Klinthoophamrong, D. Chaikiawkeaw, W. Phoolcharoen, K. Rattanapisit, P.
2135 Kaewpungsup, P. Pavasant, V.P. Hoven, *International Journal of Biological Macromolecules*
2136 149 (2020) 51-59.

2137 [168] B. Wang, X. Lv, S. Chen, Z. Li, J. Yao, X. Peng, C. Feng, Y. Xu, H. Wang,
2138 *Carbohydrate Polymers* 181 (2018) 948-956.

2139 [169] S.-P. Lin, I. Loira Calvar, J.M. Catchmark, J.-R. Liu, A. Demirci, K.-C. Cheng,
2140 *Cellulose* 20 (2013) 2191-2219.

2141 [170] U. Beekmann, L. Schmölz, S. Lorkowski, O. Werz, J. Thamm, D. Fischer, D. Kralisch,
2142 *Carbohydrate Polymers* 236 (2020) 116062.

2143 [171] L. Lamboni, Y. Li, J. Liu, G. Yang, *Biomacromolecules* 17 (2016) 3076-3084.

2144 [172] W.-S. Chang, H.-H. Chen, *Food Hydrocolloids* 53 (2016) 75-83.

2145 [173] N. Phutanon, K. Motina, Y.H. Chang, S. Ummartyotin, *International Journal of*
2146 *Biological Macromolecules* 136 (2019) 1142-1152.

2147 [174] F.A. Faisul Aris, F.N.A. Mohd Fauzi, W.Y. Tong, S.S. Syed Abdullah, *Biocatalysis*
2148 *and Agricultural Biotechnology* 21 (2019) 101332.

2149 [175] M.L. Cacicedo, G. Pacheco, G.A. Islan, V.A. Alvarez, H.S. Barud, G.R. Castro,
2150 *International Journal of Biological Macromolecules* 147 (2020) 1136-1145.

2151 [176] I. Orlando, P. Basnett, R. Nigmatullin, W. Wang, J.C. Knowles, I. Roy, *Frontiers in*
2152 *Bioengineering and Biotechnology* 8 (2020).

2153 [177] S. Mahalingam, M. Edirisinghe, *Macromolecular Rapid Communications* 34 (2013)
2154 1134-1139.

2155 [178] S. Mahalingam, S. Huo, S. Homer-Vanniasinkam, M. Edirisinghe, *Polymers* 12 (2020)
2156 1709.

2157 [179] E. Altun, M.O. Aydogdu, F. Koc, M. Crabbe-Mann, F. Brako, R. Kaur-Matharu, G.
2158 Ozen, S.E. Kuruca, U. Edirisinghe, O. Gunduz, M. Edirisinghe, *Macromolecular Materials*
2159 *and Engineering* 303 (2018) 1700607.

2160 [180] J. Ahmed, M. Gultekinoglu, M. Edirisinghe, *Biotechnology Advances* 41 (2020)
2161 107549.

2162 [181] H. Alenezi, M.E. Cam, M. Edirisinghe, *Applied Physics Reviews* 6 (2019) 041401.

2163 [182] M. Crabbe-Mann, D. Tsaoulidis, M. Parhizkar, M. Edirisinghe, *Cellulose* 25 (2018)
2164 1687-1703.

2165 [183] V. Palaninathan, S. Raveendran, A.K. Rochani, N. Chauhan, Y. Sakamoto, T. Ukai, T.
2166 Maekawa, D.S. Kumar, *Journal of Tissue Engineering and Regenerative Medicine* 12 (2018)
2167 1634-1645.

2168 [184] L. Maria Manzine Costa, G. Molina De Olyveira, P. Basmaji, L. Xavier Filho, *Journal*
2169 *of Biomaterials and Nanobiotechnology* 03 (2012) 92-96.

2170 [185] M.E. Cam, M. Crabbe-Mann, H. Alenezi, A.N. Hazar-Yavuz, B. Ertas, C. Ekentok,
2171 G.S. Ozcan, F. Topal, E. Guler, Y. Yazir, M. Parhizkar, M. Edirisinghe, *European Polymer*
2172 *Journal* 134 (2020) 109844.

2173 [186] M.O. Aydogdu, E. Altun, J. Ahmed, O. Gunduz, M. Edirisinghe, *Polymers* 11 (2019)
2174 1148.

2175 [187] E. Altun, M.O. Aydogdu, M. Crabbe-Mann, J. Ahmed, F. Brako, B. Karademir, B.
2176 Aksu, M. Sennaroglu, M.S. Eroglu, G. Ren, O. Gunduz, M. Edirisinghe, *Macromolecular*
2177 *Materials and Engineering* 304 (2019) 1800537.

2178 [188] H. Luo, H. Ao, G. Li, W. Li, G. Xiong, Y. Zhu, Y. Wan, *Current Applied Physics* 17
2179 (2017) 249-254.

2180 [189] H. Ullah, M. Badshah, A. Correia, F. Wahid, H.A. Santos, T. Khan, *Curr Pharm Des* 25
2181 (2019) 3692-3701.

2182 [190] W. Zhang, X.-c. Wang, J.-j. Wang, L.-l. Zhang, *International Journal of Biological*
2183 *Macromolecules* 140 (2019) 196-205.

2184 [191] P. Weyell, U. Beekmann, C. Küpper, M. Dederichs, J. Thamm, D. Fischer, D. Kralisch,
2185 *Carbohydrate Polymers* 207 (2019) 1-10.

2186 [192] M.L. Cacicedo, G.A. Islan, I.E. León, V.A. Álvarez, I. Chourpa, E. Allard-Vannier, N.
2187 García-Aranda, Z.V. Díaz-Riascos, Y. Fernández, S. Schwartz, I. Abasolo, G.R. Castro,
2188 *Colloids and Surfaces B: Biointerfaces* 170 (2018) 596-608.

2189 [193] M. L. Cacicedo, I. E. León, J. S. Gonzalez, L. M. Porto, V. A. Alvarez, G.R. Castro,
2190 *Colloids and Surfaces B: Biointerfaces* 140 (2016) 421-429.

2191 [194] S.O. Solomevich, E.I. Dmitruk, P.M. Bychkovsky, A.E. Nebytov, T.L. Yurkshtovich,
2192 N.V. Golub, *Carbohydrate Polymers* 248 (2020) 116745.

2193 [195] L. Chaabane, H. Chahdoura, R. Mehdaoui, M. Snoussi, E. Beyou, M. Lahcini, M.H. V
2194 Baouab, *Carbohydrate Polymers* 247 (2020) 116707.

2195 [196] J.R. Capadona, O. Van Den Berg, L.A. Capadona, M. Schroeter, S.J. Rowan, D.J.
2196 Tyler, C. Weder, *Nature Nanotechnology* 2 (2007) 765-769.

2197 [197] J. Wang, C. Gao, Y. Zhang, Y. Wan, *Materials Science and Engineering: C* 30 (2010)
2198 214-218.

2199 [198] Z. Shi, Y. Li, X. Chen, H. Han, G. Yang, *Nanoscale* 6 (2014) 970-977.

2200 [199] T. Niamsap, N.T. Lam, P. Sukyai, *Carbohydrate Polymers* 205 (2019) 159-166.

2201 [200] W. Zhang, X.-c. Wang, X.-y. Li, L.-l. Zhang, F. Jiang, *Carbohydrate Polymers* 236
2202 (2020) 116043.

2203 [201] T. Suzuki, K. Kono, K. Shimomura, H. Minami, *Journal of Colloid and Interface*
2204 *Science* 418 (2014) 126-131.

2205 [202] L. Lamboni, C. Xu, J. Clasohm, J. Yang, M. Saumer, K.-H. Schäfer, G. Yang,
2206 *Materials Science and Engineering: C* 102 (2019) 502-510.

2207 [203] D. Zhou, Y. Sun, Z. Bao, W. Liu, M. Xian, R. Nian, F. Xu, *Macromolecular Bioscience*
2208 19 (2019) 1800395.

2209 [204] M. He, Y. Zhao, J. Duan, Z. Wang, Y. Chen, L. Zhang, *ACS Applied Materials &*
2210 *Interfaces* 6 (2014) 1872-1878.

2211 [205] X. Yang, E. Bakaic, T. Hoare, E.D. Cranston, *Biomacromolecules* 14 (2013) 4447-
2212 4455.

2213 [206] S. Unal, S. Arslan, B. Karademir Yilmaz, D. Kazan, F.N. Oktar, O. Gunduz,
2214 *Carbohydrate Polymers* 233 (2020) 115820.

2215 [207] H. Luo, T. Cui, D. Gan, M. Gama, Q. Zhang, Y. Wan, *Polymer Testing* 80 (2019)
2216 106107.

2217 [208] L. Xu, A. Nirwane, Y. Yao, *Stroke and Vascular Neurology* 4 (2019) 78.

2218 [209] X. Li, J. Tang, L. Bao, L. Chen, F.F. Hong, *Carbohydr Polym* 178 (2017) 394-405.

2219 [210] Y. Li, K. Jiang, J. Feng, J. Liu, R. Huang, Z. Chen, J. Yang, Z. Dai, Y. Chen, N. Wang,
2220 W. Zhang, W. Zheng, G. Yang, X. Jiang, *Adv Healthc Mater* 6 (2017).

2221 [211] J. Wei, B. Wang, Z. Li, Z. Wu, M. Zhang, N. Sheng, Q. Liang, H. Wang, S. Chen,
2222 *Carbohydrate Polymers* 238 (2020) 116207.

2223 [212] E. Gutierrez, P.A. Burdiles, F. Quero, P. Palma, F. Olate-Moya, H. Palza, *ACS*
2224 *Biomaterials Science & Engineering* 5 (2019) 6290-6299.

2225 [213] L. Huang, X. Du, S. Fan, G. Yang, H. Shao, D. Li, C. Cao, Y. Zhu, M. Zhu, Y. Zhang,
2226 *Carbohydrate Polymers* 221 (2019) 146-156.

2227 [214] M. Schaffner, P.A. Rühs, F. Coulter, S. Kilcher, A.R. Studart, *Science Advances* 3
2228 (2017) eaao6804.
2229 [215] S. Shin, H. Kwak, D. Shin, J. Hyun, *Nature Communications* 10 (2019) 4650.
2230 [216] S. Sämfors, K. Karlsson, J. Sundberg, K. Markstedt, P. Gatenholm, *Biofabrication* 11
2231 (2019) 045010.
2232 [217] P.M. Research, *Bacterial Cellulose Market by Product Type (Industrial Grade,
2233 Technical Grade) by Application (Composites Materials, Nonwovens Adsorbent Webs, Paper
2234 and Board, Food Products) by Industry Analysis, Volume, Share, Growth, Challenges,
2235 Trends and Forecast 2019-2027*. [Online]. Available:
2236 <https://www.profsharemarketresearch.com/bacterial-cellulose-market-report/> (2021).
2237

2238